

Fakultät für Medizin

II. Medizinische Klinik und Poliklinik

Development of novel models to investigate mutant p53 functions in pancreatic cancer and determinants of deregulated expression

Nataša Stojanović

Vollständiger Abdruck der von der Fakultät für Medizin der Technischen Universität München zur Erlangung des akademischen Grades eines

Doctor of Philosophy (Ph.D.)

genehmigten Dissertation.

Vorsitzender: Univ.-Prof. Dr. Roland M. Schmid

Betreuer: Priv.-Doz. Dr. Günter Schneider

Prüfer der Dissertation:

1. apl. Prof. Dr. Dieter Saur

2. Priv.-Doz. Dr. Klaus-Peter Janssen

Die Dissertation wurde am 07.03.2014 bei der Fakultät für Medizin der Technischen Universität München eingereicht und durch die Fakultät für Medizin am 25.03.2014 angenommen.

Table of Contents

List of Tables.....	IV
List of Figures.....	V
Abbreviations.....	VII
1 Introduction.....	1
1.1 Pancreatic ductal adenocarcinoma (PDAC).....	1
1.2 Progression model of pancreatic cancer.....	1
1.3 <i>In vivo</i> models for investigating pancreatic cancer.....	3
1.4 Inducible tissue specific gene targeting.....	4
1.5 Tumour suppressor p53 – gene/protein organisation and historical overview.....	5
1.6 Alterations in the p53 gene and their influence on the cell fate.....	7
1.7 Regulation of p53 protein stability.....	8
1.8 NFκB family.....	9
1.9 Chromatin organisation.....	10
1.10 Regulation of transcription – classical model.....	11
1.11 Regulation of transcription - 'Transcription factories' model.....	11
1.12 Epigenetic regulation of gene expression and the role of chromatin modifiers.....	12
1.13 Histone deacetylases as therapeutic targets in cancer disease.....	14
1.14 Aims of this work.....	16
2 Materials.....	18
2.1 Technical equipment.....	18
2.2 Disposables.....	20
2.3 Reagents and enzymes.....	21
2.4 Kits.....	24
2.5 Antibodies.....	24
2.6 Primers.....	25
2.7 siRNA.....	28
2.8 Buffers.....	28
2.9 Histochemistry Reagents.....	29
2.10 Cell lines.....	30
2.11 Cell culture reagents.....	30
2.12 Cell culture media.....	31
3 Methods.....	32
3.1 Cell Culture.....	32
3.1.1 Isolation, handling and cryopreservation of pancreatic tumour cells.....	32
3.1.2 Isolation, handling and cryopreservation of pancreatic ductal epithelial cells (PDECs).....	32
3.1.3 siRNA transfection.....	33
3.1.4 MTT Assay.....	34
3.1.5 Caspase Assay.....	34
3.1.6 Senescence associate β-galactosidase (SA-β-gal) staining.....	34
3.1.7 Immunofluorescence.....	35
3.2 Molecular Techniques.....	36
3.2.1 DNA analysis.....	36
3.2.1.1 Isolation of genomic DNA.....	36
3.2.1.2 Polymerase chain reaction (PCR).....	36
3.2.1.3 Agarose gel electrophoresis.....	37
3.2.2 RNA analysis.....	37
3.2.2.1 RNA Isolation and Reverse Transcription.....	37
3.2.2.2 Quantitative Real-Time PCR.....	38
3.2.2.3 Comprehensive analysis of gene expression using microarrays.....	38
3.2.3 Protein analysis.....	39
3.2.3.1 Isolation of the whole cell protein extract.....	39
3.2.3.2 Determining protein concentration.....	39

3.2.3.3 Western Blot	39
3.2.4 Chromatin Immunoprecipitation (ChIP).....	40
3.3 Mouse experiments.....	41
3.3.1 Mouse strains	41
3.3.2 Genotyping	43
3.3.3 Tumour Mice Dissection	43
3.4 Histological analysis.....	44
3.4.1 Tissue fixation and sectioning	44
3.4.2 Haematoxylin and Eosin (HE) Staining of Tissue Sections	44
3.4.3 Alcian blue staining.....	44
3.4.4 Immunohistochemistry on paraffin slides	45
3.4.5 Immunohistochemistry on cryo-sections	45
3.4.6 Documentation	45
3.5 Statistical Analysis	46
4 Results.....	47
4.1 In vitro and in vivo models for investigating potential p53 ^{R172H} gain of function in pancreatic cancer.....	47
4.1.1 Characterisation of inducible p53 ^{R172H} system in vivo	47
4.1.2 Investigation of p53 ^{R172H} oncogenic potential in inducible p53 ^{R172H} model.....	49
4.1.3 PanIN-derived model system for investigating p53 ^{R172H} in pre-tumorigenic context	51
4.1.4 p53 ^{R172H} activates ribosomal pathway.....	52
4.1.5 Potential role of p65 in p53 ^{R172H} gain of function	55
4.2 p53 regulation by histone deacetylases (HDACs) and HDAC inhibitors	58
4.2.1 HDAC inhibitors reduce cell viability by inducing apoptosis and senescence	58
4.2.2 HDAC inhibitors regulate the expression of p53 mutants at protein and mRNA level	60
4.2.3 p53 protein decrease is independent of MDM2 and proteasomal degradation	62
4.2.4 HDACi regulate p53 mRNA expression.....	63
4.2.5 The role of HDAC1, 2 and 3 in p53 stabilisation.....	65
4.2.6 The Role of HDAC8 in p53 stabilisation	69
4.2.7 Role of WRAP53 in p53 mRNA regulation	70
4.2.8 Hdac1/2 mediated p53 regulation <i>in vivo</i>	71
4.2.9 The role of c-MYC in p53 regulation.....	74
4.2.10 MYC bind to the p53 gene promoter and binding is regulated by HDACi	75
5 Discussion	79
5.1 Murine models for investigating p53 ^{R172H} gain of function in PDAC	79
5.2 p53 ^{R172H} prepare the cell for the synthesis and increase metabolic processes	80
5.3 Targeting p53	81
5.4 HDAC inhibitors as destabilisers of p53 mutants	82
5.5 HDACi regulate p53 mRNA levels	83
5.6 HDAC1 and HDAC2 cooperate to stabilise p53.....	83
5.7 Regulation of p53 transcription and mRNA stability.....	84
5.8 c-MYC binding on the p53 promoter is regulated by MS275	86
5.9 MS275 treatment reveals repressed region within first intron of the p53 gene	87
5.10 Potential role of the repressive complexes in the regulation of the p53 transcription	88
6 Summary	90
7 References	91
Acknowledgements.....	106

List of Tables	Page
Table 2.1. Technical Equipment	18
Table 2.2. Disposables	20
Table 2.3. Reagents and enzymes	21
Table 2.4. Kits	24
Table 2.5. Antibodies	24
Table 2.6. Primers	25
Table 2.7. siRNAs	28
Table 2.8. Buffers	28
Table 2.9. Histochemistry reagents	29
Table 2.10. Cell lines	30
Table 2.11. Cell culture reagents	30
Table 2.12. Cell culture media	31
Table 3.1. Components of SA-β-gal staining solution	35
Table 3.2. Reaction mix and conditions for standard PCR	36
Table 3.3. Annealing temperatures and size of the wild type and mutated PCR products	37
Table 3.4. Conditions for quantitative real-time PCR	38
Table 3.5. Components of the separating and concentrating gels	40
Table 4.1. Origin of cell lines and p53 status in treated cells	53
Table 4.2. Gene set enrichment upon p53 ^{R172H} activation	53

List of Figures	Page
Figure 1.1. Progression model of pancreatic cancer	2
Figure 1.2. Schematic overview of the dual recombination system as a tool for inducible, tissue-specific gene targeting	5
Figure 1.3. p53 protein domains and 'hot spot' mutations	6
Figure 1.4. HATs and HDACs effect on chromatin accessibility	13
Figure 1.5. Chromatin patterns and status	14
Figure 1.6. Shematic representation of metal-dependent HDAC's classification and localisation	15
Figure 4.1. Recombination ratio and p53 expression in tamoxifen induced mice ...	47
Figure 4.2. p53 protein can be stabilised only in the cells with appropriate oncogenic context	48
Figure 4.3. p53 ^{R172H} accelerates cell growth and migration and shortens survival of the mice	50
Figure 4.4. Preneoplastic lesions in non-induced mice with dual recombinase system	51
Figure 4.5. PDEC cell line as an <i>in vitro</i> model for investigating p53 ^{R172H} role in an early carcinogenesis	52
Figure 4.6. p53 ^{R172H} activates ribosomal pathway in the cell	54
Figure 4.7. NFκB signalling is active in cell lines harbouring p53 ^{R172H}	55
Figure 4.8. p53 ^{R172H} stabilization in PDAC	56
Figure 4.9. Influence of p65 inactivation on the survival of KC mice with different p53 status	57
Figure 4.10. Histology of the p53 ^{R172H/lox} and p53 ^{R172H/lox} ;p65 ^{lox/lox} mice in the KC background	58
Figure 4.11. HDAC inhibitors, SAHA and MS275 reduce cell viability and induce caspase 3/7 activity	59
Figure 4.11. HDAC inhibitors, SAHA and MS275 induce senescence in human pancreatic cancer cell line PaTu8988t	60
Figure 4.13. HDAC inhibitor treatment leads to depletion of mutant p53 and its targets	61
Figure 4.14. p53 protein depletion is independent of MDM2	62
Figure 4.15. p53 protein does not undergo proteasomal degradation upon HDACi treatment	63
Figure 4.16. HDAC inhibitors SAHA and MS275 deplete p53 mRNA	64
Figure 4.17. HDAC inhibitors SAHA and MS275 do not influence mRNA stability	65

Figure 4.18. p53 regulation by Hdac1 and Hdac2	66
Figure 4.19. p53 mRNA is not decreased upon Hdac1 knock down in Hdac2- deficient cell lines	68
Figure 4.20. HDAC 8 is not off target of Hdac1 siRNA and its protein level is not affected by SAHA nor MS275 treatment	69
Figure 4.21. WRAP53 and p65 are not involved in p53 regulation	70
Figure 4.22. Pdx1Cre; LSL-ras ^{G12D} ; Hdac1 ^{lox/wt} ; Hdac2 ^{lox/lox} ; p53 ^{R172H/wt}	72
Figure 4.23. Protein levels of Hdac1, p53 and c-Myc correlate to each other in Hdac2 deficient background	73
Figure 4.24. p53 and c-Myc display similar protein expression pattern	75
Figure 4.25. c-MYC and Pol II binding towards p53 gene upon MS275 treatment	76
Figure 4.26. Activating and repressing histone marks upon MS275 treatment in the p53 gene	77
Figure 4.27. c-MYC and Pol II binding upon MS275 treatment towards p53 gene	78
Figure 5.1. Murine and human p53 promoter occupancy	85
Figure 5.2. p53 gene organization and overlap with WRAP53	87

Abbreviations

°C	Degree Celsius
4-OHT	4-hydroxytamoxifen
5-FU	5-Fluorouracil
AcH3	Acetylated histone H3
ADM	Acinar-ductal metaplasia
AFL	Atypical flat lesions
APS	Ammonium-persulfate
ATP	Adenosin-triphosphate
BAX	Bcl-2-associated X protein
Bcl-2	B-cell lymphoma 2
bp	Base pairs
BRCA2	Breast cancer 2, early onset
BrdU	5-bromo-2'-deoxyuridine
BSA	Bovine serum albumin
Caspase	Cysteine-dependent aspartate-directed proteases
CCD	Charge-coupled device
CDK	Cyclin-dependent kinase
CDKN1A	Cyclin-dependent kinase inhibitor 1 (p21)
cDNA	Complementary DNA
ChIP	Chromatin immunoprecipitation
cm	Centimeter
c-Myc	V-myc myelocytomatosis viral oncogene homolog (avian)
CO ₂	Carbon dioxide
ConTra	Conserved transcription factor binding sites
CTD	C terminal domain
DBD	DNA binding domain
ddH ₂ O	Double-distilled water
DMEM	Dulbecco's Modified Eagle Medium
DMSO	Dimethyl sulfoxide
DNA	Deoxyribonucleic acid
DNase	Deoxyribonuclease
dNTP	Deoxyribonucleotide phosphate
DTT	1,4-dithiothreitol
E	Embryonic development day

EDTA	Ethylenediaminetetraacetic acid
EGFP	Enhanced green fluorescent protein
et al.	et alii
EtBr	Ethidium bromide
EtOH	Ethanol
EZH2	Enhancer of zeste homolog 2
FCS	Fetal calf serum
FSF	Frt-Stop-Frt
g	Gram
GAPDH	Glyceraldehyde 3-phosphate dehydrogenase
GEMM	Genetically engineered mouse model
GSEA	Gene set enrichment analysis
h	Hours
H ₂ O	Water
H3K27Ac	Acetylated lysine 27 of histone H3
H3K27Me3	Trimethylated lysine 27 of histone H3
H3K4Me3	Trimethylated lysine 4 of histone H3
H3K9Me1	Methylated lysine 9 of histone H3
H3K9Me3	Trimethylated lysine 9 of histone H3
HAT	Histone acetyltransferase
HDAC	Histone deacetylase
HDACi	Histone deacetylase inhibitor
HE	Hematoxylin and eosin
HEPES	4-(2-hydroxyethyl)-1-piperazineethanesulfonic acid
HER2	Human epidermal growth factor receptor 2
HMG	High mobility group
Hras	V-Ha-ras Harvey rat sarcoma viral oncogene homolog
Hsp	Heat shock protein
IHC	Immunohistochemistry
IP	Immunoprecipitation
k, kilo	Thousand
kb	Kilobase-pairs
KC	Kras ^{G12D} ; p53 ^{R172H}
kDa	Kilodalton
kg	Kilogram
Kras	V-Ki-ras2 Kirsten rat sarcoma viral oncogene homolog
LOH	Loss of heterozygosity

LSL	LoxP-stop-LoxP
M	Molar
m, milli	Thousandth
mA	Milliampere
MBT	Malignant brain tumor
MDM2	Mouse double minute 2
μ, micro	Millionth
μg	Microgram
μL	Microliter
μm	Micrometer
μM	Micromolar
mg	Milligram
min	Minute
MIR	microRNA, miRNA
mL	Milliliter
mm	Millimeter
mM	Millimolar
MMF	Midazolam, medetomidine, fentanyl
mRNA	Messenger-RNA
MTT	3-(4,5-dimethylthiazol-2-yl)-2,5-diphenyltetrazolium bromide
mut	Mutated
n	Number
n, nano	Billionth
NAD	Nicotinamide adenine dinucleotide
NF-κB	Nuclear factor kappa-light-chain-enhancer of activated B cells
ng	Nanogram
nm	Nanometer
nM	Nanomolar
OD	Optical density
p	Phospho
PAGE	Polyacrylamide gel electrophoresis
PanIN	Pancreatic intraepithelial neoplasia
PBS	Phosphate buffered saline
PCR	Polymerase chain reaction
PDAC	Pancreatic ductal adenocarcinoma
Pdx1	Pancreatic and duodenal homeobox 1
PHD	Plant Homeo Domain

PPT	Pancreatic primary tumor
PRD	Proline rich domain
Ptf1	Pancreas transcription factor 1
PUMA	p53 upregulated modulator of apoptosis
PVDF	Polyvinylidene fluoride
PWWP	Proline-Triptophan-Triptophan-Proline
R26	Rosa 26
RNA	Ribonucleic acid
RNase	Ribonuclease
rpm	Revolutions per minute
RT	Reverse transcription
RT	Room temperature
SA β -gal	Senescence associated β -galactosidase
SAHA	Suberanilohydroxamic acid
SDS	Sodium dodecyl sulfate
sec	Second
siRNA	Small interfering RNA
SIRT	Sirtuin
STAT	Signal transducer and activator of transcription
TAD	Transactivation domain
TAE	Tris Acetate EDTA
TBP	TATA binding protein
TC	Tubular complex
TEMED	N,N,N',N'-Tetramethylethylenediamine
TP53	Tumor protein p53
Tris	Tris(hydroxymethyl)-aminomethane
tRNA	Transfer-RNA
Trp53	Transformation related protein 53
TsA	Trichostatin A
Tva	Tumor virus A
U	Unit
UV	Ultra violet
V	Volt
v/v	Volume per volume
w/v	Weight per volume
WT, wt	Wild type

1 Introduction

1.1 Pancreatic ductal adenocarcinoma (PDAC)

Pancreatic cancer is the fourth deadliest cancer worldwide. Of all cancer patients, 3% have pancreatic cancer. Still, only 6% of all pancreatic cancer patients survive more than 5 years. Estimated number of new cases of pancreatic cancer in 2014 in USA is 46420 patients and 39590 expected deaths. This means that 7% of total cancer-related deaths are due to pancreatic cancer (Siegel et al., 2014). Although a lot of effort is invested in understanding molecular mechanisms of pancreatic carcinogenesis, no drastic improvement is achieved for the last four decades (Siegel et al., 2014).

Main reasons for such a grave situation are inefficient early diagnosis and lack of improvement in therapy strategies. During early stages, PDAC displays no symptoms. Additionally, its retroperitoneal position makes pancreatic cancer practically invisible in the early stage. Therefore, patients are usually diagnosed with late stage carcinomas and only in 15-20% of the cases surgical resection is possible (Hamacher et al., 2008; Richter et al., 2003). Advanced cancer is resistant to radiation therapy and common chemotherapy. Hence, most of the treatments are based on the palliative chemotherapy. FDA approved chemotherapeutics, which are mostly in use, are nucleoside analogues, gemcitabine and 5-fluorouracil, as well as a targeted therapy with Erlotinib, the inhibitor of epidermal growth factor receptor (EGFR) tyrosine kinase (Neoptolemos et al., 2004; Pollack et al., 1999). Combined treatments are also widely in use. Combination of albumin-bound paclitaxel and gemcitabine, reached phase III clinical trial and showed significantly increased survival of the patients, compared with gemcitabine treatment alone (Von Hoff et al., 2013). Also, FOLFIRINOX – cocktail of leucovorin, fluorouracil, irinotecan and oxaliplatin showed improved survival compared to gemcitabine treatment (Conroy et al., 2011). Although significant, the improvements in survival are between 1.5 and 3 months. Clearly there is an urgent need for developing new diagnostic tools and therapeutic strategies.

1.2 Progression model of pancreatic cancer

PDAC is the most frequently diagnosed type of pancreatic cancer (85%). A progression model of the PDAC is well established and corresponds to the stepwise progression through morphological and genetic changes, which lead to highly invasive and metastatic carcinoma. Preneoplastic lesions in the carcinogenesis are termed pancreatic intraepithelial neoplasias

(PanINs) and are classified as a PanIN1A, -1B, -2 and -3 according to their morphology (Figure 1.1) (Hezel et al., 2006).

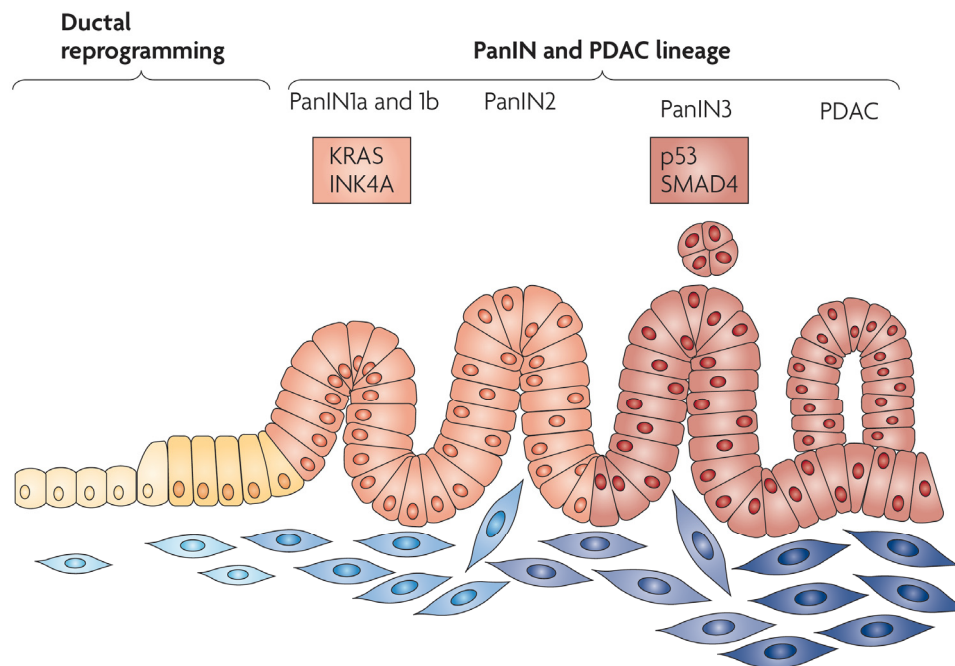


Figure 1.1. Progression model of pancreatic cancer. Progression from normal cells through a series of pancreatic intraepithelial lesions (PanIN1A, -1B, -2 and -3) to PDAC. Morphological changes correlate with distinct molecular events like activation of oncogenic *KRAS* or mutation in tumour suppressor gene, *p53* (Hruban et al., 2000a). Figure modified according to (Morris et al., 2010).

PanIN1A are characterised by elongated, column like cells. The nuclei are basally positioned and round or oval in shape. Mucin is usually present in subnuclear area. The lesion is flat without any sign of papilla. PanIN1B are similar to PanIN1A except the micropapillary structures that arise and the epithelium that becomes pseudo-stratified due to the fraction of the nuclei positioned toward apical compartment of the cell. PanIN2 are mostly papillary and in rare cases can be flat. They are characterised by improved pseudostratification, loss of polarity, enlarged nuclei, hyperchromatism and mucin secretion. PanIN3 are morphologically exclusively papillary. They are easily distinguished from PanIN2 due to the budding off clusters of epithelial cells into the lumen. This cribriforming appearance is followed by luminal necrosis. Nuclei are positioned apically towards the lumen, while the mucinous cytoplasm is orientated towards basal membrane. PanIN-3 lesions are the last precursors before PDAC and they are equal to carcinoma *in situ* (Hruban et al., 2001).

In addition to the morphological changes, progression through the PanIN lesions correlates with specific molecular events in tumour suppressors and oncogenes. In early grade PanINs (-1A, -1B and -2), mutations in *KRAS*, *p16/INK4A* as well as overexpression of

HER-2/neu occur, while in the PanIN3 the most common molecular alterations are mutations in the *TP53* (*Trp53* in the mouse, hereafter named *p53*), *DPC4* and *BRCA2* gene (Hruban et al., 2000b).

PanIN lesions have a ductal phenotype and suggest ductal origin of pancreatic cancer. However, recent studies suggest that tubular complexes (TC), which originate through acinar-ductal metaplasia (ADM), form atypical flat lesions (AFL) that may represent an alternative pathway of pancreatic cancer development (Esposito et al., 2012).

1.3 *In vivo* models for investigating pancreatic cancer

Identification of molecular changes, which take place during PDAC progression, helped scientists to develop appropriate mouse models which recapitulate PDAC development in humans. The most commonly used mouse model expresses constitutively active *Kras*^{G12D} in the pancreas, which drives development of PDAC. For pancreas-specific expression, the Cre-LoxP system is used (Orban et al., 1992). Namely, two mouse lines which express the Cre recombinase under the control of either the Pdx1 or the Ptf1a promoter are used. Pdx1 and Ptf1a are transcription factors crucial for development of pancreatic cancer and they are expressed from E8.5 and E9.5 respectively (Krapp et al., 1998; Offield et al., 1996). Due to the pancreas-specific activation of Cre recombinase, oncogenic *Kras* is expressed exclusively in pancreatic tissue from the embryonic day 8.5 (Hingorani et al., 2003). Before the recombination occurs, the *LSL-Kras*^{G12D} mice are heterozygous for wild type *Kras* (*Kras*^{+/+}) as the mutant allele is silenced by *lox-stop-lox* (*LSL*) cassette. Upon Cre activation, the stop element is excised and activated *Kras*^{G12D} is expressed from its locus at endogenous levels, resulting in a heterozygous mutant condition (*Kras*^{G12D/+}). *Pdx1-Cre; LSL-Kras*^{G12D/+} and *Ptf1a*^{Cre/+}; *LSL-Kras*^{G12D/+} mice (further referred to as KC mice) develop pancreatic cancer highly reminiscent of human disease. These mice succumb to the PDAC after roughly one year (Hingorani et al., 2003). Since the *p53* gene is often mutated in PDAC, The KC mouse model with additional *LSL-p53*^{R172H} mutation is widely used. Similar to the *Kras*^{G12D} allele, before the recombination occurs, the *LSL-p53*^{R172H} mice are heterozygous or null (depending if the *LSL-p53*^{R172H} is present only in one or in both alleles) for wild type *p53* as the mutant allele is silenced by *lox-stop-lox* (*LSL*) cassette. After Cre activation, the stop cassette is excised and mutant *p53*^{R172H} is expressed (Hingorani et al., 2005).

1.4 Inducible tissue specific gene targeting

Although the previously described mouse models are convenient due to the quickly growing tumours and the possibility to investigate interactions of a high number of genes and alleles, some of the features may represent serious limitations. The most important one is simultaneous activation of all mutated alleles during early embryogenesis. This situation does not recapitulate human carcinogenesis, which is a multi-step process instead. Therefore, dual recombination systems, which use two different recombinases, have been developed.

In these dual systems, expression of the Flp recombinase, which recombines *frt* sites, is driven by the *Pdx1* promoter. In *Pdx1-Flp; FSF (frt-stop-frt)-Kras^{G12D}* mice, the FSF cassette is removed after Flp activation, leading to oncogenic *Kras^{G12D}* expression. To get a dual system, an additional *Cre^{ERT2}* recombinase is introduced (*FSF-R26^{CAGCreERT2}*). *Cre^{ERT2}* expression here is inhibited by a preceding FSF cassette. The *Cre^{ERT2}* is placed in the ubiquitously expressed *Rosa26* locus (Soriano, 1999) and contains an additional strong promoter, CAG, which enhances the expression of the *Cre^{ERT2}*. Although expressed after Flp/*frt* recombination, *Cre^{ERT2}* recombinase is sequestered in the cytoplasm by binding to Hsp90. Only upon applying the estrogen analogue - tamoxifen, *Cre^{ERT2}* can be translocated to the nucleus and accomplish its function (Mattioni et al., 1994). In the dual system, genes, like in this case *LSL-Trp53^{R172H}* and *R26^{mT/mG}*, can be switched on by *Cre^{ERT2}* recombinase after addition of tamoxifen in a time- and tissue-dependent manner. In case of *LSL-Trp53^{R172H}*, the stop cassette is excised and p53^{R172H} is expressed. The reporter *R26^{mT/mG}* codes for *Tomato* and *eGFP*. A stop cassette is inserted between them. *Tomato* and the stop cassette both are flanked by LoxP sites. When *Cre^{ERT2}* recombinase is not active, *Tomato* is expressed, but *eGFP* expression is blocked by the stop cassette, resulting in red fluorescence. Upon *Cre^{ERT2}* activation by application of tamoxifen, *Tomato* and the stop cassette are cut out, *eGFP* is expressed and the cells change colour into green (Muzumdar et al., 2007). Schematic overview is shown in the Figure 1.2.

The benefit of the dual recombinase system is that it provides time- and tissue-specific expression or knock-out of the gene of interest. Additionally, the reporter system is useful because it provides information about recombinase efficacy and lineage tracing.

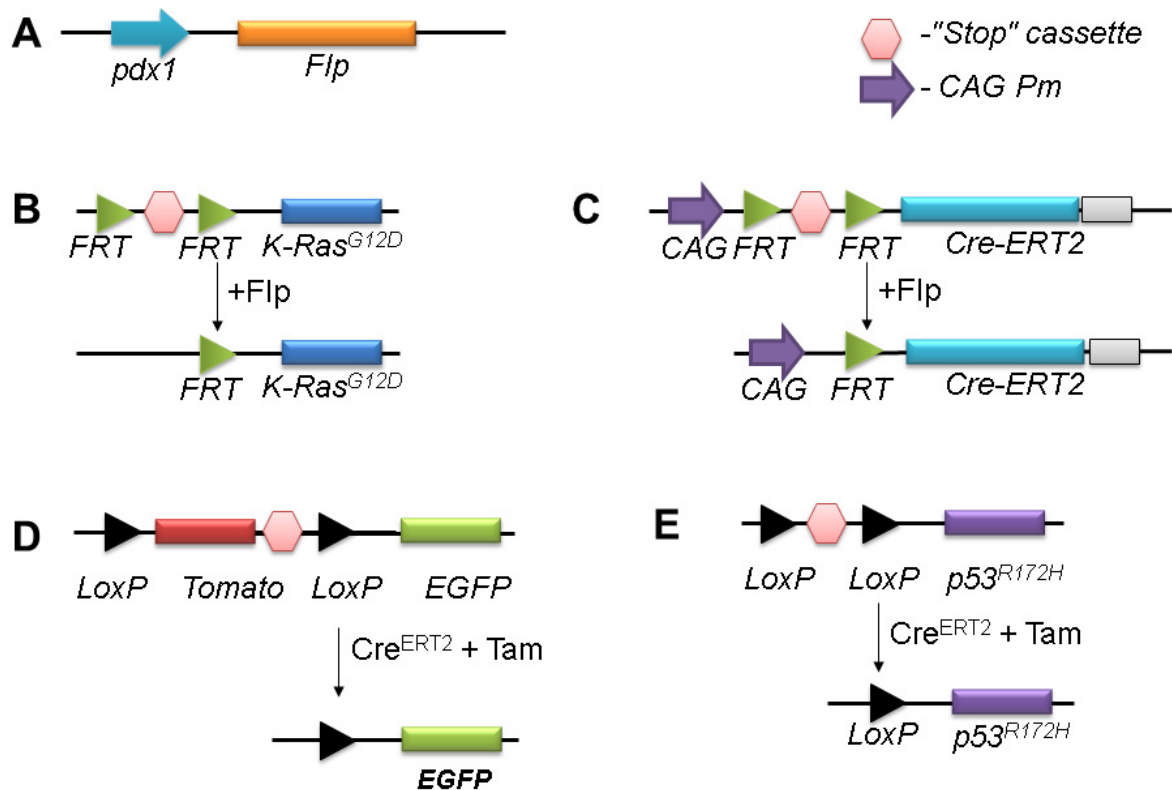


Figure 1.2. Schematic overview of the dual recombination system as a tool for inducible, tissue-specific gene targeting. **A** - *Flp* recombinase regulated by the pancreas-specific *Pdx1* promoter; **B** and **C** – exclusion of the *FSF* cassette by *Flp*-mediated recombination and activation of *Kras*^{G12D} and *Cre*^{ERT2} expression, respectively; **D** and **E** – exclusion of the *LSL* cassette by the tamoxifen-activated *Cre*^{ERT2} recombinase and switch from *Tomato* to *eGFP* expression (**D**) and activation of *p53*^{R172H} expression (**E**).

1.5 Tumour suppressor p53 – gene/protein organisation and historical overview

Tumour protein 53 (Tp53, hereafter named p53) is a transcription factor, which binds to regulatory elements of the DNA to activate or repress transcription of its target genes. The human *TP53* gene is localized at the short arm of chromosome 17 (17p.13.1) and it is coded within a 20 kB long DNA segment. The non-coding exon 1 and the 10 kB long first intron are followed by further 10 exons. The p53 protein consists of an N-terminal transactivation domain and a sequence-specific DNA binding domain. A further oligomerisation domain is necessary for the p53 tetramerisation which provides the active form and it is followed by the C-terminal regulatory domain like it is shown in the Figure 1.3 (Jeffrey et al., 1995).

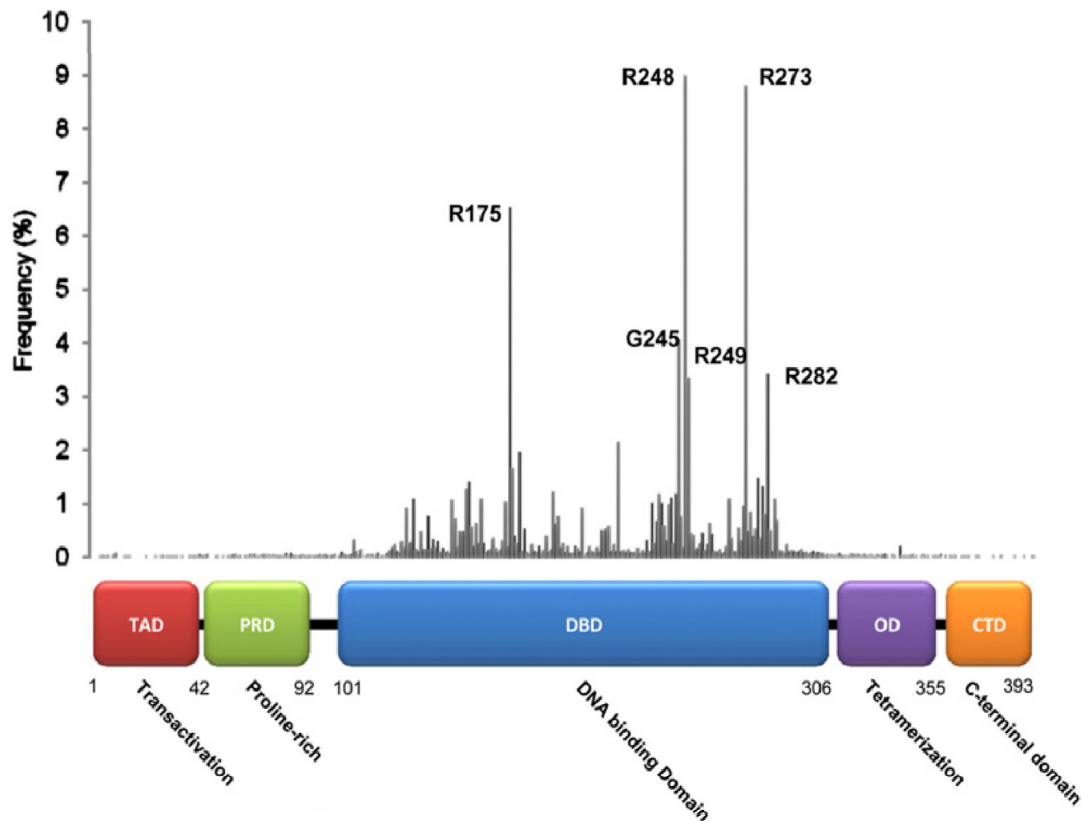


Figure 1.3. p53 protein domains and 'hot spot' mutations. Upper panel - Most common p53 mutations in humans and their positions. Lower panel - Scheme of the p53 protein structure. **TAD**-transactivation domain - N-terminal transactivation domain; **PRD** - proline-rich domain; **DBD** - DNA binding domain; **OD** - Oligomerisation domain which also contains nucleus localising sequence; **CTD** - C-terminal regulatory domain. Modified according to (Freed-Pastor and Prives, 2012).

In the last 35 years, p53 has been one of the most intensively studied tumour suppressors. It was discovered in 1979 as a 53 kDa co-precipitate of the large-T antigen in Simian virus 40 (SV40) transformed cells (Chang et al., 1979; Kress et al., 1979; Lane and Crawford, 1979; Melero et al., 1979). Initially, it was thought to be of viral origin, but soon it was found that p53 protein was expressed also in uninfected embryonic carcinoma cells (Linzer and Levine, 1979). Few years later the antibodies against the very same protein were detected in sera of children suffering from different cancer types, which was one more proof that p53 is a protein with an endogenous origin (Crawford et al., 1982). *p53* cDNA was cloned for the first time by Oren and Levine (Oren et al., 1983). Soon after, two groups showed that p53 can perform an oncogenic transformation when introduced into rat embryo fibroblasts with activated Ras signalling (Eliyahu et al., 1984; Parada et al., 1984). This discovery misled numerous scientists to the conclusion that p53 is an oncogene but it actually was first description of p53 mutant gain of function.

Almost 10 years after the discovery, several groups recognized that *p53* cDNA from different cell lines does not necessary cooperate with Ras and, when both present in cells,

they fail to form tumours (Finlay et al., 1988). After numerous analyses, it was confirmed that single nucleotide changes occur in conserved regions of cloned *p53* cDNA from transformed cells when compared with cDNA from non-transformed cells (Soussi et al., 1987). Based on this, it was concluded that the p53 proteins isolated from different tumour cell lines were actually mutated. Further experiments showed that co-transfection of a plasmid encoding wild type *p53* reduced the transformation potential of plasmids encoding mutant *p53* and an activated *Hras* gene (Eliyahu et al., 1989; Finlay et al., 1989). These experiments enlightened wild type p53 as a suppressor of cell transformation *in vitro* and showed that only one nucleotide substitution can lead to the change of p53 function.

Known as a 'guardian of the genome' (Lane, 1992), p53 protein is responsible for (i) cell cycle arrest (through regulation of target genes like *CDKN1A*), (ii) senescence (through regulation of e.g. *CDKN1A*, *PEI1*), and (iii) apoptosis (through regulation of e.g. *PUMA*, *BAX*) (Riley et al., 2008; Schmitt et al., 2002; Vousden and Lu, 2002). By regulating these processes, p53 provides time for the cell to activate an appropriate and localized response and proof check mechanisms that are in charge of keeping DNA fidelity. If irreparable DNA damage occurs, p53 leads the cell into senescence and further into apoptosis. These anti-carcinogenic mechanisms define p53 as a 'first line tumour suppressor' and keep it in the focus of cancer research (Lane, 1992).

1.6 Alterations in the p53 gene and their influence on the cell fate

p53 is an exceptional tumour suppressor in many ways. Frequently, tumour suppressors obey Knudson's 'two hit' hypothesis meaning that when one allele is mutated, the other can perform its function (Knudson, 1971). In the case of *p53*, a mutation in one allele is followed by loss of heterozygosity (LOH), suggesting that there is a selective advantage of losing wild type *p53* in a cancer cell, in order to eliminate tumour suppressive function (Baker et al., 1990). This mechanism is additional selection tool for maintaining the mutant p53. Still, loss of heterozygosity depends on the status of the p53 negative regulators MDM2 and MDM4. If p53 inhibiting pathways are activated, it is not necessary that wild type *p53* is deleted (Xiong et al., 2010).

Tumour suppressors are predominantly inactivated by nonsense or frameshift mutations (Weinberg, 1991). Contrary, most of the genetic alterations in the *p53* gene are missense mutations which occur in the DNA binding domain and cause single variations in the amino acid sequence of the full-length protein. In contrast to wt p53, which is rapidly degraded in non-stress conditions, mutations in the *p53* gene lead to a prolonged half-life of the protein (Strano et al., 2007). Out of more than 28.000 mutations in the *p53* gene

(according to the IARC database) 6 of them (Arg175, Gly245, Arg248, Arg249, Arg273, and Arg282) have high frequency of occurrence and therefore are named '*hot spot*' mutations (Harris and Hollstein, 1993). Mutations of amino-acids 248 and 273 are 'contact' mutations and other 4 are considered conformational mutants (Hainaut and Hollstein, 2000), (Figure 1.3).

Other changes in the *p53* gene are splice site and nonsense mutations, which lead to early terminated transcription and therefore to total lack of p53 or to accumulation of a truncated form (Tsuda and Hirohashi, 1994). Splice site mutations are also known but not common (Takahashi et al., 1990).

To become active, p53 forms dimers, which then align to form a tetramer (Friedman et al., 1993; Stenger et al., 1992). Only if all four monomers are aligned in a proper way, p53 can regulate its targets. If one mutated monomer is introduced, the whole tetramer gains aberrant conformation which leads to the altered target affinity of p53. For some of the targets, p53 completely loses transcriptional activity (loss of function). Others are not further regulated in a p53-specific manner (dominant negative effect) and the rest of the targets are regulated in a p53 mutant-specific way, including new targets or types of regulation which were never distinctive for p53 wt (gain of function, GOF) (Muller and Vousden, 2013).

To investigate p53 GOF, many knock in mice lines carrying different p53 mutants have been developed and usually compared to p53^{-/-} animals. The conclusion of these studies is that the type of the cancer developed as well as metastatic potential, depends on the type of the mutation and the genetic background (mouse strain). For example mutants R172H, R270H, R248W, manifest GOF by causing more tumor types and more metastasis compared with the p53-null allele, but do not shorten survival. On the other hand, R248Q/- mice show accelerated onset of all tumor types and shorter survival. This was further associated with higher T-lymphoma proliferation (Hanel et al., 2013). Furthermore, some of the mutants show higher metastatic potential, which can be considered as a GOF, compared with knock-out mice. This result is in correlation with clinical data, because it is known that, for example, breast cancer patients harbouring p53 mutant have worse prognosis than patients lacking p53 (Cadwell and Zambetti, 2001; Deppert et al., 2000; Olivier et al., 2006; Roemer, 1999).

1.7 Regulation of p53 protein stability

p53 is enrolled in transcriptional regulation of many genes and it has long been known as one of the crucial tumour suppressors. Therefore, huge effort was spent to investigate its role

as a transcription factor, its target genes, ways of regulation and p53-dependent pathways. Because of its importance and enrolment in numerous essential pathways, p53 itself has to be tightly regulated. Consequently, more than one mechanism of p53 regulation exists (Levine and Oren, 2009).

It is well known that MDM2 is the main negative regulator of p53 (Haupt et al., 1997; Jones et al., 1995). MDM2 is an ubiquitin ligase, which targets p53 for proteasomal degradation (Kubbutat et al., 1997). Furthermore, p53 regulates *MDM2* on a transcriptional level, thereby forming a loop which keeps p53 protein levels in accordance with cell state. MDM4 is a member of the same family and it is also a negative regulator of p53, but it has no ubiquitin activity (Shvarts et al., 1996). Both MDM2 and MDM4 can bind p53 mutant, but mutant p53 is not able to induce transcription of the *MDM2* gene. As a consequence, mutated p53 is stabilised in the cell (Momand et al., 1992). Except of the targeting for the degradation in proteasomes due to the ubiquitination, the p53 amino-terminus undergoes posttranslational changes like phosphorylation, acetylation and methylation, which significantly contribute to p53 stability (Meek, 1994; Sakaguchi et al., 1998).

1.8 Nuclear factor kappaB (NFκB) family

NFκB family consists of 5 transcription factors: RelA, RelB, c-Rel and two precursors NFκB1 (p105) and NFκB2 (p100), which, when processed, give rise to the mature proteins p50 and p52, respectively. All members share the Rel homology domain, which is necessary for DNA binding and dimerization (Hayden and Ghosh, 2008). NFκB members are sequestered in the cytoplasm by inhibitor molecules, the IκB family. Only upon the appropriate stimuli IκB is phosphorylated by one of the two kinases, IKKα or IKKβ and subsequently degraded in proteasomes. Released NFκB dimers translocate to the nucleus where they bind κB sites. They can bind promoter or enhancer regions and they can activate or repress transcription (Pahl, 1999). Additional regulation concerning affinity as well as binding to further transcription factors is provided by posttranslational modifications.

NFκB family members provide immune response upon viral or bacterial infections as well as inflammatory cytokines (Hayden and Ghosh, 2011). Additionally, the NFκB signalling pathway is activated upon physiological, physical and oxidative stress and it is involved in regulation of cell differentiation, proliferation and survival. Aberrant NFκB signalling leads to development of metabolic diseases, inflammatory diseases, autoimmune syndromes as well as cancer (Karin, 2006; Kumar et al., 2004).

Next to the tight regulation by sequestering in cytoplasm, NFκB signalling is kept under control by being involved in crosstalk with numerous signalling pathways, which

provide even more complex regulation. One of these pathways is p53 signalling (Schneider and Kramer, 2011). Transcription of Mdm2, which is known as a leading regulator of p53 protein stability, is activated by NFκB signalling (Tergaonkar et al., 2002). Additionally, there is a raising number of studies reporting that NFκB, especially its member p65 (RelA), is one of the mechanisms how p53 mutant gains an oncogenic function (Cooks et al., 2013).

It is already shown that p53 mutant can increase expression of NFκB targets in *in vitro* systems by direct protein-protein interaction (Schneider and Kramer, 2011). Additionally, mutant p53 promotes inflammation and inflammation-induced cancer by augmenting response of colon epithelial cells to the low amount of inflammatory cytokines and therefore provide chronic NFκB activation (Cooks et al., 2013). Cross-signalling between those two transcription factors becomes more and more appreciated as a mechanism active during all stages of tumourigenesis, metastasis formation and immune response (Wu and Zhou, 2010).

Still, it should be considered that the role of NFκB is not consistent. Lavon et al., showed that NFκB is activated in response to doxorubicin induced genotoxic stress and this activation occurred independently of p53 status. Furthermore, although p53 was also induced in this system, its induction is independent of NFκB (Lavon et al., 2003).

1.9 Chromatin organisation

In eukaryotic cells, the DNA molecule has to be organized in complex structures in order to be packed in the tiny nucleus with about 10 nm in diameter. The basic building block of DNA organization is the nucleosome, which has a precisely defined structure. It consists of 146 bp of two superhelical turns of DNA, wrapped around the histone core (Alberts B, 2012). Two nucleosomes are connected with roughly 50 bp long linker DNA. Histone core contains dimers of histones H2A, H2B, H3 and H4, which are organized in a coin-like structure but still have perturbing histone tails which are targets of intense posttranslational modifications (Kornberg and Lorch, 1999; Luger et al., 1997). Nucleosomes are further organized in solenoid-like, 30 nm broad fibres which are further involved in more complex levels of organization, finally leading to the compact chromosomes which are visible during mitosis (Alberts B, 2012).

Such a compact DNA still has to be accessible for the DNA-dependent processes such as transcription, DNA repair, and replication. For this to happen, chromatin remodelling complexes are necessary and they will be described in section 1.12.

1.10 Regulation of transcription – classical model

Transcription in eukaryotes starts by RNA polymerase II (Pol II) binding to the TATA box in the promoter upstream of the transcriptional start site. Pol II does not have intrinsic strong affinity for the promoter and therefore TATA binding proteins (TBP), TFIID complex and other general (basal) transcription factors are needed. Main characteristic of general TFs is that they do not bind in a sequence-specific manner but rather on every Pol II binding promoter (Alberts B, 2012).

Such assembled machinery can start transcription only when it interacts with the activators of transcription which are recruited to the promoter or enhancer – cis regulatory element that could be located far away from the promoter. This interaction is provided due to the activity of numerous protein complexes like for example high mobility group proteins (HMG), which are able to displace the nucleosomes to make DNA more flexible and perform looping of the DNA. By looping, transcriptional activators are brought into close proximity of the basal transcription machinery. Still, to connect these two complexes, co-activators are needed. They are part of the mediator complex and cannot bind the DNA but rather provide protein–protein interactions between activators and the basal complex (Alberts B, 2012).

Transcription factors can bind to the DNA in a sequence-specific manner but can also be recruited by other transcription factors or can be directed to certain regions by epigenetic marks (for instance, posttranslational modifications of histones) (Alberts B, 2012). Additionally, there are no universal activators or repressors in the cell. Every transcription factor regulates numerous genes and if it is going to act as an activator or repressor depends on the combination of the transcription factors available, rather than on isolated properties of one of them.

1.11 Regulation of transcription - 'Transcription factories' model

Classical models propose that members of the transcriptional machinery are recruited to the active genes. In contrast to this, more and more evidences argue that huge complexes of transcriptional regulators and Pol II ('transcription factories') are clustered and that the genes are dynamically recruited to the sites of active transcription and not *vice versa* (Osborne et al., 2004). It was reported that 'transcription factories' contain only one type of RNA Polymerase and are enriched in specific transcription factors involved in the transcription of specific group of genes (Bartlett et al., 2006). However, recent studies show that functionally unrelated transcription factors also cluster together and that almost all clustering sites are bound by cohesin (Yan et al., 2013). Cohesin is a large, ring-shaped molecule, which is able

to surround two DNA strands. Its main role is looping between enhancers and stabilization of TF binding (Faure et al., 2012; Kagey et al., 2010). For such a huge complex to access the DNA, nucleosomes have to be removed what is achieved by chromatin modifiers.

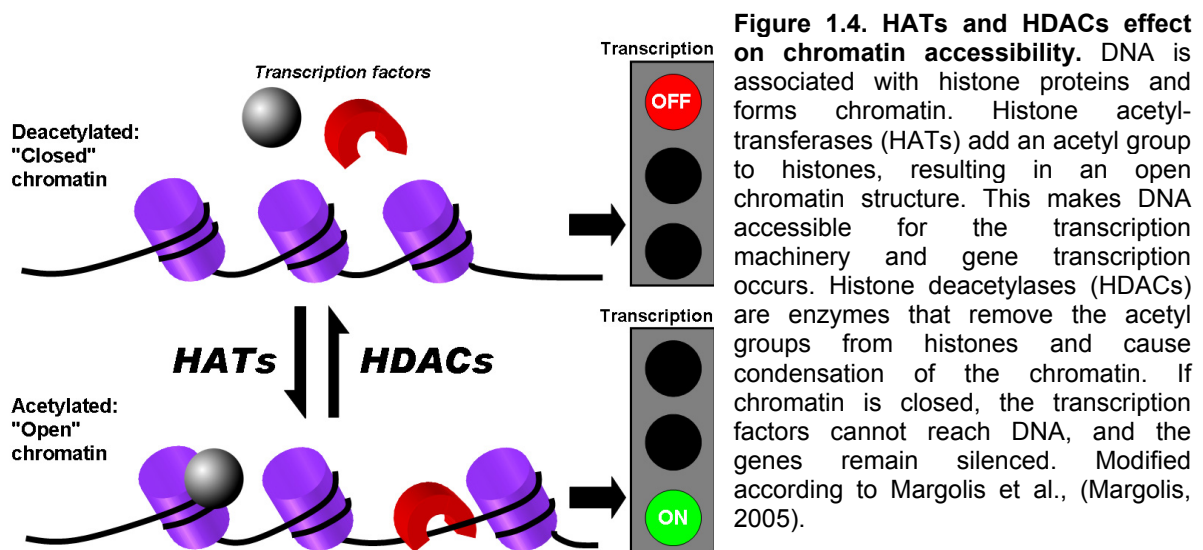
1.12 Epigenetic regulation of gene expression and the role of chromatin modifiers

Chromatin modifiers are enzymes, which are able to post-translationally alter histone proteins. Histones are mostly modified at the lysine (Lys) and arginine (Arg) residues of amino-terminal tails that protrude from the nucleosome (Alberts B, 2012). Still, some lysine residues within histone globular cores can undergo modifications like H3K56 (Das et al., 2009). In the last few decades, numerous histone modifications have been described, such as phosphorylation and ubiquitination, but the mostly investigated ones are histone methylation and acetylation.

Histone modifications can influence processes happening on the DNA molecule by manipulating the overall structure of the chromatin or by regulating binding of the effector molecules (Kouzarides, 2007).

Substrates for the protein methyltransferases are lysine and arginine residues in the histone tails but also in the histone core which can be mono-, di- or, in case of lysine residues, tri-methylated. Since it is small and electroneutral, methylation does not change chromatin structure directly, but mostly serves as a docking point for the proteins that are involved in histone assembly or regulatory proteins. These include PHD (Plant Homeo Domain) fingers and Tudor 'royal' family of domains (chromodomains, Tudor, PWWP (proline-tryptophan-tryptophan-proline) and MBT (malignant brain tumour) domains) (Kouzarides, 2007).

Acetylation of histones is controlled by balanced activity of histone acetyl transferases (HATs) and histone deacetylases (HDACs). HATs transfer acetyl groups to the lysine residues and neutralize positively charged histones. This further causes repulsion with already negatively charged DNA, uncoiling of the chromatin (euchromatin), and makes it physically accessible for the transcription machinery (Alberts B, 2012). Histone acetylated lysines are bound by bromodomains which are often possessed by HATs and chromatin remodelling complexes like Swi2/Snf2. Conversely, deacetylation of the histones by the HDACs leads to coiling of the DNA resulting in closed chromatin (heterochromatin) (Alberts B, 2012), like it is shown in the Figure 1.4.



Additional histone modifications are phosphorylation, ubiquitination, sumoylation, ADP-ribosylation, deimination, and β -N-acetylglucosamination (Kouzarides, 2007).

Individual histone modifications cannot be considered as isolated 'events'. There is rather a 'cross-talk' between them, which introduces additional levels of complexity and provides fine-tuned control of highly dynamic chromatin. Combinations of chromatin modifications provide the so-called 'histone code' which can serve as a recognition mark for the binding of numerous regulatory proteins (Turner, 2002).

Proteins which are involved in epigenetic regulation are usually part of large complexes which are able to read the 'histone code', edit it, and provide precise gene expression pattern which, as a final outcome, has appropriate cellular response. Those proteins can be grouped, according to the roles they have, into the 'writers', 'erasers' and 'readers' (Arrowsmith et al., 2012). Already mentioned histone acetylases and protein methyltransferases add acetyl or methyl groups on the lysine or arginine residues at the histone tails (writers). Bromodomain containing proteins bind acetylated lysins, while Tudor domains, MBT domains, chromodomains and PWWP domains containing proteins bind methyl marks on lysine or arginine residues (readers). Histone deacetylases and lysine demethylases remove those marks (erasers) (Arrowsmith et al., 2012).

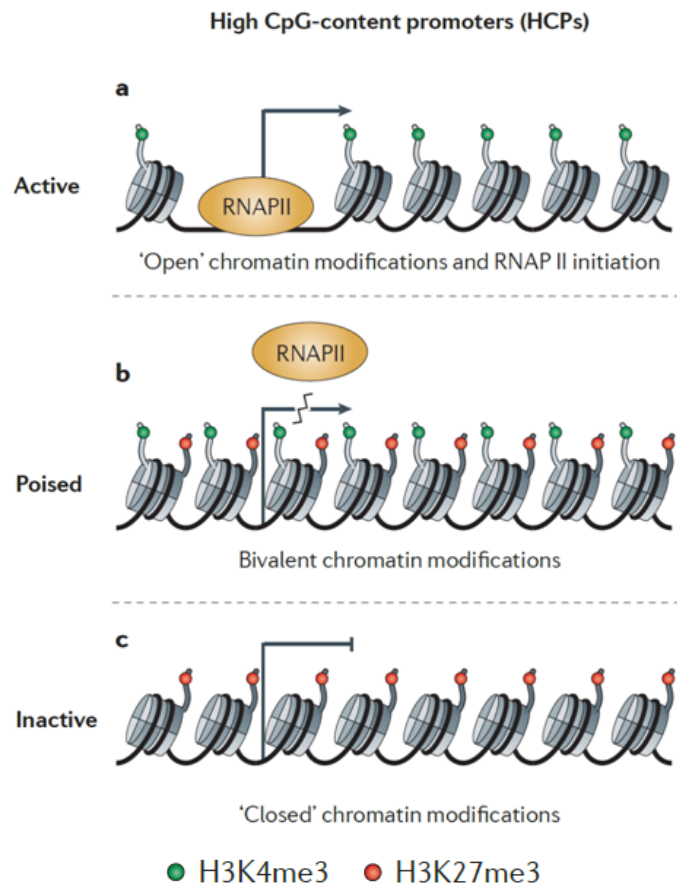


Figure 1.5 Chromatin patterns and status. Promoters are subject to distinct chromatin patterns and regulation. **a** - Active promoters are enriched for histone H3 lysine 4 trimethylation (H3K4me3). **b** - Poised promoters are marked by the bivalent combination of H3K4me3 and H3K27me3. **c** - Inactive promoters carry 'repressive' chromatin modifications such as H3K27me3 and are relatively inaccessible to RNAPII. Modified according to (Zhou et al., 2011).

Next to the active and inactive chromatin, genes can also have poised status. These genes are available for Pol II binding, but the transcription does not take place until appropriate signal comes (Guenther et al., 2007). This 'steady' state is typical for the genes that require fast response. All grades of chromatin, active, poised and repressed, are characterised by a specific pattern of histone modification. Overview of the common histone modification as well as the chromatin status is given in Figure 1.5.

1.13 Histone deacetylases as therapeutic targets in cancer disease

Although cancer is considered to be a consequence of genetic alterations which ultimately lead to aberrant gene expression, there is increasing evidence that the epigenome is widely changed in cancer. Next to the well-known increased methylation and resulting silencing of tumour suppressor genes, numerous histone marks are altered (Jones and Baylin, 2007). This changes are caused by the deregulation of chromatin modifiers and as an ultimate

consequence, inadequate gene expression occurs. One of the examples is the overexpression of class I HDACs in pancreatic ductal adenocarcinoma (Schneider et al., 2010).

Histone deacetylases are divided into five classes according to the homology with yeast proteins (Fig. 1.6): class I includes HDAC1, HDAC2, HDAC3 and HDAC8; class IIa includes HDAC4, HDAC5, HDAC7 and HDAC9; class IIb includes HDAC6 and HDAC10; class III includes the sirtuins SIRT1–SIRT7; and class IV contains HDAC11 (de Ruijter et al., 2003). Enzymes from classes I, II and IV require a bivalent metal ion for catalysis (Finnin et al., 1999). Sirtuins are structurally and biochemically unrelated to the other classes. They are NAD⁺ - dependent enzymes and next to the protein deacetylase they also have ADP-ribosylase activity (Sauve et al., 2006).

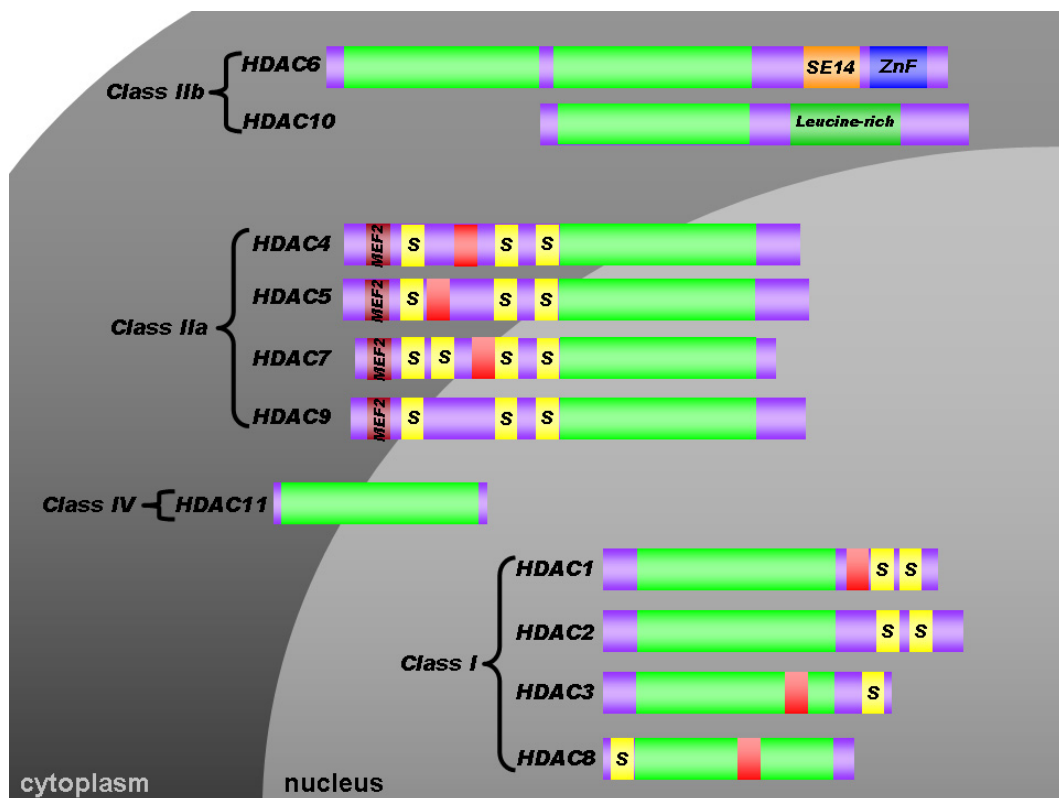


Figure 1.6. Schematic representation of metal-dependent HDAC's classification and localisation. Histone deacetylases are divided into five classes according to the homology with yeast proteins. Class I includes HDAC1, HDAC2, HDAC3 and HDAC8; class IIa includes HDAC4, HDAC5, HDAC7 and HDAC9; class IIb includes HDAC6 and HDAC10; and class IV contains HDAC11. The deacetylase catalytic domain (green), nuclear localization signal (red), myocyte enhancer factor 2 binding domain (violet), serine binding motif (yellow), SE14 - serine–glutamate tetradecapeptide, ZnF - zinc finger protein binding domain and leucine rich domain are depicted. Subcellular localization is shown. Modified after (Karagiannis and Ververis, 2012).

Two HDAC inhibitors (SAHA and romidepsin) are already approved for the treatment of cutaneous T cell lymphoma and are widely used in the clinic (Prince et al., 2009) (Grant et al., 2007). Numerous inhibitors like LBH-589, PXD101, MS275 and others are in different phases of clinical trials (Arrowsmith et al., 2012).

The main challenge for designing efficient HDAC inhibitors is their low specificity. They often target more than one HDAC and have lot of side effects. Hence, efforts are made to design HDAC inhibitors specific for individual HDACs. Still, one huge hurdle is the fact that HDACs are usually part of the vast complexes. Therefore, if the inhibitor is successful in blocking isolated HDAC, this does not guarantee that it will be equally efficient in inhibiting the very same HDAC as a part of the greater complex (Bantscheff and Drewes, 2012).

When adjusting chromatin condensation, the main targets of HDACs are histone proteins. Lately, more and more non-histone targets of HDACs are revealed (Glozak et al., 2005). This feature might be beneficial for use of HDACi for targeting hardly drugable molecules like sequence-specific transcription factors (c-MYC, p53) (Darnell, 2002). According to the data obtained so far, HDACi might not succeed as a monotherapy at the clinic but it is certain that they increase the efficacy of conventional and targeted therapies.

1.14 Aims of this work

p53 mutations have high frequency in pancreatic cancer. p53 mediates resistance towards conventional therapy, which is partly caused by new functions that p53 mutant gains. Thus, I recognised a need to investigate molecular background of p53^{R172H} gain of function. Therefore, I aimed to:

- 1) establish models for investigating p53^{R172H} gain of function. Those are: *in vivo* mouse model, *Pdx1-Flp; FSF-KRas^{G12D}; FSF-R26^{CAG-CreERT2}; LSL-p53^{R172H/lox}; R26^{mT/mG}*, in which mutant *p53* can be induced in a time-dependent manner specifically in pancreas; inducible *in vitro* systems - primary tumour cell lines and PDECs.
- 2) demonstrate a gain of function in *in vivo* models

Since NFκB signalling is highly involved in tumour development and maintenance I found it important to investigate the role of NFκB subunit p65 in different p53 backgrounds (p53^{R172H} or p53^{lox}). For this purpose, I aim to establish conventional *in vivo* model *Pdx1-Cre; LSL-KRas^{G12D}; LSL-p53^{R172H/lox}; LSL-p65^{lox/lox}*, as well as appropriate *in vitro* systems and to investigate:

- 3) p53^{R172H} dependency on p65.

I further aimed to investigate the role(s) of histone deacetylases in regulation of mutant p53. I've used the genetic approach (siRNA) as well as chemical inhibitor MS275, and HDAC1 and HDAC2 deficient mouse models of pancreatic cancer (*Pdx1-Cre;LSL-KRas^{G12D}; LSL-Hdac1^{lox/wt};LSL-Hdac2^{lox/lox} LSL-p53^{R172H/wt}*). I focused on the molecular mechanism of transcriptional regulation.

2 Materials

2.1 Technical equipment

Table 2.1. Technical Equipment

Instruments	Source
96-well magnetic ring-stand	Applied Biosystems Inc., Carlsbad, CA, USA
Analytical balance A120s	Sartorius AG, Goettingen
Autoclave 2540EL	Tuttnauer, Europe, B.V., EH BREDA, NL
Avanti J25 centrifuge	Beckman Coulter Inc., Brea, CA, USA
AxioCam MRc	Carl Zeiss AG, Oberkochen
AxioCam MRc	Carl Zeiss AG, Oberkochen
Biometra WT 18	Biometra GmbH, Göttingen
Bioruptor UCD – 200 TM	Diagenode s.a. Belgium, Europe, Liege, B
Centrifuge 5417R	Eppendorf AG, Hamburg
Centrifuge micro 220R	Hettich, Germany
CO ₂ incubator HERAcell 240	Thermo Fisher Scientific Inc., Waltham, MA, USA
CO ₂ incubator HERAcell	Heraeus Instruments GmbH, Osterode
Cryostat Microm HM560	Thermo Fisher Scientific Inc., Waltham, MA, USA
Dewar Carrying Flask, type B	KGW-Isotherm, Karlsruhe
Dual Gel Caster Hoefer	GE Healthcare Europe GmbH, Freiburg
Electrophoresis chamber WB Mighty Small II SE250	Hoefer Scientific Instruments San Francisco
Elektrophoresis-power supply PowerPac 200	Bio-Rad Laboratories GmbH, München
Elisa Plate reader Anthos 2001	Anthos Mikrosysteme GmbH, Krefeld
Eppendorf 5432 mixer	Eppendorf AG, Hamburg
FluoSTAR optima BMG	Labtech GmbH, Offenburg
Foil sealing instrument	Severin Electrogeraete GmbH, Sundern
Gel doc XR+ documentation system	Bio-Rad Laboratories GmbH, München
Gel electrophoresis chamber Sunrise	Biometra GmbH, Goettingen
Gene Amp PCR system 9700	Applied Biosystems Inc., Foster City, CA
Heated paraffin embedding module EG1150H	Leica Microsystems GmbH, Wetzlar
Hemocytometer (Neubauer improved)	LO-Laboroptik GmbH, Bad Homburg
HeraSafe biological safety cabinet	Thermo Fisher Scientific Inc. Waltham, MA, USA
Homogenizer Silent Crusher M with tool 6F	Heidolph Instruments GmbH, Schwabach
Horizontal gel electrophoresis system	Biozym Scientific GmbH, Hessisch Oldenburg
Incubator HERAcell 240	Thermo Fisher Scientific Inc., Waltham, MA, USA

Instruments	Source
Laminar flow HERAsafe	Heraeus Holding GmbH, Hanau
Leica EG 1150 H embedding system	Leica Mikrosysteme Vertrieb GmbH, Wetzlar
Luminometer Lumat LB 9501	Berthold Technologies GmbH, Bad Wildbad
Magnetic stirrer COMBIMAG IKAMAG	IKA-Werke GmbH, Staufen
Microliter syringe	Hamilton Bonaduz AG, Bonaduz, Switzerland
Microplate Photometer Anthos2001	Anthos Mikrosysteme GmbH, Krefeld
Microscope Axio Imager A1	Carl Zeis AG, Oberkochen
Microscope Axiovert 25	Carl Zeiss AG, Oberkochen
Microscope DM LB	Leica Mikrosysteme Vertrieb GmbH, Wetzlar
Microtome HM355S	Thermo Scientific, Walldorf
Microwave oven	Siemens, München
Mini-PROTEAN3 cell	Bio-Rad Laboratories GmbH, München
Multipette stream	Eppendorf AG, Hamburg
Odyssey infrared imaging system	LI-COR Bioscience Corporate, Lincoln, NE; USA
Paraffin tissue floating bath Microm SB80	Thermo Fisher Scientific Inc., Waltham, MA, USA
PCR cycler TPersonal/TGradient	Biometra biomedizinische Analytik GmbH, Göttingen
PCR-Thermocycler T-1	Biometra biomedizinische Analytik GmbH, Göttingen
pH meter 521	WTW Wissenschaftlich-Technische Werkstaetten GmbH, Weilheim
Pipettes Reference, Research	Eppendorf AG, Hamburg
Pipetus	Hirschmann Laborgeräte GmbH&CoKG, Eberstadt
Power supply E844, E822, EV243	Consort, Turnhout, Belgium
Power supply EPS601	GE Healthcare Europe GmbH, Freiburg
Precision balance Kern FTB	Gottlieb Kern & Sohn GmbH, Balingen-Frommerns
Schott Duran glass ware	Schott UK Ltd, Stafford, UK
Spectrophotometer ND-1000	PEQLAB Biotechnologie GmbH, Erlangen
StepOnePlus Real-Time PCR system	Applied Biosystems Inc., Carlsbad, CA, USA
Stereomikroskope Stemi SV11	Carl Zeis AG, Oberkochen
Stripettor Plus	Corning, Germany
Thermomixer compact	Eppendorf AG, Hamburg
Thermoshake	Gerhardt GmbH, Königswinter
Tissue infiltration system	Leica Microsystems GmbH, Wetzlar
VacuGene pump	GE Healthcare Europe GmbH, Freiburg

Instruments	Source
VacuGene XL	GE Healthcare Europe GmbH, Freiburg
Vortex Reax 2000	Heidolph Instruments GmbH, Schwabach
Vortex VF2	IKA-Werke GmbH, Staufen
Wallac MicroBetaTrilux 1450	PerkinElmer Inc., Waltham, MA, USA
Water bath 1003	GFL Gesellschaft für Labortechnik GmbH, Burgwedel
Western blot system SE 260 Mighty Small II	Hoefer Inc., Holliston, MA, USA
Wet blotting chambers (Mini Protean Tetra System)	Bio-Rad Laboratories GmbH, München
Zeiss LSM 510 Axiovert 100 microscope	Carl Zeiss AG, Oberkochen

2.2 Disposables

Table 2.2. Disposables

Disposable	Source
27-gauge needles	BD Bioscience, Franklin Lakes, NJ, USA
Amersham Hybond-N membrane	GE Healthcare Europe GmbH, Freiburg
Amersham micro columns Illustra ProbeQuant G-50	GE Healthcare Europe GmbH, Freiburg
Amersham Rediprime II DNA labelling system	GE Healthcare Europe GmbH, Freiburg
BioPur combitips	Eppendorf AG, Hamburg
Cell culture disposables	BD Bioscience, Franklin Lakes, NJ, USA; TPP Tissue Culture Labware, Trasadingen, CH; Sarstedt AG, Nuembrecht
Cell scrapers	TPP Tissue Culture Labware, Trasadingen, CH
Chromatography paper 3 mm	Whatman plc, Kent, UK
Combitips BioPur	Eppendorf AG, Hamburg
Cover slips	Menzel-Gläser, Braunschweig
Cryotubes	Nunc Brand Products, Naperville, IL, USA
Embedding cassettes	AMP Stensved, Denmark
Ethilon 5-0	Ethicon, Johnson&Johnson MEDICAL GmbH, Norderstedt
Express-Plus 0.22 µm Stericup	Millipore Corporate, Billerica, MA, USA
Feather disposable scalpel	Feather Safety Razor Co., Ltd, Osaka, Japan
Gene pulser/Micropulser cuvettes (0.2 cm gap)	Bio-Rad Laboratories GmbH, München
Glass Pasteur Pipette	Hirschmann Laborgeräte GmbH & Co KG, Eberstadt
Immobilon-P transfer membrane, PVDF	Millipore Corporate, Billerica, MA, USA

Disposable	Source
Kodak BioMax MS film	Sigma-Aldrich Chemie GmbH, Steinheim
MicroAmp optical 96-well reaction plate	Applied Biosystems Inc., Carlsbad, CA USA
Microtiterplate 96-well µclear white	Greiner Bio-One GmbH, Frickenhausen
Microtome blades S35 and	Feather Safety Razor Co, Ltd., Osaka, Japan
PCR reaction tubes	Eppendorf AG, Hamburg; Brand GmbH + Co.KG, Wertheim
Petri dishes	Sarstedt AG&Co., Nümbrecht
Phase lock gel light tubes	5' prime GmbH, Hamburg
Plastic foil	Rische + Herfurth GmbH, Hamburg
Polystyrene tubes (round-bottom)	Sarstedt AG, Nümbrecht
Reaction tubes 1.5 and 2 mL	Eppendorf AG, Hamburg
Safe-lock reaction tubes BioPur	Eppendorf AG, Hamburg
Serological pipettes	BD Bioscience, Franklin Lakes, NJ, USA
Single use needles Sterican 27 gauge	B. Braun Melsungen AG, Melsungen
Single use syringes Omnifix	B. Braun Melsungen AG, Melsungen
Sterile pipet tips	Biozym Scientific GmbH, Hessisch Oldendorf
Superfrost Plus glass slides	Menzel-Gläser, Braunschweig
Syringe filter Filtropur S 0,2	Sarstedt AG, Nuembrecht
Wound clips	MEDICON eG, Tuttlingen

2.3 Reagents and enzymes

Table 2.3. Reagents and enzymes

Reagent	Source
1 kb extension ladder	Invitrogen GmbH, Karlsruhe
2log DNA ladder	New England Biolabs, Frankfurt
3-(4,5-deimethylthiazol-2-yl)-2,5-diphenyl tetrazolium bromide (MTT)	Carl Roth GmbH, Karlsruhe
3,3',5-Triiodo-L-thyronine	Sigma-Aldrich Chemie GmbH, Steinheim
4-hydroxytamoxifen (4-OHT)	Sigma-Aldrich Chemie GmbH, Steinheim
Agarose	PEQLAB Biotechnologie GmbH, Erlangen
Ammonium - persulphate	Sigma-Aldrich Chemie GmbH, Steinheim
BBXF agarose gel loading dye mixture	BIO 101, Inc. Carlsbad, CA, USA
Blotting grade blocker non fat dry milk	Bio-Rad Laboratories GmbH, München
Bovine Pituitary Extract	BD Biosciences, Franklin Lakes, NJ, USA
Bovine serum albumin fraction V	Sigma-Aldrich Chemie GmbH, Steinheim

Reagent	Source
Bradford reagent, 5x	Serva Electrophoresis GmbH, Heidelberg
Bromphenol blue	Sigma-Aldrich Chemie GmbH, Steinheim
Chloroform	Carl Roth GmbH + Co.KG, Karlsruhe
Cholera toxin	Sigma-Aldrich Chemie GmbH, Steinheim
Collagen	BD Biosciences, Franklin Lakes, NJ, USA
Collagenase typeV	Sigma-Aldrich Chemie GmbH, Steinheim
Complete protease inhibitor cocktail tablets, EDTA free	Roche Diagnostics Deutschland GmbH, Grenzach-Wyhlen
Dexamethasone	Sigma-Aldrich Chemie GmbH, Steinheim
D-Glucose	Sigma-Aldrich Chemie GmbH, Steinheim
Dimethylsulfoxide (DMSO)	Carl Roth GmbH + Co.KG, Karlsruhe
DNase I	Qiagen GmbH, Hilden
dNTP mix, 10mM each	Fermentas GmbH, St. Leon-Rot
Dodecylsulphate Na-salt in pellets (SDS)	Serva Electrophoresis GmbH, Heidelberg
Dulbecco's phosphate buffered saline, powder	Biochrom G, Berlin
Epidermal Growth Factor	BD Biosciences, Franklin Lakes, NJ, USA
Ethanol, 100%	Merck KGaA, Darmstadt
Ethidium bromide (10 mg/mL)	Sigma-Aldrich Chemie GmbH, Munich
Etoposid	EMD Biosciences, San Diego, USA
Etoposide, Calbiochem	Merck KGaA, Darmstadt
Forene isoflurane	Abbott GmbH & Co.KG, Ludwigshafen
Fungizone	Invitrogen GmbH, Karlsruhe
GDP (10x)	Millipore Corporate, Billerica, MA, USA
Gel Loading Dye, 6X	New England Biolabs, Frankfurt
Glycerol	Sigma-Aldrich Chemie GmbH, Steinheim
Glycin	Carl Roth GmbH, Karlsruhe
HBSS	Invitrogen GmbH, Karlsruhe
HCl	Carl Roth GmbH, Karlsruhe
HEPES	Sigma-Aldrich Chemie GmbH, Steinheim
Hoechst 33342	Sigma-Aldrich Chemie GmbH, Steinheim
HotStarTaq DNA polymerase	Qiagen GmbH, Hilden
Isofluran Forene	Abbott GmbH, Wiesbaden
Isopropanol	Carl Roth GmbH, Karlsruhe
ITS+Premix	BD Biosciences, Franklin Lakes, NJ, USA
Magnesium-chloride	Carl Roth GmbH, Karlsruhe

Reagent	Source
Metacarn	Boehringer Ingelheim Pharma GmbH, Ingelheim am Rhein
Methanol	Carl Roth GmbH, Karlsruhe
Mitomycine C	ApliChem, Germany
Mouse diet LASCRediet CerActive TAM400	LaSvendi GmbH, Soest
MS275 (Entinostat)	LC Laboratories, Woburn, USA
Na-Acetate	Sigma-Aldrich Chemie GmbH, Steinheim
NaCl	Merck KGaA, Darmstadt
NaOH	Carl Roth GmbH, Karlsruhe
Nicotinamide	Sigma-Aldrich Chemie GmbH, Steinheim
Nonidet NP-40	Sigma-Aldrich Chemie GmbH, Steinheim
Nu-SerumIV	BD Biosciences, Franklin Lakes, NJ, USA
Nutlin -3	Cayman Chemical, Ann Arbor, MI, USA
Odyssey blocking reagent	LI-COR Corp. Offices, Lincoln, NE, US
PageRuler™ Prestained Protein Ladder	Thermo Scientific
Paraformaldehyde, 37%	Sigma-Aldrich Chemie GmbH, Steinheim
Penicilin/Streptomycin	Invitrogen GmbH, Karlsruhe
Phosphatase inhibitor mix I	Serva Electrophoresis GmbH, Heidelberg
Phosphatase inhibitor set	Roche Diagnostics Deutschland GmbH, Mannheim
PI-103	Selleck Chemicals LLC, Houston, TX, USA
Polyethylenimine (PEI)	Sigma-Aldrich Chemie GmbH, Steinheim
Power SYBR Green PCR master mix	Applied Biosystems, Warrington, UK
Proteinase K, recombinant, PCR grade	Roche Diagnostics Deutschland GmbH, Grenzach-Wyhlen
REDTaq ReadyMix PCR reaction mix	Sigma-Aldrich Chemie GmbH, Steinheim
RnaseA	Fermentas GmbH, St. Leon-Rot
Roti – Histofix, 4%	Carl Roth GmbH, Karlsruhe
Roti Phenol/Chloroform/Isoamyl-alcohol	Carl Roth GmbH, Karlsruhe
Rotiphorese Gel 30	Carl Roth GmbH, Karlsruhe
SAHA	Cayman Chemical, Ann Arbor, MI, USA
Saponin	Sigma-Aldrich Chemie GmbH, Steinheim
Sodiumdeoxycholate	Sigma-Aldrich Chemie GmbH, Steinheim
Soybean Trypsin Inhibitor type I	Sigma-Aldrich Chemie GmbH, Steinheim
SuperScript II reverse transcriptase	Invitrogen GmbH, Karlsruhe
Tamoxifen	Sigma-Aldrich Chemie GmbH, Steinheim
TEMED	Carl Roth GmbH, Karlsruhe

Reagent	Source
TO-PRO3-iodid	Invitrogen GmbH, Karlsruhe
TrisHCl	Carl Roth GmbH, Karlsruhe
TritonX-100	Sigma-Aldrich Chemie GmbH, Steinheim
Trypsin-Inhibitor	Sigma-Aldrich Chemie GmbH, Steinheim
Tween-20	Carl Roth GmbH, Karlsruhe
Vectashield mounting medium with DAPI	Vector Laboratories, Burlingame, CA, USA
X-Gal	Melford Laboratories, Chelsworth, Ipswich, UK
β -Mercaptoethanol	Sigma-Aldrich Chemie GmbH, Steinheim

2.4 Kits

Table 2.4. Kits

Kits	Source
Ambion WT expression kit	Applied Biosystems, Inc., Carlsbad, CA, USA
Caspase-Glo 3/7 Assay	Promega GmbH, Mannheim
Gene Chlp poly-A RNA control kit	Affymetrix, Inc., Santa Clara, CA, USA
Gene Chlp WT terminal labeling kit	Affymetrix, Inc., Santa Clara, CA, USA
GeneChip mouse gene 1.0 St array	Affymetrix, Inc., Santa Clara, CA, USA
One-Cycle Target Labeling and Control Reagents	Affymetrix, Inc., Santa Clara, CA, USA
QIASchredder	Qiagen GmbH, Hilden
RNAse – free DNase set	Qiagen GmbH, Hilden
RNeasy Mini kit	Qiagen GmbH, Hilden
SimpleChIP Enzymatic Chromatin IP Kit (Magnetic Beads)	Cell Signaling Technology, Inc., Danvers, MA, USA

2.5 Antibodies

Table 2.5 Antibodies

Antibody	Source
AlexaFluor680 goat anti-mouse IgG (#A21058)	Invitrogen GmbH, Karlsruhe
AlexaFluor 680 goat anti-rabbit IgG (#A21076)	Invitrogen GmbH, Karlsruhe
Anti-AcH3 (rabbit) #06-599	Upstate/Millipore Corporate, Billerica, MA, USA
Anti-c-myc sc-764	Santa Cruz Biotechnology, Inc., Heidelberg
Anti-H3K27Ac (rabbit) #8173	Cell Signaling Technology, Inc., Danvers, MA, USA
Anti-H3K27Me3 - C36B11 (rabbit) #9733	Cell Signaling Technology, Inc., Danvers, MA, USA

Antibody	Source
Anti-H3K4Me3 (C42D8) 9751s	Cell Signaling Technology, Inc., Danvers, MA, USA
Anti-H3K9Me1 (mouse) CS200549	Millipore Corporate, Billerica, MA, USA
Anti-H3K9Me3 (rabbit) 9754	Cell Signaling Technology, Inc., Danvers, MA, USA
Anti-HDAC1, 05-614	Upstate/Millipore Corporate, Billerica, MA, USA
Anti-HDAC2 rabbit H54 sc-7899	Santa Cruz Biotechnology, Inc., Heidelberg
Anti-HDAC3 rabbit, 06-890	Upstate/Millipore Corporate, Billerica, MA, USA
Anti-HDAC8 rabbits c-11405	Santa Cruz Biotechnology, Inc., Heidelberg
Antimouse IgG(H+L) DyLight (R) 680, Conjugate	Cell Signaling Technology, Inc., Danvers, MA, USA
Anti-p53 DO1 mouse	Santa Cruz Biotechnology, Inc., Heidelberg
Anti-p65 C-20 rabbit	Santa Cruz Biotechnology, Inc., Heidelberg
Anti-Pol II N20 (rabbit) sc-899	Santa Cruz Biotechnology, Inc., Heidelberg
Antirabbit IgG(H+L) DyLight (R) 680, Conjugate	Cell Signaling Technology, Inc., Danvers, MA, USA
Anti-survivin D-8 mouse	Santa Cruz Biotechnology, Inc., Heidelberg
Anti- β -Actin (mouse) (#A5316)	Sigma-Aldrich Chemie GmbH, Steinheim
CTCF – C20 (goat) sc-15914	Santa Cruz Biotechnology, Inc., Heidelberg
Ezh2 (D2C9) #5246	Cell Signaling Technology, Inc., Danvers, MA, USA
Novocastra Anti-p53 CM5 (Rabbit)	Leica Byosystems, UK

2.6 Primers

All primers were synthesized by MWG (sequencing, real-time PCR) or Operon (cloning). If not stated otherwise, genotyping primer pairs are used for genomic tail PCR.

Table 2.6. Primers

<i>Primers for quantitative real time PCR</i>		
Name of PCR	Name of primer	Sequence (5'-3')
Cyclophin, murine	Cyclophilin F6 CyclophinR16	ATGGTCAACCCCACCGTG T TCTGCTGTCTTTGGGACCTTGTC
Cyclophilin, human	Cycloph FW Cycloph REV	ATGGTCAACCCCACCGTGT TCTGCTGTCTTTGGGACCTTGTC
Bcl6	mBcl6 FW mBcl6 REV	TCAAGGCCAGTGAAGCAGAA TCCGGCTGTTCAGGAACTCT
p53 human	p53fw p53rev	ATG TGC ACG TAC TCT CCT CC AGC CAG GCC ATC ACC ATC

Primers for quantitative real time PCR		
p53 murine	mp53986 FW mp1217 REV	AGAGACCGCCGTACAGAAGA CTGTAGCATGGGCATCCTTT
WRAP53 1 α , human	huWRAP53 1alfa FW huWRAP53 1alfa REV	CGGAGCCCAGCAGCTACC TTGTGCCAGGAGCCTCGCA
WRAP53 total human	huWRAP53 ex3-4 FW huWRAP53 ex3-4 REV	GACGGTTCCTGCATCTTGAC GACAGGGACCATTCTGCAT
HDAC1	mHDAC1 fw mHDAC1 rev	CTGAATACAGCAAGCAGATGCAGAG TCCCGTGGACAACACTGACAGAAC
Primers for ChIP		
Name of PCR	Name of primer	Sequence (5'-3')
p53 TSS	hp53TSSfw hp53TSSrev	CCAGTCTTGAGCACATGGGA GTCCAGCTTTGTGCCAGGA
p53 Prom1	hp53prom1fw hp53prom1rev	TCCTTCACAACCCTTATCACTCT GGCTTACGTTTCCATGTACTGA
p53 Prom2	hp53prom2fw hp53prom2rev	CTAGGGCTTGATGGGAACGG TTCGGTCCACCTTCCGATTG
p53 Prom3	hp53prom3fw hp53prom3rev	TCCTTCAGACCAGGACCCAG TGGCATCAGTTCAGAGTCCG
p53 Prom4	hp53prom4fw hp53prom4rev	AGATACCTCTGGGGAACCCG TCTCCCAGACTCCCACTC
p53 Prom5	hp53prom5fw hp53prom5rev	TCAGCCCTAGCCCTACACTT CCGTCAGGAGCCCTAGAAAC
p53 Exon1	hp53ex1fw hp53ex1rev	TGTCACCGTCGTGGAAAGC AAAGTCTAGAGCCACCGTCC
p53 Intr1-1	hp53intr1-1fw hp53intr1-1rev	AAGCTCCACTCCTCTGCCTA ACTTAGCGAGTTTGGGGGTG
p53 Intr1-2	hp53intr1-2fw hp53intr1-2rev	GTGCATGGGAAGAACTGCG GTTCTTCTGGTAGGAGGCG
p53 Intr1-3	hp53intr1-3fw hp53intr1-3rev	CAAGCGATTCTCCTGCCTCA CGGGCGGATTACTTGAGGAT
p53 Intr1-4	hp53intr1-4fw hp53intr1-4rev	TGGCCAATAGGCACATGAAAA ACAGCCTTCCGGACATTAGG
p53 Intr1-5	hp53intr1-5fw hp53intr1-5rev	AGGCAAGCAACAGATCAGAAGA TGTTCAAGTTGTGGGACTGCT
p53 Exon2	hp53ex2fw hp53ex2	GCTCGACGCTAGGATCTGAC CCCAGGGTTGGAAGTGTCTC
p53 3'UTR	3UTR-2 fw 3UTR-2 rev	AATCCTTGGTGAGAGGCTGC GCACAAGGTTCTCTCCCTCC

Primers for genotyping		
Name of PCR	Name of primer	Sequence (5'-3')
LSL-Kras ^{G12D}	Kras-UP1-WT	CACCAGCTTCGGCTTCCTATT
	Kras-URP- LP1	AGCTAATGGCTCTCAAAGGAATGTA
	KrasG12Dmut-UP	CCATGGCTTGAGTAAGTCTGC
LSL-Trp53 ^{R172H}	Trp53R172H-WT-UP2	AGCCTTAGACATAACACACGAACT
	Trp53R172H-URP-LP	CTTGGAGACATAGCCACACTG
	Trp53R172H-mut UP4	GCCACCATGGCTTGAGTAA
FSF-Stop	pGL3-pA-pause-4645-UP	CTTTATGTTTTTGGCGTCTTCC
	Cre-neu-LP	CCTGGAAAATGCTTCTGTCCG
LSL-Rosa26TVA-lacZ	R26-Tva-GT-UP	AAAGTCGCTCTGAGTTGTTAT
	R26-Tva-GT-SA-mut-LP	GCGAAGAGTTTGTCTCAACC
	R26-Tva-GT-WT-LP	GGAGCGGGAGAAATGGATATG
LSL-p53 ^{lox}	p53-A-berns	CACAAAAACAGGTTAAACCCAG
	p53-B-berns	AGCACATAGGAGGCAGAGAC
Pdx1Flp	pdx5utr-scUP	AGAGAGAAAATTGAAACAAGTGCAGGT
	Flpopt-scLP	CGTTGTAAGGGATGATGGTGAAC
	Gabra-UP	AACACACACTGGAGGACTGGCTAGG
	Gabra-LP	CAATGGTAGGCTCACTCTGGGAGATGATA
R26 ^{CreERT2}	Cre-ER-T2-sc-UP3	GAATGTGCCTGGCTAGAGATC
	Cre-ER-T2-sc-LP1	GCAGATTCATCATGCGGA
FSF-Kras ^{G12D}	Kras-WT-UP1	CACCAGCTTCGGCTTCCTATT
	Kras-URP-LP1	AGCTAATGGCTCTCAAAGGAATGTA
	R26-Tva-SA-mut-LP	GCGAAGAGTTTGTCTCAACC
R26-td-EG	CAG-sc-LP	GTACTTGGCATATGATACACTTGATGTAC
	R26-Tva-GT-UP	AAAGTCGCTCTGAGTTGTTAT
	R26-Tva-GT-WT-LP	AAAGTCGCTCTGAGTTGTTAT
R26-FSF-CAG	R26-td-E-mutLP	TCAATGGGCGGGGGTCGTT
	R26-Tva-GT-UP	AAAGTCGCTCTGAGTTGTTAT
	R26-Tva-GT-WT-LP	AAAGTCGCTCTGAGTTGTTAT
Pdx1Cre	Cre-neu-UP	CCTGGAAAATGCTTCTGTCCG
	Cre-neu-LP	CAGGGTGTTATAAGCAATCCC
	Gabra1-UP	AACACACACTGGAGGACTGGCTAGG
	Gabra1-LP	CAATGGTAGGCTCACTCTGGGAGATGATA
p65 ^{lox}	P65-loxp-1:	GAGCGCATGCCTAGCACCAG
	P65-loxp-2:	GTGCACTGCATGCGTGCAG

Primers for genotyping		
HDAC1 ^{lox}	H1_EX3_UP	AATTCCTGCGTTCTATTGCGC
	H1_IN3-WT_LP	CACAGGAGCCCTAACTGGACAAG
	H1_IN3_LP1 (postloxp2)	AAGAGCATGAACTGATGGCGAG
HDAC ^{wt}	HDAC2 lox WT_UP (In1)	GCACAGGCTACTACTGTGTAGTCC
	HDAC2 lox rev (WT_In1)	CCACCACTGACATGTACCCAAC
HDAC2 ^{mut}	HDAC2 lox MT_UP (post-loxp1)	GTCCCTCGACCTGCAGGAATTC
	HDAC2 lox rev (WT_In1)	CCACCACTGACATGTACCCAAC

2.7 siRNA

Table 2.7. siRNAs

Target	Sequence
SDI	CAGUCGCGUUUGCGACUGG
siHDAC1a	GUGCUGUGAAGCUUAAUAA
siHDAC1b	GUACCACAGUGAUGACUAC
siHDAC2a	CUUGCCAUUGCUGAUGCUC
siHDAC2b	CGAGCAUCAGACAAACGGUAU
siHDAC3a	GAAGAUGAUCGUCUUCAAG
siHDAC3b	GAGCCUUAUUGCCUUCAAC
siip65-144	GAUCAUUGGCUACACAGGA

2.8 Buffers

All buffers were prepared with bidestilled H₂O.

Table 2.8. Buffers

Buffer	Component
Blocking buffer	5% skim milk powder 0,1% TWEEN in PBS
Concentrating gel buffer	0.5 M Tris, adjusted to pH 6.8 with HCl
G solution	500 ml HBSS 4 ml Penicilin/Streptomycin 5 ml Fungizone 0,45 g Glucose 200 µl 0,119 M CaCl ₂
Gitschier's Buffer, 10x	670 mM TRIS pH 8.8

	166 mM (NH ₄) ₂ SO ₄ 67 mM MgCl ₂
Buffer	Component
IP buffer, pH 7.9	50 mM HEPES 150 mM NaCl 1 mM EDTA 0,5% Nonidet 540 10% Glycerol Phosphatase inhibitor (add prior to use) Protease inhibitor (add prior to use)
PCR lysis (Soriano)	0.5% Triton X-100 1% β-Mercaptoethanol 10% 10x Gitschier's buffer 400 µg/mL proteinase K (add prior to use)
Protein loading buffer pH 6.8 (Laemmli buffer), 5x	10% SDS 50% glycerol 228 mM TrisHCl 0.75 mM bromphenol blue 5% β-mercaptoethanol
Running buffer, 10x	25 mM TrisHCl 192 mM glycine 0.1% SDS
Separating gel buffer	1.5 M Tris adjusted to pH 6.8 with HCl
Transfer buffer	192 mM glycine 0.1% SDS 20% methanol M TrisHCl

2.9 Histochemistry Reagents

Table 2.9. Histochemistry reagents

Reagent	Source
Acetic acid (glacial)	Merck KGaA, Darmstadt
Alcian blue 8GX	Sigma-Aldrich Chemie GmbH, Munich
Alcian blue, pH 2.5	1% Alcian blue+3% Acetic acid
Aluminium sulfate	Honeyell Specialty Chemicals Seelze GmbH, Seelze
Antigen unmasking solution, citric acid based	Vector Laboratories, Burlingame, CA, USA
Avidin/Biotin blocking kit	Vector Laboratories, Burlingame, CA, USA
Biotinylated anti-rabbit IgG (H+L)	Vector Laboratories, Burlingame, CA, USA
DAB peroxidase substrate kit , 3,3'-diaminobenzidine	Vector Laboratories, Burlingame, CA, USA

Eosin	Waldeck GmbH & Co KG, Münster
Reagent	Source
Goat serum (G9023)	Sigma-Aldrich Chemie GmbH, Munich
H ₂ O ₂	Merck KGaA, Darmstadt
Haematoxylin	Merck KGaA, Darmstadt
Pertex mounting medium	Medite GmbH, Burgdorf
Roti Histofix (4%)	Carl Roth GmbH + Co. KG, Karlsruhe
Roti Histol	Carl Roth GmbH + Co. KG, Karlsruhe
Saccharose	Merck KGaA, Darmstadt
Vectashield mounting medium with DAPI	Vector Laboratories, Burlingame, CA, USA
Vectastain Elite ABC solution	Vector Laboratories, Burlingame, CA, USA

2.10 Cell lines

Table 2.10. Cell lines

Cell line	Source
MiaPaCa2	ATCC, Manassas, VA, USA
Panc1	ATCC, Manassas, VA, USA
PaTu8988t	ATCC, Manassas, VA, USA

2.11 Cell culture reagents

Table 2.11. Cell culture reagents

Reagent	Source
3,3',5-Triiodo-L-thyronine	Sigma-Aldrich Chemie GmbH, Munich
Bovine Pituitary Extract	BD Biosciences, Franklin Lakes, NJ, USA
Cholera toxin	Sigma-Aldrich Chemie GmbH, Munich
Collagenase type 2 and 4	Worthington, Biochemical Corporation, Lakewood, NJ, USA
Collagen Type I	BD Biosciences, Franklin Lakes, NJ, USA
Dexamethasone	Sigma-Aldrich Chemie GmbH, Munich
DMEM/F12 medium	Invitrogen GmbH, Karlsruhe
Dulbecco's modified eagle medium (D-MEM) with L-glutamine	Invitrogen GmbH, Karlsruhe
Dulbecco's phosphate buffered saline (PBS)	Invitrogen GmbH, Karlsruhe
Epidermal Growth Factor	BD Biosciences, Franklin Lakes, NJ, USA
Fetal calf serum (FCS)	Biochrom AG, Berlin

ITS+Premix BD Biosciences, Franklin Lakes, NJ, USA

Reagent	Source
Nicotinamide	Sigma-Aldrich Chemie GmbH, Munich
Non-essential amino acids (100x)	Invitrogen GmbH, Karlsruhe
Nu-SerumIV	BD Biosciences, Franklin Lakes, NJ, USA
OptiMEM	Invitrogen GmbH, Karlsruhe
Penicillin-Streptomycin	Invitrogen GmbH, Karlsruhe
Sodium pyruvate	Invitrogen GmbH, Karlsruhe
Soybean Trypsin Inhibitor type I	Sigma-Aldrich Chemie GmbH, Munich
Trypsin-EDTA	Invitrogen GmbH, Karlsruhe

2.12. Cell culture media

Table 2.12. Cell culture media

Medium	Composition
Freezing Medium	70% DMEM 20% FCS 10% mL DMSO
Tumor cell/cell line medium	DMEM 10% FCS 1% Penicillin-Streptomycin
DMEM/F12 full medium – Medium for primary ductal epithelial cells	500 ml DMEM/F12 medium (15mM HEPES, 3.2 mg/ml glucose, phenol red) 2,5 mg D-Glucose (5mg/ml, RT) 50 mg Soybean Trypsin Inhibitor type I (0,1 mg/ml) 2,5 ml ITS+Premix 12,5 mg Bovine Pituitary Extract (25mg/ml) 100 µl Epidermal Growth Factor 50 µl 3,3',5-Triiodo-L-thyronine (5nM) 5 µl Dexamethasone (1µM) 0,61 g Nicotinamide (1.22mg/ml) 25 ml Nu-SerumIV (5%) 50 µl Cholera toxin (100ng/ml) 5 ml Penicillin/Streptomycin (1x)

3 Methods

If not stated different, the procedures were carried out according to manufacturer's protocol.

3.1 Cell Culture

All the cells were cultured under sterile conditions in a laminar flow bench. Cells were cultivated in appropriate media (Table 2.12) at 37°C and 5% CO₂.

3.1.1 Isolation, handling and cryopreservation of pancreatic tumour cells

Isolation of the murine primary tumour cells was done under sterile conditions. During dissection of the animal, pancreatic tumour was sampled from the 2 or 3 different regions of the pancreas. Three mm diameter pieces were placed in a 10 cm culture dish with a sterile PBS. The dish was transferred into a laminar flow bench, sliced into tiny peaces with scalpel and resuspended in 5 ml of tumour cell medium with 200 U/ml of collagenase type II. After 24 h of incubation at 37°C, cells were centrifuged for 5 min at the 1100 rpm. Supernatant was discarded and the cells again resuspended in 5 ml of tumour cell medium and placed into 25 cm² flask for further culturing.

Isolated tumour cells and human pancreatic cancer cell lines Panc1 and PaTu8988t were regularly supplied with fresh pre-warmed media. When reaching 80% confluence, cells were passaged. To passage them, cells were washed with sterile PBS, trypsinised 2-5 min at 37 °C and the portion of the cells transferred into a new vessel with a fresh medium. Cell numbers were determined using Neubauer hemocytometer.

For long-term storage, cells were frozen in liquid nitrogen. Upon trypsinisation, cells were resuspended in fresh medium and centrifuged at 1000 rpm for 5 min. Supernatant was discarded, the pellet was resuspended in ice-cold freezing medium and stored at –80°C for 24h and then transferred to liquid nitrogen.

3.1.2 Isolation, handling and cryopreservation of pancreatic ductal epithelial cells (PDECs)

Mice were dissected as explained in the section 3.2.3. As fast as possible, pancreas was removed without traces of any other tissue. Approximately half of the organ was fixed in

paraformaldehyde (PFA) and used for the histology analysis. The other half was placed into the glass flask with 5 ml of G solution (section 2.8) and used for isolation of PDECs. The dish was transferred to the laminar flow bench, where the tissue was sliced with scissors into tiny pieces. Another 20 ml of G solution was added, flask was swirled and left for few seconds so that pancreatic tissue can precipitate. The floating fatty tissue was carefully removed with glass Pasteur pipette. This washing step was repeated twice.

Sterile filtered collagenase solution (25 ml) was added and the tissue was incubated in the closed flask for 20 minutes at 37°C on the magnetic stirrer. Collagenase was inactivated by adding G solution. Tissue was transferred to 50 ml tube and centrifuged for 5 min at 1000 rpm. Supernatant was then removed. Cells were resuspended in 2 ml of trypsin and incubated at room temperature (RT) for 2 min. Digestion was stopped by adding 5 ml of trypsin inhibitor. Then, G solution was added up to 50 ml. Cells were centrifuged (5 min, 1000 rpm), supernatant was removed and pellet resuspended in 25 ml of DMEM/F12 (full medium (Table 2.12)). After one more centrifugation and removal of the supernatant, cells were resuspended in 12 ml of DMEM/F12 with fungisone and carefully plated on the 6-well collagen plates.

Upon reaching 80% confluence, cells were passaged. Medium was carefully removed from the plates. The cells with collagen were transferred to 50 ml of collagenase solution and incubated at 37°C until the collagen was totally resolved. Cells were then centrifuged for 5 min at 1000 rpm, supernatant was removed and pellet resuspended in 1 ml of trypsin and incubated for 5 min at RT. Reaction was stopped by resuspending the suspension in 2 ml of trypsin inhibitor. DMEM/F12 medium was added up to 20 ml, cells resuspended and centrifuged (5 min, 1000 rpm). Supernatant was removed, cells resuspended in 30 ml of DMEM/F12, and carefully plated on three 10 cm collagen-coated plates. For long-term storage, cell pellets were resuspended in DMEM/F12 with 5% DMSO and frozen at -80 °C. After 24h, cells were transferred to liquid nitrogen.

3.1.3 siRNA transfection

siRNA mediated knock down was performed according to the protocol previously described by our group (Wirth et al., 2011). Cells were seeded in 6 well plates (50.000 cells/well). On the next day, medium is replaced with 800 µl of serum-free medium. Two µl of transfection reagent polyethylenimin (PEI) were diluted in 598 µl of Optimem medium (Mix1) and incubated for 5 min. Two and half µl of siRNA were diluted in 597.5 µl of Optimem (final conc. 100 nM; Mix2). Six hundred µl of Mix1 was added to Mix2, incubated for 20 min and applied onto the cells. On the next day medium was replaced with DMEM/F12 full medium (with

FCS). After 48 or 72 hours, cells were harvested for protein or RNA isolation. Volumes refer to the 1 well of 6-well plate.

3.1.4 MTT Assay

MTT assay was used to determine cell viability (Mosmann, 1983). This assay is based on colorimetric reaction in which MTT (3-(4,5-Dimethylthiazol-2-yl)-2,5-diphenyltetrazolium bromide) is reduced to a purple formazan by mitochondrial reductase. In each well of 96 wells microplate, 5000 cells were seeded. On the next day, cells were treated with MS275 or with SAHA and cell viability was determined after 24, 48 or 72h. In each well, 10 μ L of MTT reagent (5 mg/mL MTT in PBS) per 100 μ L of cell medium were added and plates were incubated at 37 °C for 4h. Next, medium was carefully removed, cells lysed in 200 μ L of DMSO:EtOH (1:1), incubated at RT on the shaker for 10 min and OD determined at 600 nm wavelength. Analysis of the three technical replicates in three independent experiments were performed.

3.1.5. Caspase Assay

Caspase assay measures caspase activity. Active caspase 3 is a key marker of apoptosis and therefore this assay was used to detect apoptosis upon MS275 or SAHA treatment. Cells were grown in the 96 microwell plates and 24h after the treatment, luciferin, cleavable by caspase 3 or 7, was added to the cells (Caspase-Glo-3/7-Assay). After 1h incubation in the dark, the luminescence was measured on the FLUOstar-Luminometer. The amount of the luminescence correlated with the amount of the active caspase 3.

3.1.6 Senescence associate β -galactosidase (SA- β -gal) staining

SA- β -gal staining is a cytochemical assay based on production of a blue-dyed precipitate that results from the cleavage of the chromogenic substrate X-Gal. The precipitate is observed only in senescent cells (Dimri et al., 1995). Cells were plated on the glass cover slips in 6 well plates and treated with SAHA or MS275 for 72h. Subsequently, medium was removed and cells washed 3 times with PBS (pH 7.4). Next, cells were fixed with 2% PFA for 5 min at the RT, washed 3 times with PBS and staining solution was added. Staining components are given in the table 3.1 and they should be prepared prior to use. Plates were wrapped with Parafilm, to protect the staining from CO₂ and to keep the pH value constant. Plates were then placed in the incubator for 24h. On the next day, staining solution was removed, and

cells were washed 3 times with PBS (pH 7.4). Cells were mounted with mounting medium containing DAPI.

Component	Final concentration
X-Gal	20 mg/ml
Citric acid / sodium phosphate, pH 6.0	40 mM
K ₃ Fe(CN) ₆	5 mM
K ₄ Fe(CN) ₆	5 mM
NaCl	150 mM
MgCl ₂	2 mM

3.1.7. Immunofluorescence

Immunofluorescence is a technique that targets specific biomolecules in the cell with fluorescently labelled antibodies and therefore allows visualisation of the distribution of the target molecule within the sample. We used immunofluorescence on cultured cell lines to analyse the distribution of p53 protein upon SAHA or MS275 treatment.

Cells were seeded on the sterile cover-slips in 6 well plates. On the next day, they were treated with SAHA or MS275 for 48h. Subsequently, medium was removed, cells were washed three times with PBS and fixed with 4% formaldehyde, diluted in PBS. Permeabilization was performed for 3 min with 0.25% TritonX-100 diluted in PBS. Coverslips with fixed and permeabilized cells were placed in the Petri dishes with a wet tissue on the bottom, to provide humidity. Primary antibody was diluted in PBS (1:1000) and 25 μ l of antibody solution were applied on each coverslip. Cells were further covered with Parafilm and incubated for 1h at the RT. Subsequently, slides are washed three times in PBS and secondary antibody is applied in the same way like the primary antibody. After 1h incubation protected from the light, washing steps were repeated and cover-slips were mounted with a DAPI containing mounting medium on the microscope slides. After 48h microscopic analysis was performed on the fluorescent microscope.

3.2 Molecular Techniques

3.2.1 DNA analysis

3.2.1.1 Isolation of genomic DNA

Genomic DNA was isolated by adding 50 μ l of lysis (Soriano) buffer (Table 2.8) to the tissue or cell pellet. Lysis was performed by incubation on 55°C for 90 min. Next, proteinase K was added and suspension incubated on 95°C for 15 min. Lysates were vortexed for 10 sec and centrifuged for 10 min at the maximum speed. Supernatant was carefully removed, placed into the PCR tubes and stored at -20°C until further use.

3.2.1.2 Polymerase chain reaction (PCR)

PCR was used for genotyping of the mice. General procedure was done as already published (Mullis et al., 1986). Reaction was performed using REDTaq ReadyMix, with 1.5 μ l of DNA. PCR conditions are shown in the Table 3.2. Amplification was done for 40 cycles. PCR products were stored at -20°C until analysing on the agarose gel by electrophoresis.

Reaction mix		Conditions		
12.5 μ l	REDTaq Ready Mix	95°C	5min	
0.5-1-2 μ l	Forward primer (10 μ M)	95°C	45 sec	
0.5-1-2 μ l	Reverse primer (10 μ M)	53-64 °C	1 min	40x
1.2 μ l	DNA	72 °C	1min, 30sec	
Up to 25 μ l	H ₂ O	72°C	5 min	

Specific primer set was used for different genotypes, so that wild type and mutated products could be distinguished according to the size on the 1.5% agarose gel. Annealing temperatures and product sizes are depicted in the Table 3.3.

Name of the PCR	Annealing temperature	Wild type	Mutated
FSF-Kras ^{G12D}	55°C	270 bp	351 bp
Pdx1 ^{Cre}	60 °C	no product	390
LSL-Trp53 ^{R172H}	62 °C	570 bp	270 bp
LSL-p53 ^{lox}	64°C	288 bp	370 bp
Pdx1 ^{Flp}	56°C	300 bp	620 bp
R26 ^{CreERT2}	55°C	no product	190 bp
LSL-Rosa26 ^{lVA-lacZ}	62°C	600 bp	310 bp
LSL-R26 ^{mT/mG}	62°C	650 bp	450 bp
R26-FSF-CAG	62°C	650 bp	450 bp
FSF-Stop	60°C	no product	600 bp
p65 ^{lox}	58°C	270 bp	300 bp
hdac1 ^{lox}	60°C	260 bp	322 bp
hdac2 ^{lox}	60°C	no product	500 bp
hdac2 ^{wt}	60°C	472 bp	no product

3.2.1.3 Agarose gel electrophoresis

PCR products as well as RNA quality were analysed on 1.5-2% agarose gels. Gels are prepared by boiling of agarose in 1xTAE buffer. Upon cooling down to the 55°C 6µl of etidiumbromide per 100µl boiled agarose was added and gels are pured in horizontal electrophoresis chambers. After polymerisation, 12 µl of PCR product was used and the electrophoresis was running for 1h and 30min or longer if it was needed. Results were analysed by UV translumination.

3.2.2 RNA analysis

3.2.2.1 RNA Isolation and Reverse Transcription

For RNA isolation, cells were washed with PBS and lysed with mixture consisting of 594 µl of lysis buffer (RLT) and 6 µl of β-merkaptoethanol (for 10 cm dish). Lysates were stored at -80°C until further processing or they were immediately used for RNA isolation with QIAshredder columns and RNeasy mini kit. DNA was degraded with RNase-free DNase set. RNA concentration was determined by the spectrophotometer NanoDrop 1000. RNA samples were stored at -80°C until further processing. For generating 100 µl of cDNA 2 µg

RNA were used. Reverse transcription was performed with a TaqMan reverse transcription reagents. Samples were further stored at -80°C until further use.

3.2.2.2 Quantitative Real-Time PCR

Real-time PCR primers were designed using Primer 3 online tool (Rozen and Skaletsky, 2000). Real-time PCR was performed with SYBR Green PCR Master Mix and 100 nM each primer using StepOnePlus real-time PCR system and software.

All samples were normalized to cyclophilin as a housekeeping gene. Relative quantification was performed by using $\Delta\Delta Ct$ method (Livak and Schmittgen, 2001). Equations are shown below.

$$\Delta Ct = Ct(\text{target gene}) - Ct(\text{endogenous control}) \quad [\text{calculated for every sample}]$$

$$\Delta\Delta Ct = \Delta Ct(\text{treated sample}) - \Delta Ct(\text{reference sample})$$

$$\text{Relative expression} = 2^{-\Delta\Delta Ct}$$

PCR conditions can be seen in Table 3.4. Primer sequences are listed in Table 2.6. Analyses were performed in technical triplicates in three independent experiments.

Temperature	Time	Number of cycles
50 °C	2 min	1
95 °C	10 min	1
95 °C	15 sec	40
60 °C	1 min	

3.2.2.3 Comprehensive analysis of gene expression using microarrays

Microarray analysis of gene expression enables comprehensive assessment of the transcriptome in multiple samples and their comparison. Using this approach, it is possible to infer 'gene signatures' of certain phenotypic states as well as the underlying signalling pathways. Microarray analyses were used as an unbiased approach to determine genes and pathways involved in early response to p53^{R172H} expression. For this purpose, total RNA from the cell lines derived from murine pancreatic cancer as well as PDECs was used.

RNA is extremely sensitive to degradation due to the ubiquitous presence of the RNases. Before any downstream analysis, RNA integrity and quality was investigated. This was achieved by the gel electrophoresis of RNA. Only 28S and 18S rRNA were visible and

the ratio of their bands was approximately 2:1 (28S:18S), without traces of any degraded RNA.

Samples were further processed with the Ambion WT expression kit. Purified single strand DNA was then fragmented and labelled using the GeneChip WT terminal labelling kit. Hybridisation to GeneChip mouse gene1-0 ST array chips was performed by cooperation partners at University of Düsseldorf (Prof. K. Koehrer, Biomedical Research Center (BMFZ)).

3.2.3 Protein analysis

3.2.3.1 Isolation of the whole cell protein extract

For collecting the whole cell lysate, transfected or chemically treated cells were washed with ice cold PBS and lysed in IP buffer with additional protease and phosphatase inhibitors. Lysates were frozen in liquid nitrogen and stored at -80°C until further use. Prior to use, protein lysates were thawed on ice and centrifuged in precooled centrifuge for 20 min at 4°C . Supernatant was transferred to the new tubes and stored at -80°C or further processed.

3.2.3.2 Determining protein concentration

Protein concentration was measured by colorimetric reaction established by Bradford (Bradford, 1976). In 300 μl of 1x Bradford reagent, 1 μl of protein lysate was added. As a standard curve, defined dilutions of BSA were made. Measurement is performed in triplicates and OD values were obtained from photometer at the wave length of 600 nm. Values are extrapolated from the standard curve. Samples were further brought to equal concentration by adding IP buffer and 5X Laemmly buffer and incubated for 5 min at 95°C . For further analysis 30-50 μg of proteins were used.

3.2.3.3 Western Blot

Proteins were separated according to the size by using sodium dodecyl sulphate – polyacrylamide gel electrophoresis (SDS-PAGE) (Burnette, 1981). For this purpose, 12% denaturing polyacrylamide gel was poured into the gel chambers and covered with 1 ml of isopropanol. After polymerisation, isopropanol was removed and concentrating gel poured over the separating gel. Components of the both gels are given in the table 3.5.

Component	Separating gel	Concentrating gel
dH ₂ O	3400 µl	3000µl
Concentrating gel buffer	-	1300 µl
Separating gel buffer	2600 µl	-
30% Acrylamide	4000 µl	750 µl
10% SDS	100 µl	50 µl
10% APS	50 µl	25 µl
TEMED	15 µl	10 µl

Protein separation was carried out at 80 - 160V in running buffer for 1.5 - 2.5 hours. After separation proteins were immobilised on Immobilon-P transfer membrane (Milipor). For the transfer purposes wet blot was used for 2h at 300 mA or overnight at 90mA (Towbin et al., 1979).

Unspecific binding of antibodies was blocked by incubating in 2.5% skim milk for 20 min. Membrane was than incubated in primary antibody (dilution 1:1000) with gentle shaking at 4 °C, overnight. After washing, secondary antibody (dilution 1:5000) was applied for 2h at room temperature and protected from the light. Membrane was washed again and detection was performed in Odyssey® infrared imaging system (LI-COR) at 700 nM or 800 nM wavelength. β -actin is used as loading control. If it is not stated differently in the *Results* section, experiment was performed once.

3.2.4 Chromatin Immunoprecipitation (ChIP)

For investigating the recruitment of transcription factors of interest, as well as for examining the changes in chromatin modifications, we performed ChIP analysis. Twenty five million cells per treatment were used. Cells were treated with vehicle or with MS275 for 24h, fixed with 1% PFA for 10 min. Cells were further processed by using the SimpleChIP *Enzymatic Chromatin IP Kit* with a magnetic beads according to the manufacturer protocol. Antibodies used in a ChIP assay are listed in a table 2.5. After purification, amount of bound DNA is quantified with qPCR using $\Delta\Delta C_t$ method.

3.3 Mouse experiments

All mice were bred and kept in the Centre for preclinical research (ZPF) of the 'Klinikum rechts der Isar' in specific pathogen free (SPF) area. Allowance for the animal experiments was provided by government Oberbayern and the experiments were conducted according to the standards of Federation for Laboratory Animal Science Associations (FELASA).

Results from animal experiments were generated in a joint effort with the group of Prof. Dieter Saur (Klinikum rechts der Isar, II Medical Department, Technical University Munich, Germany).

3.3.1 Mouse strains

Conditional *Cre-loxP* as well as inducible dual recombinase *Flp-frt;Cre^{ERT2}-loxP* systems were used for tissue-specific deletion of the gene or for expression of the mutated alleles (Feil et al., 1997; Orban et al., 1992; Zhu and Sadowski, 1995).

This is provided by interbreeding mice carrying Cre or Flp recombinase under control of a tissue-specific promoter, with mouse lines carrying mutated allele silenced by a transcriptional stop element flanked by *loxP* or *frt* sites, or with mice carrying transgenes also flanked by *loxP* or *frt* sites. Due to the Cre/Flp activity, *loxP/frt* sites are recognised and recombined allowing expression or partial deletion of the gene of interest in the offspring (Hingorani et al., 2003; Zhu and Sadowski, 1995). Additionally, the *Flp-frt;Cre^{ERT2}-loxP* system was used for time-dependent expression of the mutated allele.

Pdx1-Cre (Hingorani et al., 2003). This mouse line was kindly provided by Prof Andrew Lowy (UC San Diego Health System, San Diego, USA). Expression of the Cre recombinase is under control of the pancreas-specific Pdx1 promoter. Pdx1 is expressed in the pancreas during the embryonic development, starting from the E8.5. Pdx1-Cre mouse line has no phenotype.

Pdx1-Flp (unpublished data Prof. D. Saur). This mouse line was kindly provided by Prof. Dieter Saur, (Klinikum rechts der Isar, II Medical Department, Technical University Munich, Germany). In this transgenic mouse line, expression of the Flp recombinase is under control of the pancreas-specific Pdx1 promoter. The Pdx1-Flp mouse line has no phenotype.

LSL-Kras^{G12D} (Hingorani et al., 2003; Jackson et al., 2001). This knock in mouse line was kindly provided by Prof Tyler Jacks, PhD (Massachusetts Institute of Technology, Cambridge, MA, USA). Mutations in *KRAS* gene are driving mutations in human pancreatic cancer (Hingorani et al., 2003). Upon Cre activation and excision of the stop cassette, mice carrying *LSL-Kras^{G12D}*, express KRAS protein with substitution in the codon 12 (Glycine to

Aspartic acid). Mutated protein had lost GTP-ase activity and therefore leads to the constitutive activation of Ras signalling pathway (Hingorani et al., 2003).

FSF-Kras^{G12D} (Schönhuber et al., 2014). This mouse line was kindly provided by Prof Dieter Saur, (Klinikum rechts der Isar, II Medical Department, Technical University Munich, Germany). This line is equal to the *LSL-Kras^{G12D}* mouse line, except of the 5' positioned frt flanked stop genetic element instead of the LSL-cassette. Heterozygous FSF-Kras^{G12D} mice do not show any phenotype because the oncogenic Kras^{G12D} expression is blocked by frt flanked stop cassette.

FSF-CAG-R26^{CreERT2} (Schönhuber et al., 2014). This mouse line was kindly provided by Prof Dieter Saur, (Klinikum rechts der Isar, II Medical Department, Technical University Munich, Germany). The knock in mouse line expresses a fusion protein of Cre recombinase from P1 bacteriophage and mutated ligand binding domain of the human estrogen receptor (ER^{T2}). Expression is blocked by a frt flanked stop cassette positioned on the 5' end. It is positioned in the first intron of *Rosa26* locus and under control of CAG promoter. Constructs knocked into the *Rosa26* locus do not show any phenotype (Zambrowicz et al., 1997). Upon Flp activation, frt sites are recombined and CreERT2 is expressed but still sequestered in the cytoplasm. Transfer to the nucleus is possible by applying tamoxifen.

R26^{mT/mG} (Muzumdar et al., 2007). This reporter mouse line harbours loxP flanked coding sequence for the dimer Tomato and enhanced green fluorescent protein (EGFP) in the *Rosa26* locus. The Tomato gene is flanked by two loxP sites. Therefore, cells without any active Cre recombinase show red fluorescence (Muzumdar et al., 2007). Upon Cre-mediated recombination, the loxP sites are recombined, Tomato is excised and EGFP is expressed.

LSL-p53^{R172H} (Hingorani et al., 2005; Olive et al., 2004). This knock in mouse was kindly provided by Prof. Tyler Jacks, PhD (Massachusetts Institute of Technology, Cambridge, MA, USA). *LSL-p53^{R172H/+}* mice harbour a missense mutation (Arginine to Histidine at the codon 172) homolog to the human mutation in codon 175 observed in numerous spontaneous tumours as well as patients with Li-Fraumeni syndrome (Olive et al., 2004). After deletion of the loxP flanked stop element at the 5' end of the construct, oncogenic p53^{R172H} protein is expressed (de Vries et al., 2002; Liu et al., 2000).

LSL-p53^{F2-10} (LSL-p53^{lox}) (Jonkers et al., 2001). *LSL-p53^{F2-10}* mouse line was kindly provided by Prof. Anton Berns, PhD (The Netherlands Cancer Institute, Amsterdam, Netherlands). These mice harbour p53 coding sequence with one loxP site placed within intron 1 while the second loxP site is placed in the intron 10. Upon Cre activation, exons 2-10 of the p53 gene are excised leading to the lack of p53 tumour suppressor (Jonkers et al., 2001).

LSL-relA^{flox} (LSL-p65^{flox}) (Algul et al., 2007). This mouse line was kindly provided by Prof Roland Schmid, Dr med. (Klinikum rechts der Isar, II Medical Department, Technical University Munich, Germany). The relA^{flox} mouse line contains a modified p65 endogenous locus, in which exons 7-10 are floxed with loxP sites. Exons 7-10 code for Rel homology domain and nuclear localization site. Upon activation of Cre recombinase, loxP sites are recombined and exons 7-10 excised, resulting in an inactive truncated form of RELA, which cannot be transferred to the nucleus (Algul et al., 2007).

HDAC1^{flox} (kindly provided by Prof. A. Bradley, EUCOMM, UK). This mouse line was kindly provided by Prof. Allan Bradley, PhD (The Wellcome Trust Sanger Institute, Cambridge, UK). HDAC1^{flox} mice contain loxP sites flanking exon 3. Upon Cre activation, loxP sites are recombined and exon 3 is excised, providing a non-functional form of HDAC1.

HDAC2^{flox} (Montgomery et al., 2007). This knock in mouse line was kindly provided by Prof. Eric Olson, Ph.D. (University of Texas Southwestern Medical Center, Dallas, TX, USA). In HDAC2^{flox} mice, exon 2, 3 and 4 of the Hdac gene are flanked by loxP sites. Upon the activation of Cre recombinase, the loxP sites are recombined and exons 2 - 4 are excised providing a non-functional form of HDAC2 (Montgomery et al., 2007).

All the animals have mixed genetic background (129/Sv / C57BL/6).

3.3.2 Genotyping

Two to three weeks old mice were anesthetised with isofluran and 2 mm long piece of the tail was cut off. The wound was closed by silver nitrate applicator. For later identification every mouse got an ear mark representing a number code. DNA from tails was isolated as it is described in the section 3.2.1.1.

3.3.3 Tumour Mice Dissection

Prior to dissection mice were injected with 5mg/kg 5-bromo-2'-deoxyuridine (BrdU) dissolved in sterile PBS. BrdU immunohistochemistry is used later for determining proliferation ratio. Mice were euthanized by isofluran inhalation, fixed and disinfected with 70% ethanol. Dissection is carried out in sterile conditions. Samples for DNA, RNA and protein isolation were collected and stored on -80°C. Sample for the cells isolation was placed in sterile PBS and further procedure is described in the section 3.1.1. Weight of the pancreas, spleen and liver is documented. Samples for cryosectioning as well as all the internal organs were fixed in 4% PFA.

3.4 Histological analysis

3.4.1 Tissue fixation and sectioning

Tissue collected from the mice was fixed in 4% PFA for 24h, washed with PBS, dehydrated with ASP300, embedded in paraffin and stored at RT until further use. For further analysis 1.5 - 2µm thick sections were cut using microtome.

Cryosections were fixed in 4% PFA for 1.5h, washed with PBS and transferred to 15% sucrose. On the next day samples were transferred to 30% sucrose and after 24h embedded in Tissue-Tek O.C.T. and stored at -80°C. Thirty µm thick sections were cut with cryostat Microm HM 560 and stored at -20°C until further use.

3.4.2 Haematoxylin and Eosin (HE) Staining of Tissue Sections

Deparaffination of the paraffin embedded tissue was performed by using Roti Histol. Subsequently, rehydration was performed by the decreasing alcohol series (2x 100%, 2x 98% and 2x 80% EtOH). Sections were then stained in haematoxylin for 5 sec, washed in tap water for 10 min and stained in eosin for approx. 20 sec. Dehydration was achieved by an increasing alcohol series (2x 80%, 2x 96% and 2x 100% ethanol). After 2 x 5 min in Roti Histol, slides were mounted with Pertex mounting medium.

3.4.3 Alcian blue staining

Paraffin embedded sections were deparaffinised and rehydrated as described in the section 3.4.2. Slides were then stained in alcian blue staining for 5 min. Counterstaining was performed in nuclear fast red solution for 5 min. Slides were further dehydrated as described in the section 3.4.2.

3.4.4 Immunohistochemistry on paraffin slides

Tissue sections were deparaffinised and rehydrated as described in the section 3.4.2. Antigen retrieval was performed by using citric acid based unmasking solution and incubating in a microwave at 360W for 12 min. Slides were cooled down for 20 min and were washed in H₂O. Endogenous peroxidase reactivity was blocked by incubating the slides in 3% H₂O₂ for 10 min. After washing once in water and twice in PBS, slides were incubated with 5% serum in PBS for 1 h to block unspecific antibody binding. Primary antibody was diluted in blocking solution in ranges 1:50 to 1:500 and incubated over night at 4°C. Additionally, avidin/biotin blocking kit was applied.

Primary antibody was removed by washing with PBS. Biotinylated secondary antibody was diluted 1:200 and incubated for 1h at RT. After washing in PBS, Vectastain Elite ABC solution was added and subsequently slides were incubated with 3,3'-diaminobenzidine tetrahydrochloride (DAB) until brown staining appeared. Slides were finally counterstained with haematoxylin and mounted as described in the section 3.4.2.

3.4.5 Immunohistochemistry on cryo-sections

Cryo-sections were used for confocal microscopy and were prepared like described in the section 3.4.1. Prior to the staining procedure slides were left over night to dry, fixed with 4% PFA and washed with PBS for 5 min. On each slide 200 µl of blocking solution C (PBS, 3% BSA, 1% saponin, 1% Triton-X) was added and incubated for 1h. Subsequently, antibody was diluted in C solution (1:100), added at the slide, covered with a Parafilm and incubated for 48h at 4°C. Then, antibody was removed and slides were washed with solution C for 30 min, four times. Secondary antibody was diluted (1:1000) in a solution C, applied on slides and incubated for additional 48h. Next, secondary antibody was removed, slides were washed with C solution two times for 30 min, and with solution D (PBS, 3%BSA, 1% saponin) additional 2 times for 30 min. Slides were than washed with PBS for 10 min, dried with a tissue and mounted with a Vectashield mounting medium.

3.4.6 Documentation

Slides were photographed using microscope Axio Imager.A1 with AxioCam HRc and software AxioVision 4.8. For the confocal microscopy Zeiss LSM510 Axiovert 100 was used with x40/1.3 oil-immersion objective (optical section thickness 4.4 µm). Images with a frame size of 1,024x1,024 pixels and an image size of 225x225 µm were collected. Images were merged and converted with Zeiss LSM 510 software (Klein et al., 2013).

3.5. Statistical Analysis

Descriptive and general statistical analyses were performed using GraphPad Prism 5 software package (La Jolla, USA). Data are presented as arithmetic mean +/- standard error of the mean, if not stated otherwise. Survival curves were done by Kaplan-Meier survival analysis. To analyze statistical significance of different groups t-test or log rank test were used and p values are indicated within the figures or figure legends. Bonferroni correction was applied if more than one test was performed on one data set. To analyze correlation between data sets Pearson's nonparametric correlation was applied. As significance levels error probability p was employed ($p < 0.05$ (*), $p < 0.005$ (**), $p < 0.001$ (***)).

Gene set enrichment analysis (GSEA) detects enriched sets of transcript involved in certain biological process, thereby serving as a surrogate indication that such pathway is upregulated in test samples, compared to control samples, and *vice versa* (Subramanian et al., 2005). GSEA software was provided by the Broad Institute of the MIT, Cambridge, USA (www.broadinstitute.org). Gene sets were obtained from the Molecular signatures database 3.1, and the following parameters were used: permutation type - gene set; permutation number - 1000; metric for ranking genes - signal2noise; enrichment statistic - weighted; gene set size restrictions - min 15 / max 500. Enrichment score (ES) gives the degree by which the gene set is enriched. Positive ES suggests the up-regulation of the gene set, while negative ES suggests its down-regulation. Normalized ES (NES) was used to compare results across different gene sets, and is derived by dividing ES by the mean of all permutations of the dataset. Significant gene sets were identified using a FDR q-value < 0.05 and a nominal p-value < 0.05 .

4 Results

4.1 In vitro and in vivo models for investigating potential p53^{R172H} gain of function in pancreatic cancer

Previous studies demonstrated that p53^{R172H} gains an oncogenic function in pancreatic cancer models (Morton et al., 2010). Still, the molecular mechanisms are not defined clearly and they certainly depend on the context (e.g. function in the carcinogenesis and in the tumor maintenance). Since p53 is mutated 50–70% of pancreatic cancers appropriate models to investigate molecular processes directed by a p53 mutant were generated (Barton et al., 1991; Redston et al., 1994; Ruggeri et al., 1992).

4.1.1 Characterisation of inducible p53^{R172H} system in vivo

Although the conventional murine pancreatic cancer model (section 1.3) recapitulates several aspects of the human disease, it fails to recapitulate the multi-step carcinogenesis, due to the simultaneous activation of all mutated alleles during early embryogenesis.

To generate appropriate models allowing the sequential genetic manipulation of p53 after *Kras*, we bred *Pdx1-Flp; FSF-Kras^{G12D/+}; FSF-R26^{CAG-CreERT2}; R26^{mT/mG}* mice with *LSL-p53^{R172H/lox}* mice. Mice with a final genotype were treated with tamoxifen in order to activate CreERT2 recombinase. To investigate tamoxifen induced recombination in vivo, we analysed pancreata of tamoxifen treated and non-treated mice by using confocal fluorescence microscopy.

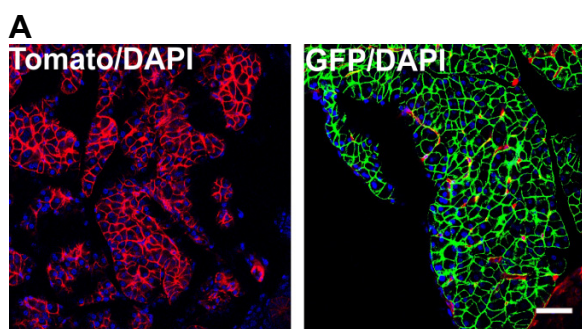


Figure 4.1. Recombination ratio and p53 expression in tamoxifen induced mice. Recombination of the cells in pancreatic tissue of the tamoxifen treated and untreated mice by the use of a reporter allele. *Pdx1-Flp; FSF-Kras^{G12D/+}; FSF-R26^{CAG-CreERT2}; R26^{mT/mG}; LSL-p53^{R172H/lox}* mice at the age of 3 weeks were divided into two groups. One group was exposed to tamoxifen enriched and another to the normal food for 4 weeks. After the treatment, mice were sacrificed and cryo-sections of the pancreas were analysed using a confocal microscope. **A** – Recombination ratio in the pancreata of tamoxifen exposed (green) and tamoxifen non-exposed mice (red). Blue – nuclear staining with DAPI. **B** – p53 expression in the recombined cells (red). Scale bar – 50µM.

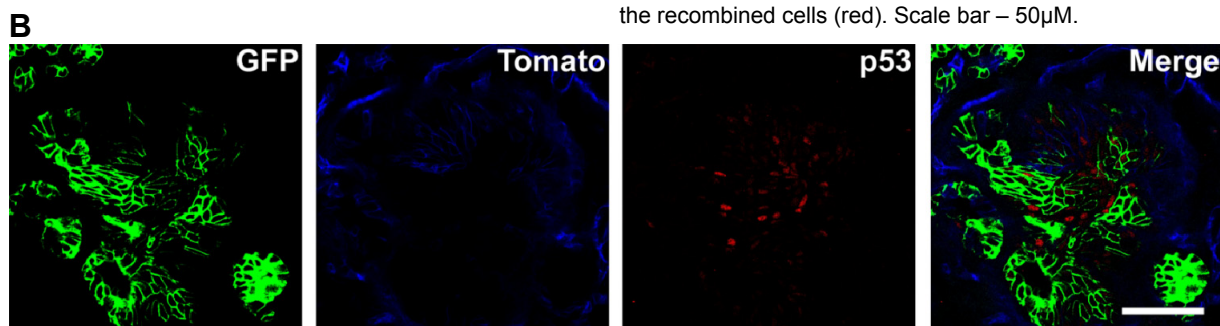


Figure 4.1A shows recombination of the cells in pancreatic tissue of the tamoxifen treated and untreated mice by the use of a reporter allele. Figure 4.1B shows, next to the recombined (green) and non-recombined cells (blue), the expression of p53 (red). Although most of the cells were recombined, p53 was expressed only in the cells of pre-neoplastic lesions.

Restricted expression of the p53 mutant was also obvious in immunohistochemical p53 staining (Figure 4.2). Upper panel shows a preneoplastic lesion from untreated mice, where no nuclear p53 staining is visible. Middle and bottom panels show preneoplastic lesions from two tamoxifen-treated mice, with one or two *LSL-p53^{R172H}* alleles, respectively. Also, untransformed pancreatic tissue was negative for p53 nuclear staining. These data suggest that p53 can be stabilised only in cells with an appropriate oncogenic context.

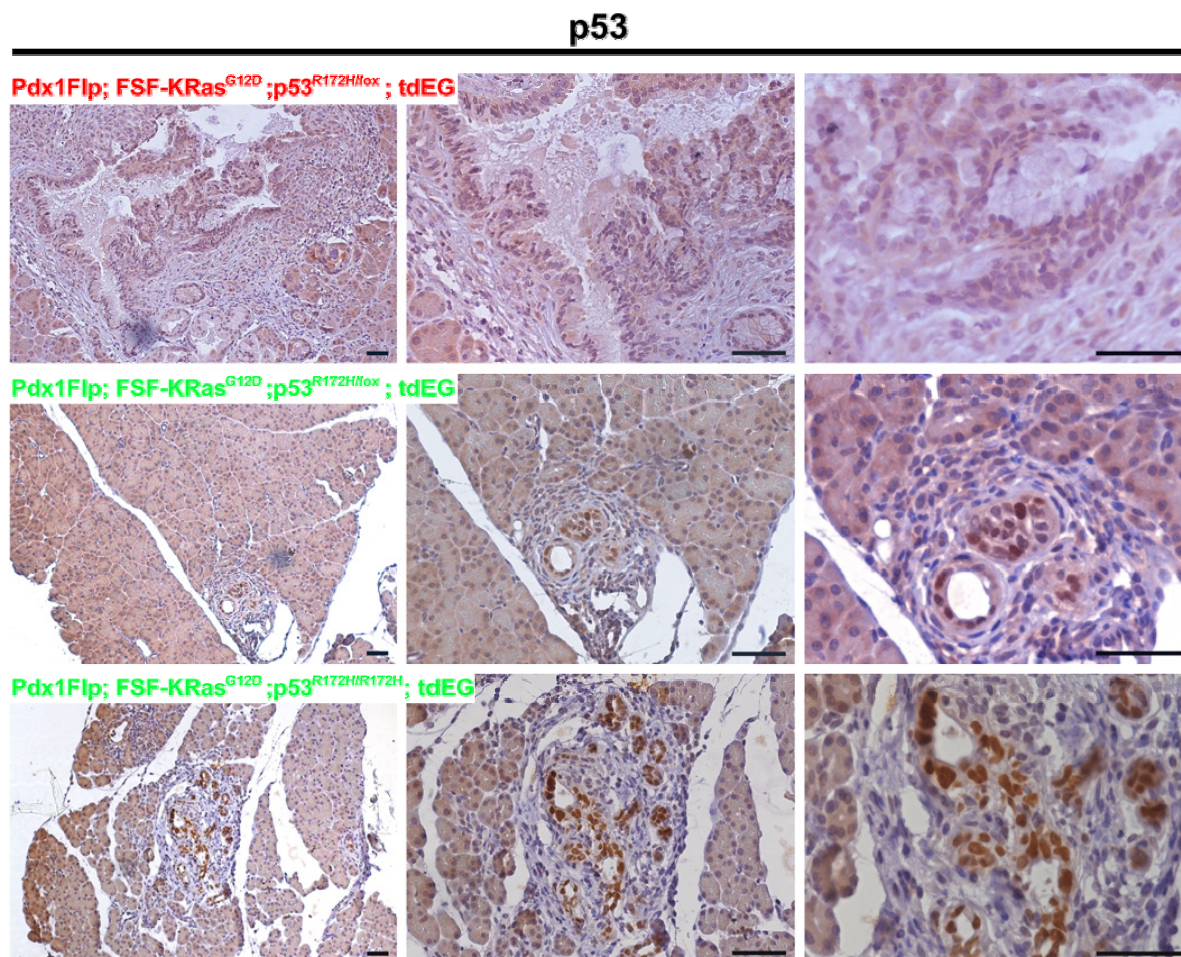


Figure 4.2. p53 protein can be stabilised only in the cells with appropriate oncogenic context. Immunohistochemical staining of p53 in paraffin sections of pancreata of tamoxifen-treated (green – NS856;NS859) and untreated (red – NS866) mice. p53 is expressed only within preneoplastic lesions. Scale bar – 50 μ m. The mice which were induced with tamoxifen food for one month, starting from the age of three weeks. Mice were sacrificed when tamoxifen treatment was finished at the age of 7 weeks. The experiment was done once and included one control and three treated mice (two of them are shown). The mice were littermates.

4.1.2 Investigation of p53^{R172H} oncogenic potential in inducible p53^{R172H} model

Mice with a dual recombinase system (Flp/Cre) that are not treated with tamoxifen and therefore do not express p53 mutant still develop tumours and die on average at the age of 5 months. The tumour development is due to the presence of oncogenic Kras and lack of one p53 allele (the *LSL-p53^{R172H}* allele is null before Cre dependent recombination). Mice which were treated with tamoxifen, and therefore expressed p53^{R172H}, had shorter survival than the untreated once (Figure 4.3A). Additionally, morphology of the tumours developed in the mice with dual recombination system (Flp/Cre) was similar to the mice from conventional model (Cre; see below).

Furthermore, we isolated cell lines from pancreatic cancers of mice not treated with tamoxifen and generated PDAC *in vitro* models which allowed us to activate p53^{R172H} and elucidate its effect in isogenic backgrounds. The recombination efficacy, tested by the R26T/E reporter allele, was less than 100% in these cells (Figure 4.1). Therefore, to enrich the recombined cells, we sorted them using flow cytometry. Figure 4.3B displays the western blot showing that p53^{R172H} is expressed exclusively in activated cells in all three experiments. Next, we performed wound healing/scratch assay to investigate migratory potential of the cells. As shown in Figure 4.3C, cells expressing p53 mutant migrated faster than the control cells. Additionally, we compared the cell growth of the non-activated and activated cells lines during 6 days, using MTT assay. Cell line expressing p53 mutant was growing faster, indicating proliferation-promoting effect of the mutated p53 (Figure 4.3D). These *in vitro* data suggest that p53 gains oncogenic function by promoting cell survival and cell migration.

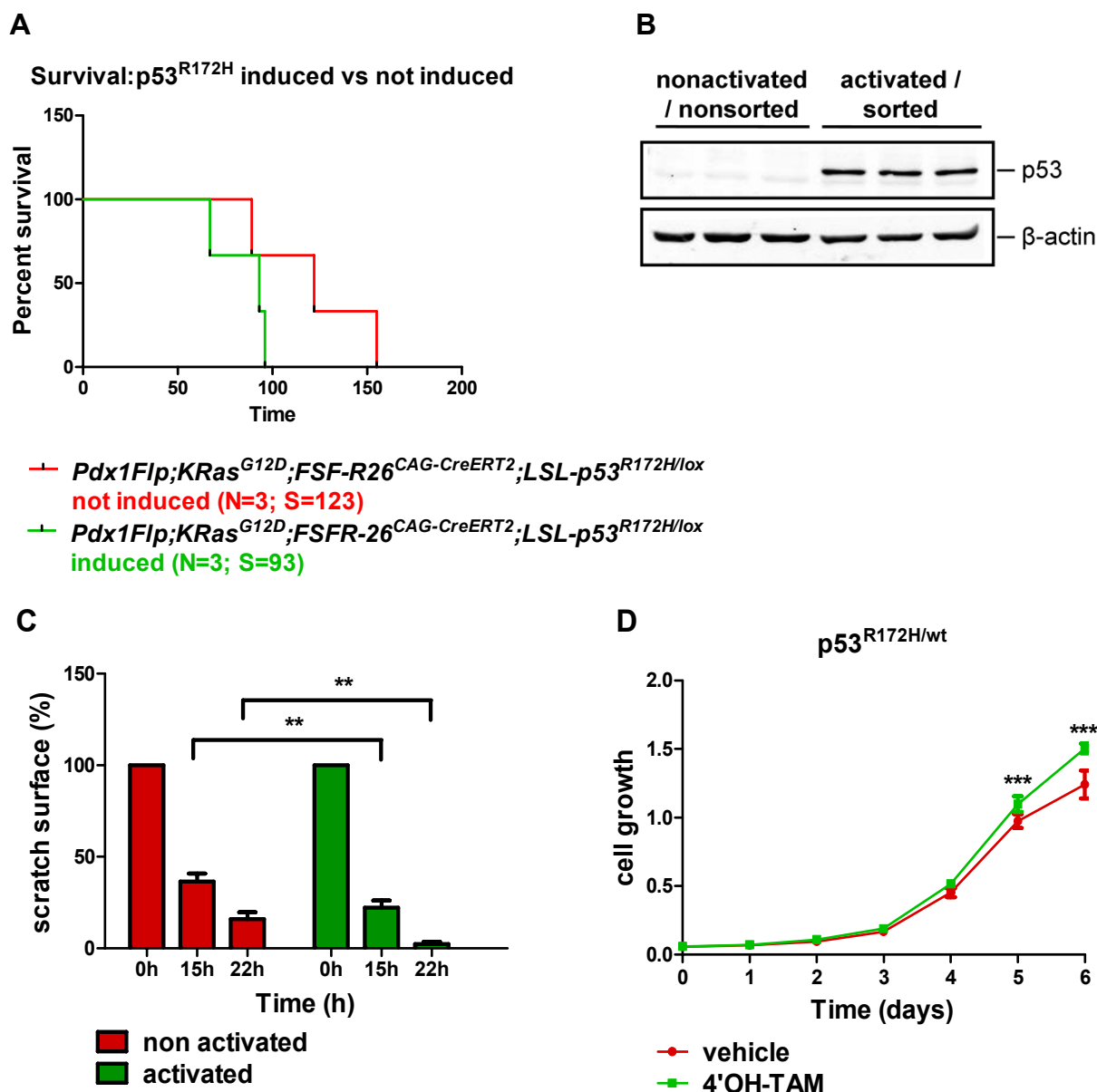


Figure 4.3. p53^{R172H} accelerates cell growth and migration and shortens survival of the mice. **A** – Survival of the control mice and mice treated with tamoxifen. The mice were exposed to the tamoxifen enriched food at the age of three weeks. After one month of treatment, they were exposed to the normal food until they succumbed to tumour. Log-rank test: $p=0,1966$. **B** – Western blot showing p53 protein stabilisation only in the cells which were treated with 4-OH TAM (500 nM) for 48h and then sorted for expression of GFP. Three bands in each group represent three experiments. **C** – Quantification of wound healing/scratch assay (cell line NS481). Cells were treated with 4-OH TAM (500 nM) or with vehicle for 48h and sorted for the expression of GFP. After seeding, the cells were pre-treated for 2 hours with mitomycin. Scratch is made at the time point 0 and cell migration was followed at the time point 0, 15 and 22h. Bars show scratch surface as a percentage. The difference is tested with two way ANOVA test including Bonferroni correction for the multiple testing ($p<0.01$). Red bars – control cells, not expressing p53^{R172H}; Green bars – cells expressing p53^{R172H}. **D** – Cell growth of p53^{R172H}-expressing (treated with 500 nM 4-OH TAM) and control cells (vehicle treated) during 6 days assessed with MTT assay (cell line S-505). The difference is statistically significant on 5th and 6th day ($p<0.001$). Tested with ANOVA test including Bonferroni correction for the multiple testing. All the in vitro experiments were done three times.

4.1.3. PanIN-derived model system for investigating p53^{R172H} in pre-tumorigenic context

To investigate the function of the p53 mutant in *in vitro* surrogate model of preneoplastic lesions, we used pancreatic ductal epithelial cells (PDECs) from a *Pdx1-Flp*; *FSF-KRas*^{G12D}; *FSF-R26*^{CAG-CreERT2}; *p53*^{R172H/R172H}; *R26*^{mT/mG} mouse (NS814). The pancreas of this mice contained PanIN lesions but not invasive cancers (Figure 4.4). Hence, the PDECs isolated from this mouse may reflect a preneoplastic state and therefore gave us the opportunity to investigate the role of p53^{R172H} in early neoplastic stages.

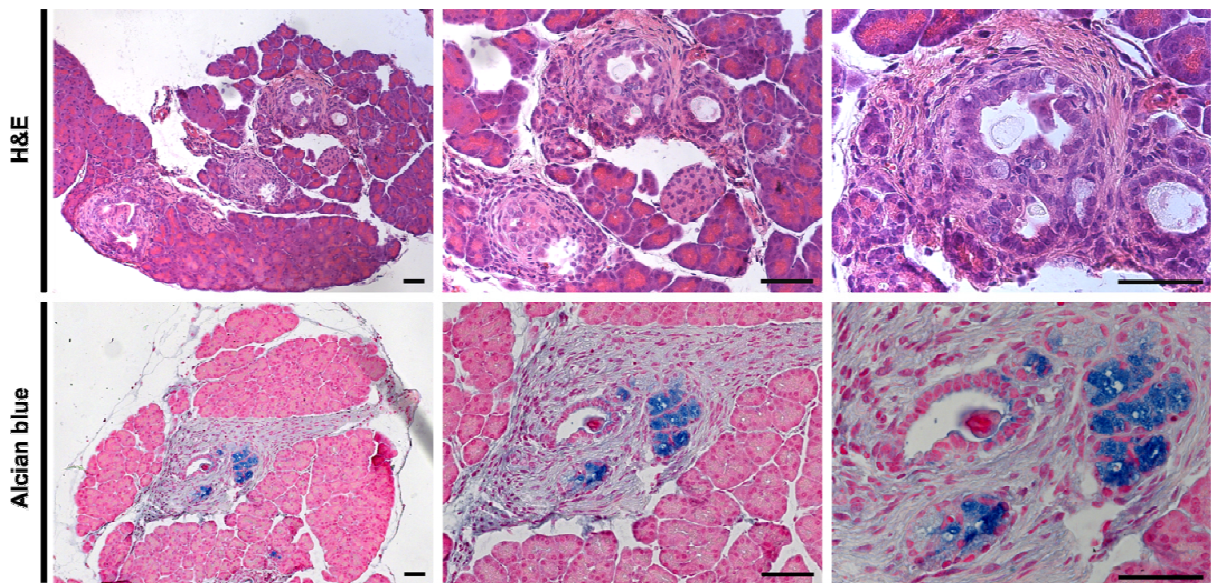


Figure 4.4. Preneoplastic lesions in non-induced mice with dual recombinase system. Pancreas of 6 weeks old mouse with a genotype *Pdx1-Flp*; *FSF-KRas*^{G12D}; *FSF-R26*^{CAG-CreERT2}; *LSL-p53*^{R172H/lox}; *R26*^{mT/mG} (NS814); Upper panel – H&E staining of paraffin sections; bottom panel – alcian blue staining, typical for PanIN lesions 1 and 2. Scale bar - 50µM.

In *in vitro* conditions, tamoxifen treatment efficiently leads to the recombination of the reporter allele, which was detected by a switch in fluorescence from red to green (Figure 4.5A). To investigate the expression of the p53 mutant, we performed western blotting. The expression of p53 was detected after 24 hours, as it can be seen in Figure 4.5B. Furthermore, expression was stable over an investigation period of 3 days. To confirm that the cells do not harbour wt p53, we treated them with doxorubicin which is a typical DNA damage inducer and leads to the stabilisation of wt p53, if present. Indeed, p53 was induced only in the positive control which contained p53 wt but not in the PDEC cell line, as depicted in Figure 4.5C.

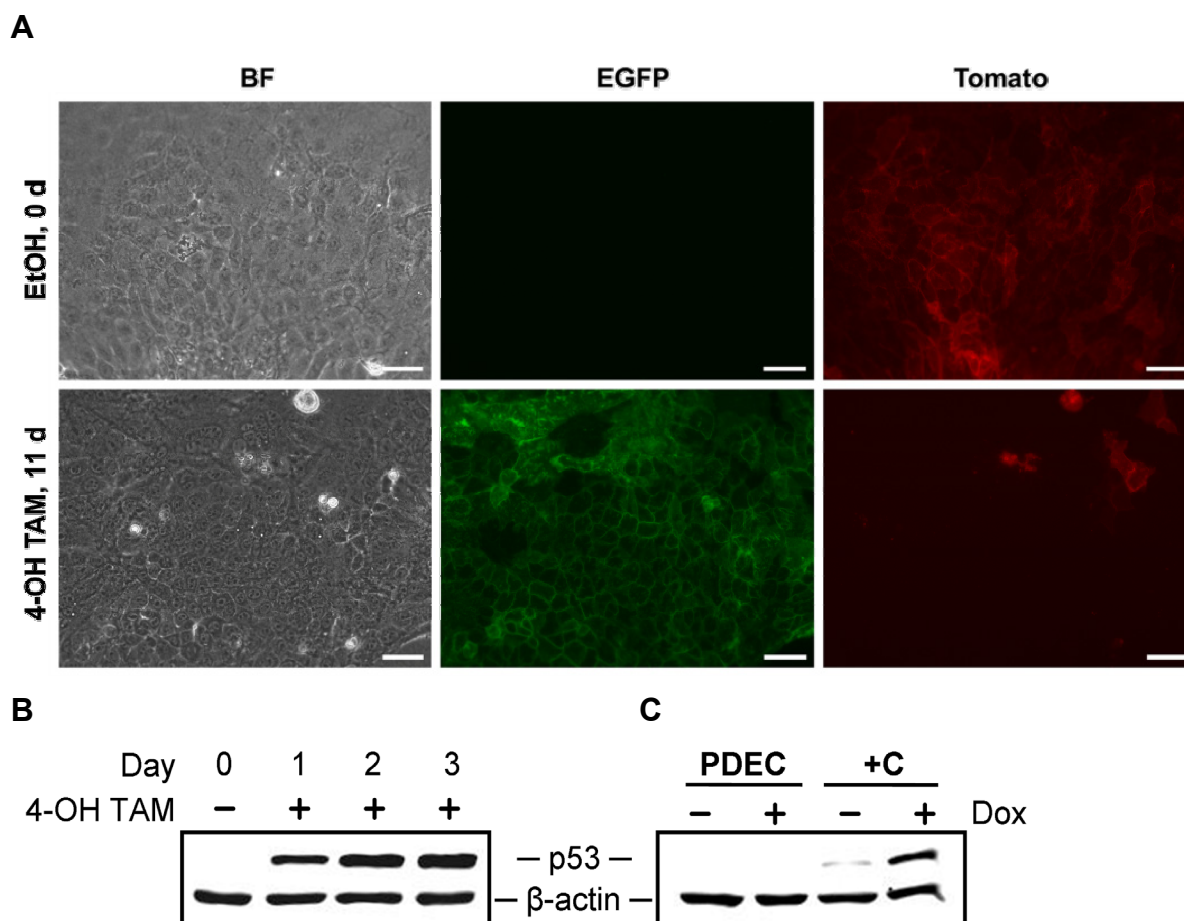


Figure 4.5. PDEC cell line as an *in vitro* model for investigating p53^{R172H} role in an early carcinogenesis. **A** – Collagen culture of PDECs (NS814) fully recombined after three days of 4-OH TAM (500 nM) treatment. The recombination was stable also after day 11. Green – GFP; Red – Tomato. Scale bar – 50µM. **B** – Western blot showing p53 induction already 24h after 4-OH TAM (500 nM) treatment. **C** – Western blot showing lack of wt p53 in PDEC cells. Cells were treated with doxorubicin (0.5 µg/µl) for 24h. As a positive control, we used murine cells from pancreatic cancer harbouring wt p53. All the experiments were done twice.

4.1.4 p53^{R172H} activates ribosomal pathway

To grasp the molecular mechanism of p53^{R172H} activity, we used a non-biased approach and performed comprehensive gene expression analysis. For this purpose, we used PDECs and tumour cell lines which were treated with tamoxifen for 24 hours and analyzed transcriptomes of these cells. The origin of cell lines, as well as the status of the p53 gene before and after treatment, are given in the table 4.1. As controls, we used appropriate cell lines which were treated with vehicle and therefore did not express p53 mutant. We confirmed the expression of p53^{R172H} 24h after 4-OH TAM treatment with a western blot, and we excluded the possibility of wt p53 expression by treating the cells with doxorubicin similar like in the PDEC cell line (Figure 4.5C data not shown).

Origin	p53 status		Cell line
	vehicle	4-OH Tam	
Tumour	p53 ^{-/-}	p53 ^{R172H/R172H}	NS481
Tumour	p53 ^{-/-}	p53 ^{R172H/-}	NS815;NS817
PDEC	p53 ^{-/-}	p53 ^{R172H/-}	NS814

We performed gene set enrichment analysis (GSEA). Significantly up- and downregulated pathways from the KEGG database are shown for each cell line in table 4.2. Ribosome pathway was significantly upregulated in NS481 (p53^{R172H/R172H}) and NS815 (p53^{R172H/-}) upon expression of mutant p53 (Figure 4.6A and B). Therefore, we decided to explore it further. Overlapping genes from the enrichment core for both cell lines which were significantly regulated are shown in the heat map (Figure 4.6C). Still, individual targets remain to be validated.

Cell line (p53 status of vehicle vs 4'-OH TAM treated cells) / Origin of cells	NES	P (nominal)	FDR
NS481 (p53^{-/-} vs p53^{R172H/R172H}) / Tumour			
↗ SPLICEOSOME	2.24	<0.0001	<0.001
↗ RIBOSOME	2.17	<0.0001	0.001
↗ NUCLEOTIDE EXCISION REPAIR	2.17	<0.0001	0.001
↗ RNA POLYMERASE	2.15	<0.0001	0.001
↗ VALINE LEUCINE AND ISOLEUCINE DEGRADATION	2.11	<0.0001	0.001
↗ PROTEIN EXPORT	2.11	0.002	0.001
↗ AMINOACYL TRNA BIOSYNTHESIS	2.06	<0.0001	0.002
↗ DNA REPLICATION	2.01	<0.0001	0.004
↗ HOMOLOGOUS RECOMBINATION	1.91	0.003	0.010
↗ AMINO SUGAR AND NUCLEOTIDE SUGAR METABOLISM	1.88	<0.0001	0.011
↗ BASAL TRANSCRIPTION FACTORS	1.86	0.009	0.013
↗ RNA DEGRADATION	1.82	<0.0001	0.019
↗ PROTEASOME	1.81	0.003	0.020
↗ PYRIMIDINE METABOLISM	1.79	<0.0001	0.021
↗ FRUCTOSE AND MANNOSE METABOLISM	1.77	<0.0001	0.023
↗ HUNTINGTONS DISEASE	1.74	<0.0001	0.029
↗ ONE CARBON POOL BY FOLATE	1.72	0.022	0.033
↗ SELENOAMINO ACID METABOLISM	1.67	0.017	0.043
↗ P53 SIGNALING PATHWAY	1.65	0.003	0.048
↘ NEUROACTIVE LIGAND RECEPTOR INTERACTION	-1.92	<0.0001	0.017
↘ ASTHMA	-1.68	0.015	0.150

Table 4.2. B – Gene set enrichment upon p53 ^{R172H} activation. Table lists significantly positively (↗) and negatively (↘) enriched KEGG signatures			
NS815 (p53^{-/-} vs p53^{R172H/-}) / Tumour			
↗ RIBOSOME	1.83	<0.0001	0.049
↘ CITRATE CYCLE TCA CYCLE	-1.96	<0.0001	0.034
↘ KEGG ADHERENS JUNCTION	-1.91	<0.0001	0.029
↘ AMINOACYL TRNA BIOSYNTHESIS	-1.91	0.002	0.021
NS817 (p53^{-/-} vs p53^{R172H/-}) / Tumour			
↗ ALLOGRAFT REJECTION	1.85	<0.0001	0.033
↘ DRUG METABOLISM CYTOCHROME P450	-2.10	<0.0001	0.005
↘ METABOLISM OF XENOBIOTICS BY CYTOCHROME P450	-1.99	<0.0001	0.009
↘ PEROXISOME	-1.85	<0.0001	0.042
↘ VALINE LEUCINE AND ISOLEUCINE DEGRADATION	-1.81	0.005	0.047
NS814 (p53^{-/-} vs p53^{R172H/-}) / PDEC			
↘ METABOLISM OF XENOBIOTICS BY CYTOCHROME P450	-2.33	<0.0001	<0.0001
↘ GLUTATHIONE METABOLISM	-2.26	<0.0001	<0.0001
↘ VALINE LEUCINE AND ISOLEUCINE DEGRADATION	-2.10	<0.0001	0.001
↘ PROPANOATE METABOLISM	-2.10	<0.0001	<0.0001
↘ DRUG METABOLISM CYTOCHROME P450	-2.04	<0.0001	0.002
↘ PYRUVATE METABOLISM	-1.80	0.002	0.019
↘ RETINOL METABOLISM	-1.76	0.004	0.028
↘ BETA ALANINE METABOLISM	-1.76	0.002	0.026
↘ PEROXISOME	-1.71	0.002	0.036

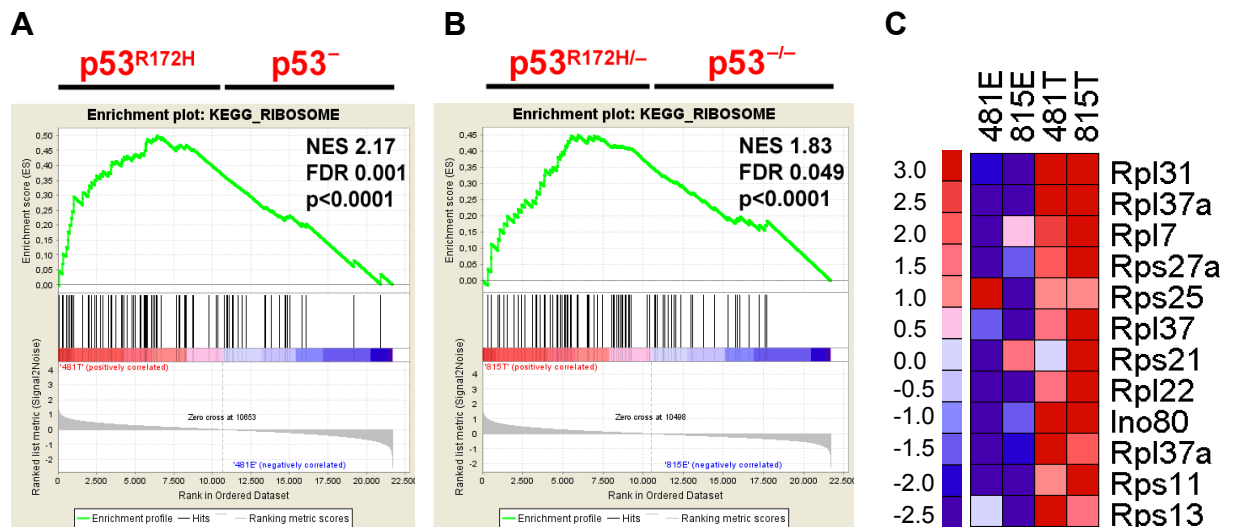


Figure 4.6. p53^{R172H} activates ribosomal pathway in the cell. PDEC and tumour cell lines were treated with tamoxifen for 24h. Isolated RNA is used for gene expression analysis. Gene set enrichment analysis show statistically significant enriched pathway in the cell lines expressing p53^{R172H} homo- (**A**, NS481) or heterozygously (**B**, NS815). FDR – false discovery rate; NES – normalized enrichment score; p – nominal p value. **C** – Heat map of overlapping genes from the enrichment core for both cell lines which were significantly regulated. E, vehicle control; T, Tamoxifen treatment.

4.1.5 Potential role of p65 in p53^{R172H} gain of function

According to the previously shown data and already published reports from pancreatic cancer research p53^{R172H} gains an oncogenic function. Our objective was to further investigate molecular basis of this process. The crosstalk between NFκB family member p65 and p53 signalling was shown to be pivotal for cancer development and drug resistance (Cooks et al., 2013; Schneider et al., 2010). When we performed GSEA of the murine pancreatic cancer cell lines lacking p53 vs cell lines harbouring p53^{R172H}, p65 signature was significantly enriched in latter cell lines (Figure 4.7). Therefore, we examined if the described p53 gain of function might act through the activation of p65.

In order to explore the molecular mechanism underlying a potential p53 gain of function in PDAC next to the dual recombination system *in vivo*, we used KC mouse model with modified p53 locus. The goal was to interbreed in p53^{lox/lox} alleles in KC mice which were missing both p53 alleles (p53^{lox/lox}) and KC mice harbouring one (p53^{R172H/lox}) or two mutated p53 alleles (p53^{R172H/R172H}). Further, we wanted to investigate if the p65 deletion had more pronounced effect on the KC mice harbouring mutant p53 than on the mice lacking p53. To do so, we firstly characterised KC mice with p53^{R172H} and mice lacking p53.

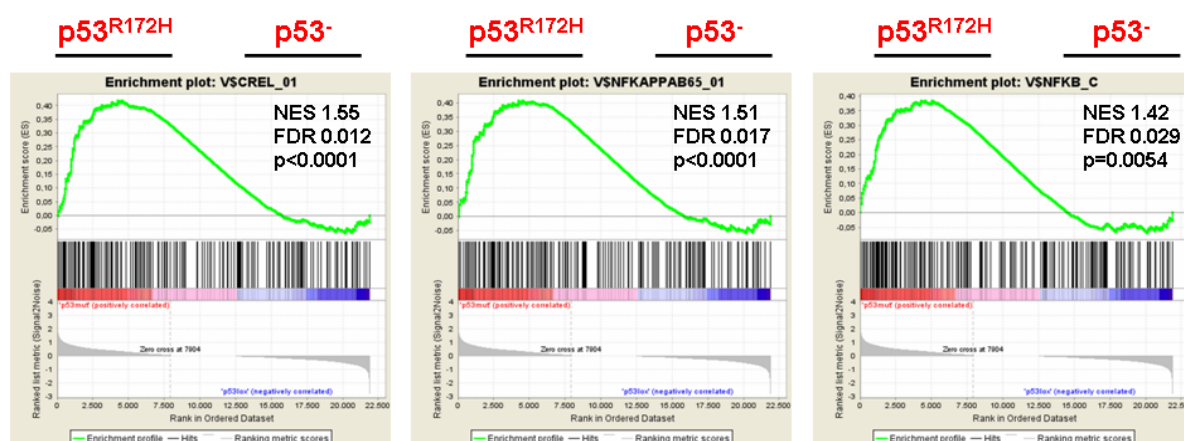
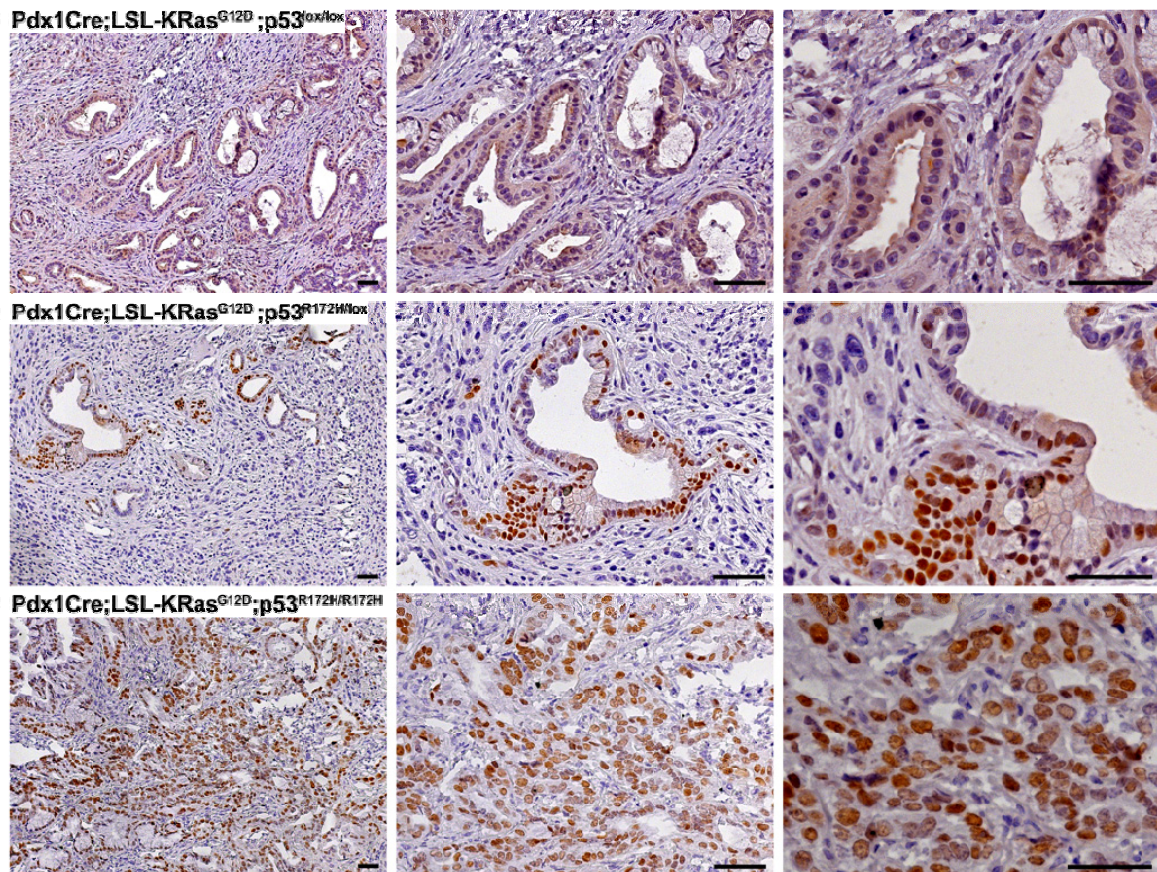


Figure 4.7. NFκB signalling is active in cell lines harbouring p53^{R172H}. GSEA analysis of tumour cell lines lacking p53 (W22,6554) and harbouring p53^{R172H} (5193; 3107; 6051; 434; 5436; 3139) in KC background. FDR – false discovery rate; NES – normalized enrichment score; p-nominal p value.

The goal of the experiment was to investigate if there is a difference between KC mice which were missing both p53 alleles (p53^{lox/lox}) and KC mice harbouring one (p53^{R172H/lox}) or two mutated alleles (p53^{R172H/R172H}). We first considered the levels of p53 protein in tumour tissue of the mice with different genotypes. Immunohistochemical staining shown in Figure 4.8A clearly demonstrates the lack of p53 protein in the KC p53^{lox/lox} mice and its stabilisation in mice harbouring the mutated protein. Mice with both homo- or heterozigously expressed p53^{R172H} developed tumours with heterogeneous morphology and

varied p53 expression within single tumours. Fragments of the tumour were differentiated (Figure 4.8A, middle panel), while the others were undifferentiated (Figure 4.8A, bottom panel). Additionally, we did not find any macroscopic metastasis in liver and lungs from those mice. We also investigated if there is a difference in survival between the mice with different genotypes. The mice with $p53^{lox/lox}$, $p53^{lox/R172H}$ and $p53^{R172H/R172H}$ in KC background, have a mean survival of 56.5, 47 and 52 days, respectively (Figure 4.8B).

A



B

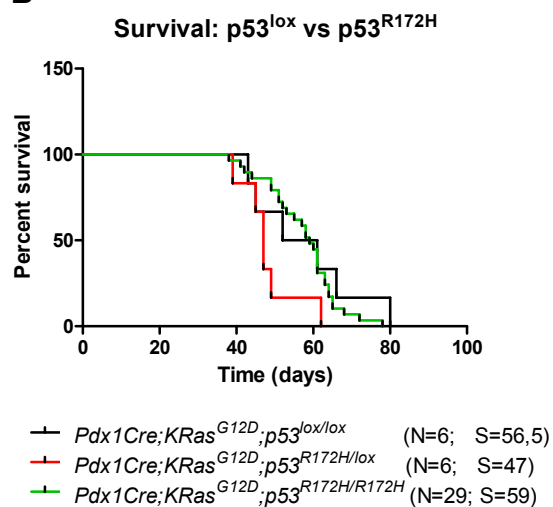


Figure 4.8. A – Representative immunohistochemical staining with anti-p53 antibody, showing p53 protein stabilisation in the pancreas of the mice harbouring mutant $p53^{R172H}$. Three mice per group were analysed and representative IHC from mice 13866, NS762 and AA190 are presented. Scale bar – 50 μ M. **B** – Kaplan-Meier curves showing survival of the mice with indicated genotypes (labelled in different colours). N – number of the animals included in the survival curve; S – median survival in days. P values of a long rank test:

$$p53^{lox/lox} \text{ vs } p53^{R172H/R172H} \quad p=0,4157$$

$$p53^{R172H/lox} \text{ vs } p53^{R172H/R172H} \quad p=0,011^*$$

$$p53^{lox/lox} \text{ vs } p53^{R172H/lox} \quad p=0,1897$$

Then, we compared survival of $p65^{\text{lox/lox}}$ within already described KC mice missing wt p53 allele ($p53^{\text{lox/lox}}$) or carrying p53 mutant allele ($p53^{\text{R172H/lox}}$) (Figure 4.9A, B and C). Kaplan-Meier curve shows that independently of the background ($p53^{\text{lox}}$ or $p53^{\text{R172H}}$), loss of p65 prolonged survival, statistically significant in $p53^{\text{R172H/lox}}; p65^{\text{lox/lox}}$ mice.

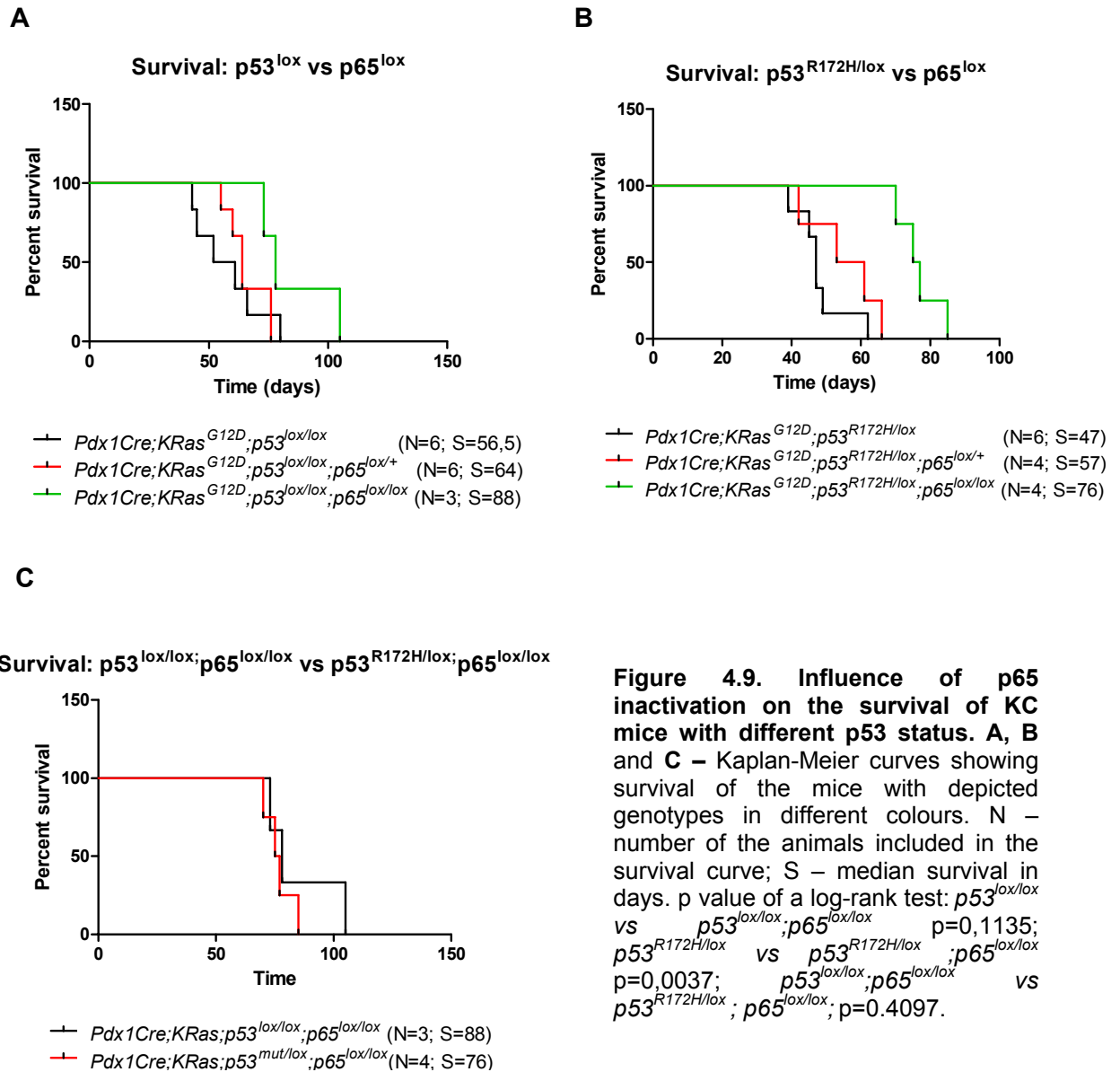


Figure 4.9. Influence of p65 inactivation on the survival of KC mice with different p53 status. A, B and C – Kaplan-Meier curves showing survival of the mice with depicted genotypes in different colours. N – number of the animals included in the survival curve; S – median survival in days. p value of a log-rank test: $p53^{\text{lox/lox}}$ vs $p53^{\text{lox/lox}}; p65^{\text{lox/lox}}$ $p=0,1135$; $p53^{\text{R172H/lox}}$ vs $p53^{\text{R172H/lox}}; p65^{\text{lox/lox}}$ $p=0,0037$; $p53^{\text{lox/lox}}; p65^{\text{lox/lox}}$ vs $p53^{\text{R172H/lox}}; p65^{\text{lox/lox}}$ $p=0.4097$.

Histological examination of the pancreatic tumour tissues showed that $p65^{\text{lox/lox}}$ mice still contained areas with untransformed acini (Figure 4.10). Furthermore, only mice with $p53^{\text{R172H/lox}}; p65^{\text{lox/lox}}$ in KC background developed macro-metastasis in liver and lung (2 out of 4 mice).

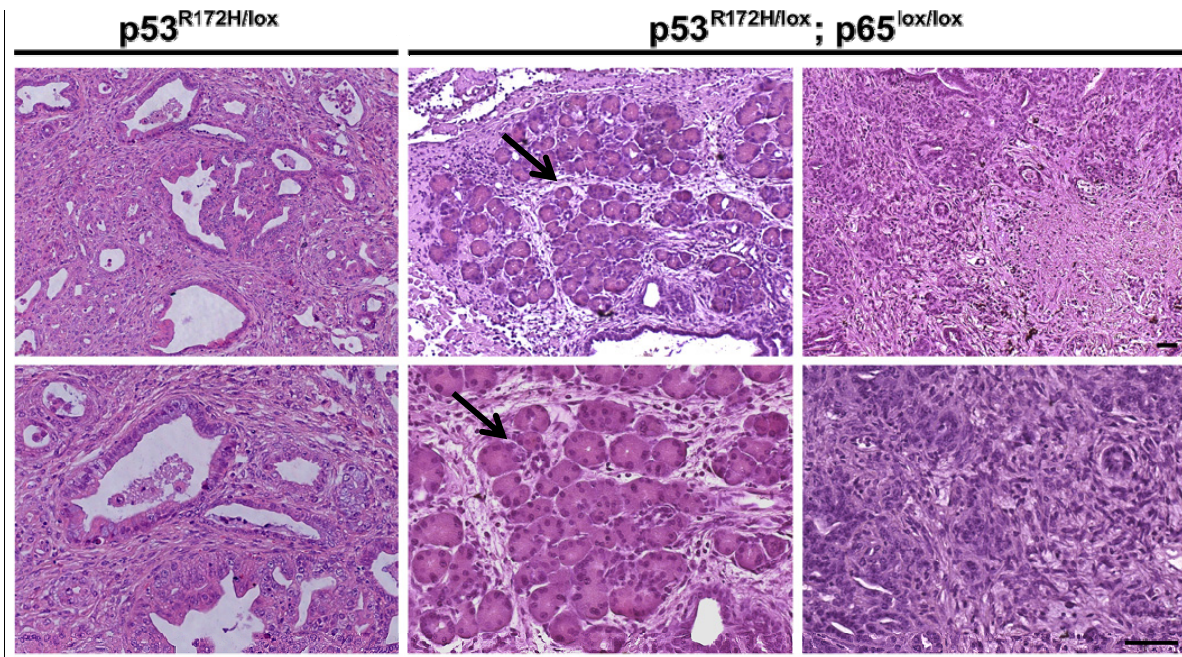


Figure 4.10. Histology of the $p53^{R172H/lox}$ and $p53^{R172H/lox};p65^{lox/lox}$ mice in the KC background. Paraffin sections were stained with haematoxylin & eosin staining and three mice per group were analysed. Localised normal acini in $p53^{R172H/lox};p65^{lox/lox}$ mice (arrow). Scale bar – 50 μ m.

4.2. p53 regulation by histone deacetylases (HDACs) and HDAC inhibitors

The p53 tumour suppressor is one of the most investigated non-histone targets of histone deacetylases. When deacetylated, transcriptional activity of both wt and mutant p53 is altered due to the changes in its DNA binding ability (Harms and Chen, 2007; Li et al., 2011). In this section we describe the analysis of the molecular mechanism of p53 mutant regulation by the HDACs and HDAC inhibitors.

4.2.1 HDAC inhibitors reduce cell viability by inducing apoptosis and senescence

HDAC inhibitors (HDACi) can induce death of tumour cells in doses which do not affect healthy, non-transformed cells (Insinga et al., 2005). To assess the effect of HDACi in our model system, we performed MTT and caspase 3/7 activity assay in different human and murine pancreatic cancer cell lines treated with HDACi.

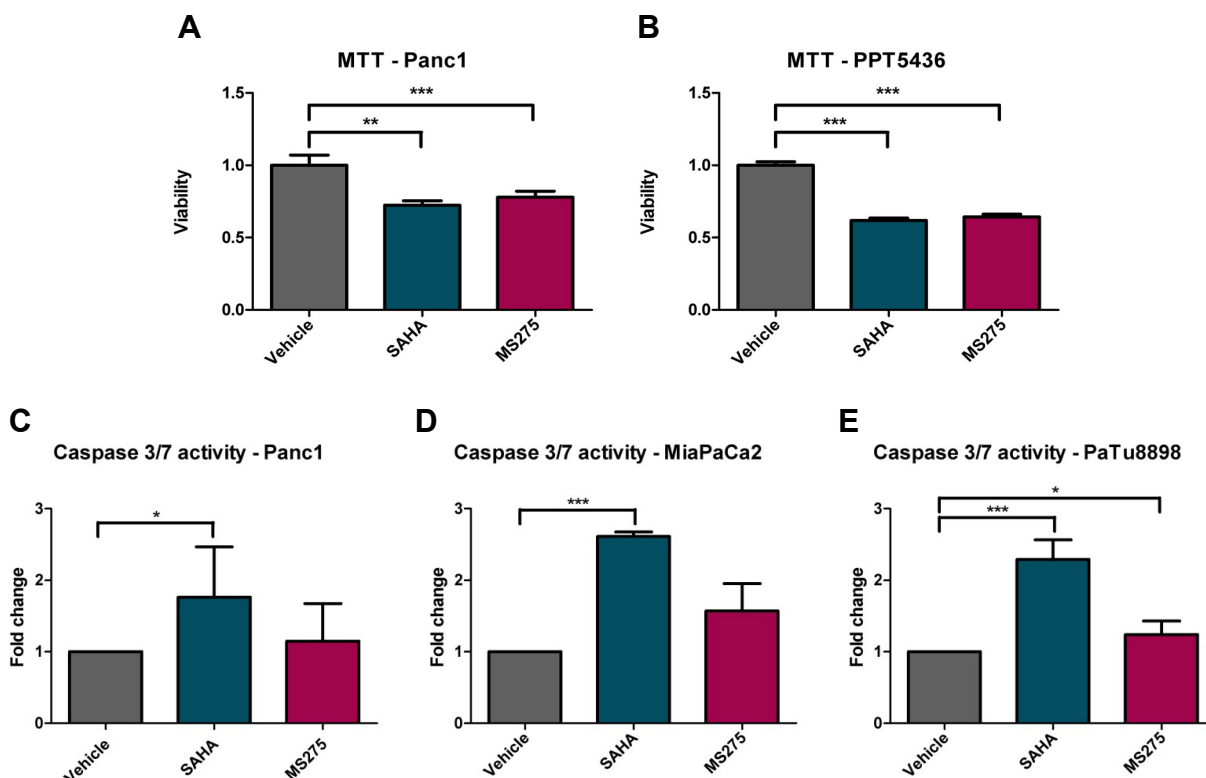


Figure 4.11. HDAC inhibitors, SAHA and MS275 reduce cell viability and induce caspase 3/7 activity. **A** and **B** – MTT assay in Panc1 and PPT5436 cell lines. Cells were treated with SAHA (4 μ M) or MS275 (4 μ M) for 48h when the relative viability is determined. **C**, **D** and **E** – Caspase 3/7 activity assay in MiaPaCa2, Panc1 and PPT5436 cell lines. Cells were treated with SAHA (4 μ M) or MS275 (4 μ M). After 24h caspase 3/7 activity is measured and fold change increase in apoptosis is calculated. Experiments were done 3 times. Every experiment contained 3 technical replicates. Mean values with SD are plotted. Statistical analyses were done with unpaired two tailed Student t-test and significance is depicted with asterisks above the columns.

As shown in Figure 4.11A and B, within 48 hours HDACi reduced cell viability between 35% and 45%, depending on inhibitor used and on the cell line. Additionally, caspases 3 and 7 activities were slightly increased upon the treatment, as it can be seen in Figure 4.11C, D and E.

During longer treatments (72h) we observed that cells underwent striking morphological changes as shown in Figure 4.12A. They became flattened, enlarged and resembled a senescent-like phenotype. It was already reported that HDACs are involved in numerous phenotypic changes associated with cellular senescence (Place et al., 2005). To confirm it in our model, we performed senescence associated (SA-) β -galactosidase staining which can be seen in Figure 4.12B. As expected, accumulation of SA- β -galactosidase occurred only in the HDACi treated cells.

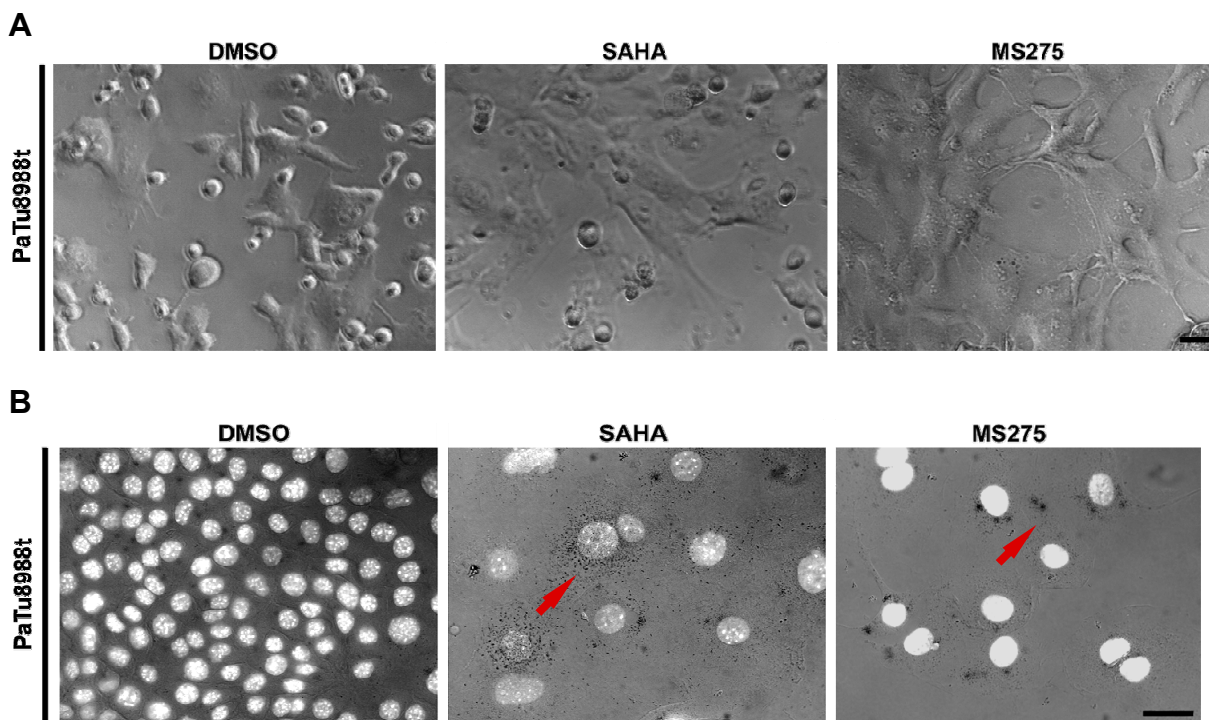


Figure 4.12. HDAC inhibitors, SAHA and MS275 induce senescence in human pancreatic cancer cell line PaTu8988t. A – Phenotypic changes of the cells upon HDACi treatment. **B** – Cells were treated with SAHA (4 μ M) or MS275 (4 μ M). Senescence associated β -galactosidase staining was performed 72h later. As depicted with the arrows, SA- β -galactosidase was accumulated only in HDACi treated cells. Nuclei are stained with DAPI (bright) and fluorescent and bright fields are merged. Pictures are taken with monochromatic camera. Scale bar – 100 μ m.

4.2.2 HDAC inhibitors regulate the expression of p53 mutants at protein and mRNA level

To investigate the role of HDACs in p53 mutant regulation, we used three human and murine cell lines derived from pancreatic cancer, which harbour different point mutations in the *Trp53* gene (PaTu8988t – $p53^{R282W}$, Panc1- $p53^{R273H}$, and murine PPT5436- $p53^{R172H}$). As it is shown in Figure 4.13A and B, both HDAC inhibitors, SAHA and MS275, decreased p53 mutant protein level. As a control we investigated survivin expression, known to decrease upon HDACi treatment (Zhao et al., 2012) As expected, survivin was also decreased in our setting (Figure 4.13A and B).

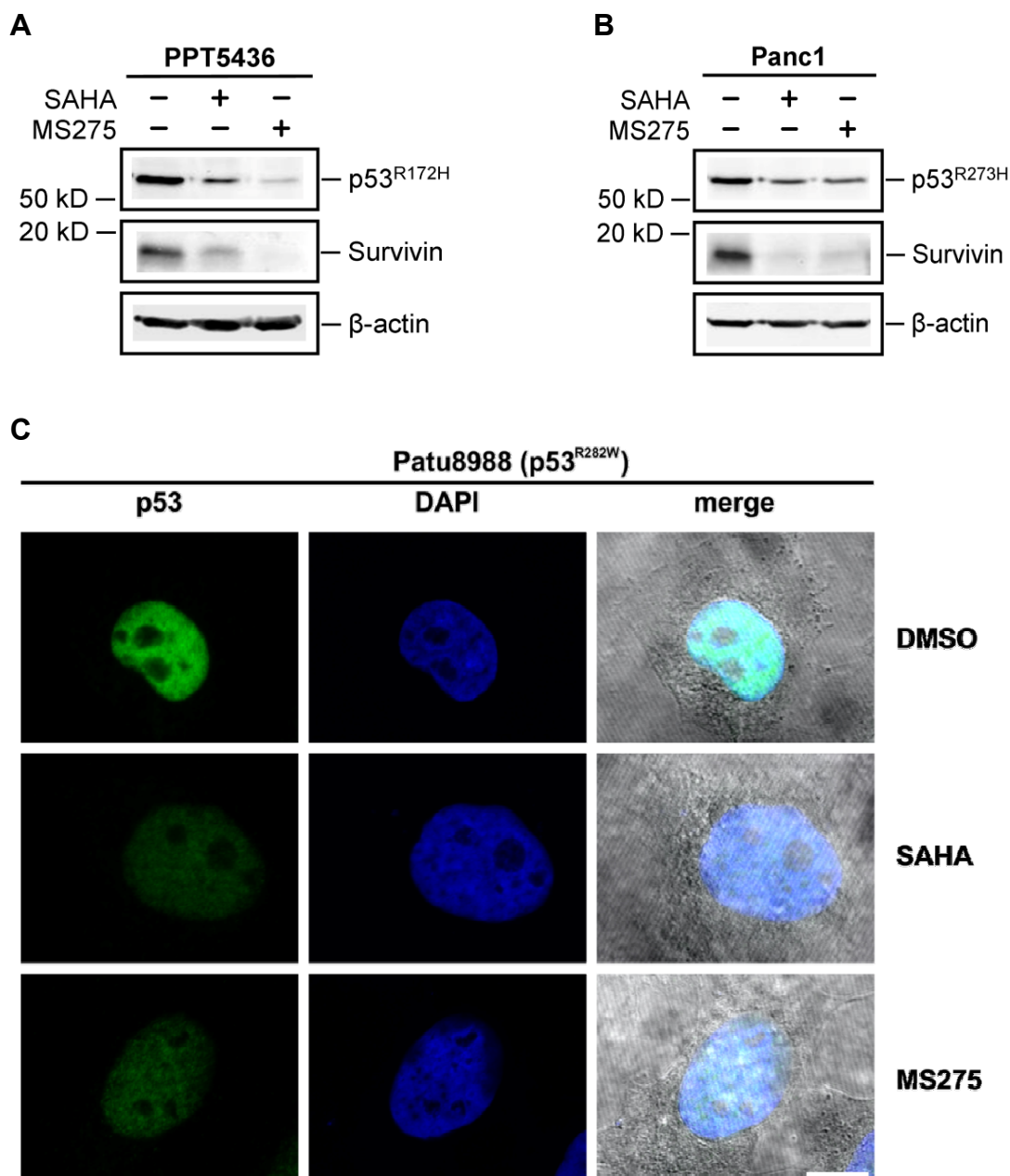


Figure 4.13. HDAC inhibitor treatment leads to depletion of mutant p53 and its targets. Western blot analysis of p53 and survivin protein levels in human Panc1 (**A**) and murine PPT5436 (**B**) cell line, 48h after SAHA (4 μ M) or MS275 (4 μ M) treatment. β -actin is used as a loading control. Experiment is performed twice. **C** – PaTu8988t cell line was treated with SAHA (4 μ M) or MS275 (4 μ M) for 48h. Cells were fixed and immunocytochemical staining against p53 is performed. Green – p53, blue – DAPI; Scale bar – 10 μ m.

This result was further confirmed with staining of p53 in human pancreatic cancer cell line PaTu8988t. As shown in Figure 4.13C, the fading of the nuclear p53 staining (green) occurs after HDACi treatment, corroborating reduced p53 protein expression.

4.2.3 p53 protein decrease is independent of MDM2 and proteasomal degradation

MDM2 is known major negative regulator of p53. It binds to p53 protein, blocks its transcriptional activity (Momand et al., 1992) and targets p53 for proteasomal degradation (Haupt et al., 1997; Kubbutat et al., 1997). To address the question if p53 protein is destabilised via MDM2, we used MDM2 specific inhibitor, Nutlin3a. As shown in Figure 4.14, blocking interaction of MDM2 and p53 with Nutlin3a does not increase p53 protein to its initial level. This result suggests that MDM2 is marginally, or not at all, involved in p53 destabilisation upon HDACi treatment. There is a slight effect in Panc 1 cell line, independently of the HDAC inhibitor (SAHA or MS275) or the time point investigated, but no effect in the other cell lines is observed.

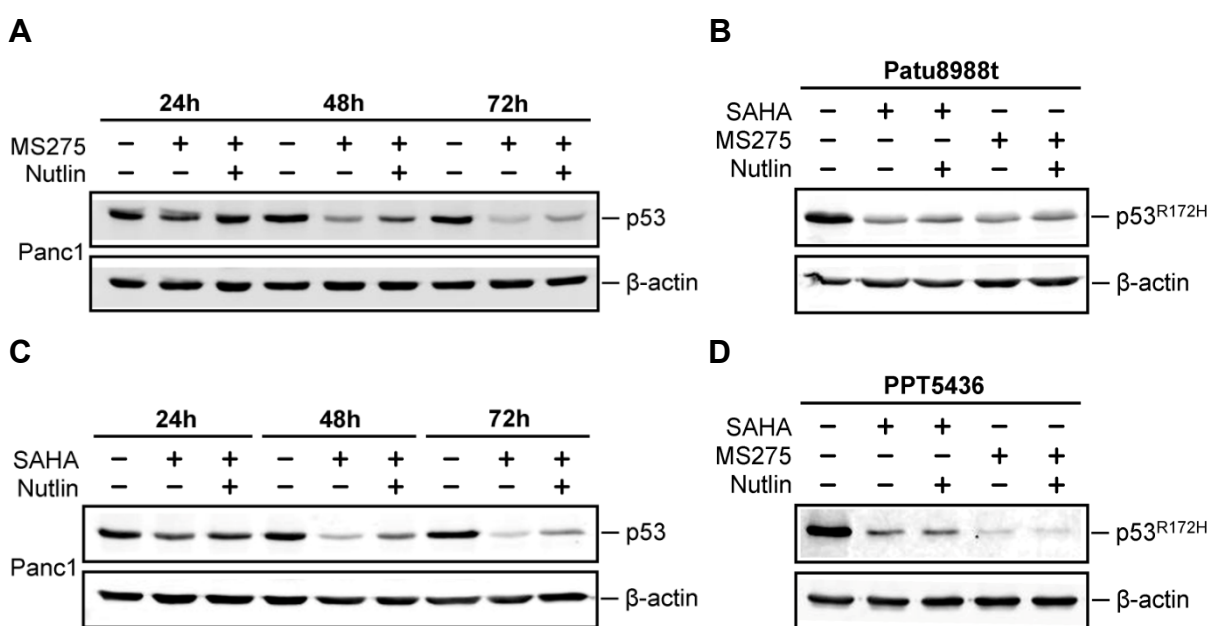


Figure 4.14. p53 protein depletion is independent of MDM2. **A** and **C** – Western blot showing kinetic of p53 depletion (24, 48, 72h) upon SAHA (4 μ M) or MS275 (4 μ M) treatment (respectively) and the p53 protein level in combined treatment (HDACi + Nutlin3a) in Panc1 cell line. Cells in combined treatment were pre-treated with (10 μ M) Nutlin3a for 2 hours and then MS275/SAHA is added. **B** and **D** – Western blot in PaTu8988t and PPT5436 cell lines (respectively) showing p53 protein level decrease upon HDACi treatment. Cells were treated with SAHA (4 μ M) or MS275 (4 μ M) for 48h or, in combined treatment, pre-treated with (10 μ M) Nutlin3a for 2 hours and then treated with HDACi and Nutlin3a for additional 24, 48 and 72h. Experiments were done twice.

The main mechanism by which cells degrade proteins is by the proteasome pathway. To investigate if p53 is degraded via the proteasome, we used a potent proteasome inhibitor MG132. Cells derived from human pancreatic cancer (Panc1 and PaTu8988t) were pre-treated with HDACi (SAHA or MS275). After 24h cells were treated again, only with HDACi or with HDACi and proteasome inhibitor MG132. As a control for effective proteasome

inhibition, we assessed the level of HSP70. As shown in Figure 4.15A and B, the combined treatment did not rescue the HDACi induced p53 down-regulation, arguing that HDACi engage a different pathway.

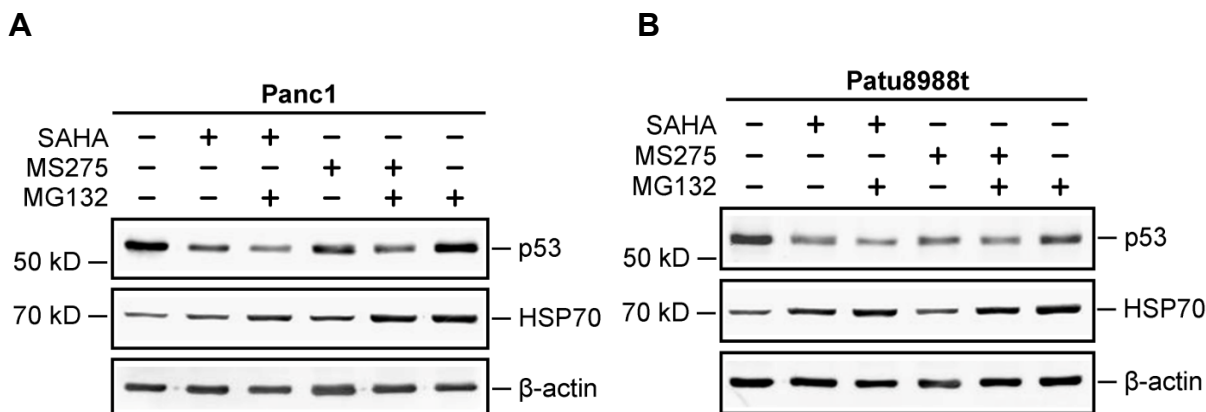


Figure 4.15. p53 protein does not undergo proteasomal degradation upon HDACi treatment. Two different human cell lines derived from pancreatic cancer, Panc1 (A) and PaTu8988t (B) were treated with HDACi, SAHA (4 μ M) or MS275 (4 μ M) for 24h. The cells were then again treated only with HDACi or simultaneously with HDACi and MG132 (10 μ M) for additional 6 hours. p53 as well as HSP70 protein levels, were determined with western blot. β -actin is used as a loading control. Experiments were done two times.

4.2.4 HDACi regulate p53 mRNA expression

The data shown in section 4.2.2 and 4.2.3 indicate that p53 protein depletion upon HDACi treatment in pancreatic cancer cell lines does not depend on a MDM2-dependent proteasomal pathway. Therefore, we investigated p53 mRNA levels in the same set-up. As shown in Figure 4.16, already after 24 hours p53 mRNA level was decreased upon SAHA or MS275 treatment in human Panc1 (Fig 4.16A) and murine PPT5436 (Fig 4.16B). The effect was even more pronounced after 48 hours.

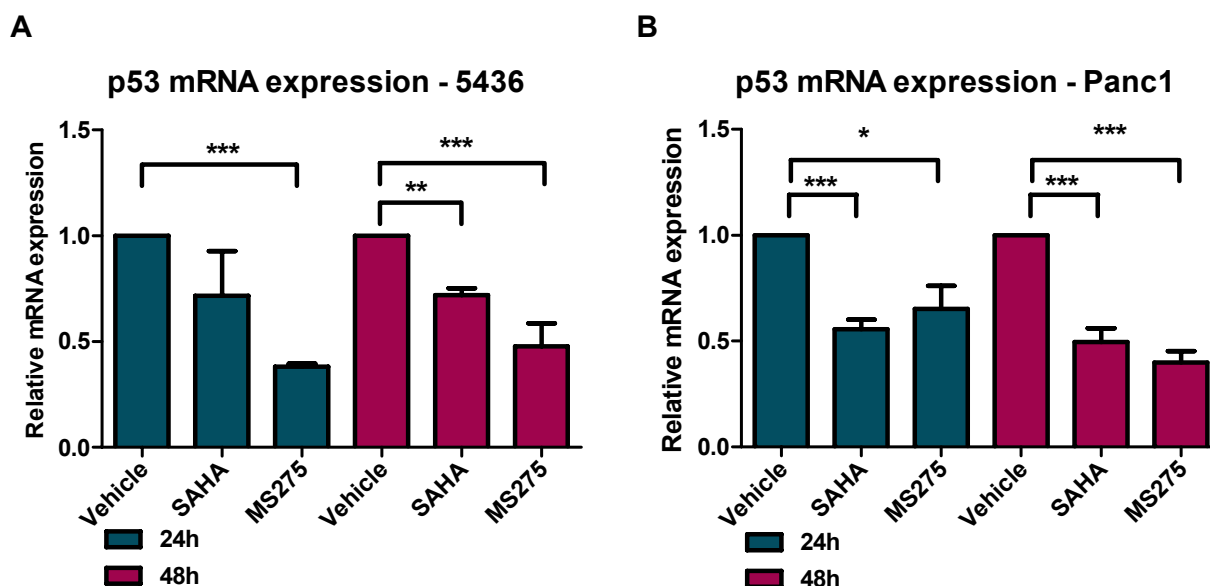


Figure 4.16. HDAC inhibitors SAHA and MS275 deplete p53 mRNA. **A** and **B** – real time quantitative PCR in PPT5436 and Panc1 cell lines, respectively. Cells were treated with SAHA (4 μ M) or MS275 (4 μ M) for 24 and 48h. Values were normalised to vehicle treated cells. Experiment was done three times with three technical replicates each. Relative mRNA levels were calculated with $\Delta\Delta$ Ct method using cyclophilin for normalisation. Mean values with SD are plotted. Statistical analyses were done with paired two tailed Student t-test and significance is depicted with asterisks above the columns. Correction for multiple testing is performed. Panc1: vehicle vs SAHA: $p=0,0004$; vehicle vs MS275: $p=0,048$; 5436: vehicle vs SAHA: $p=0,0012$; vehicle vs MS275: $p=0,0002$.

The amount of mRNA in the cell depends on transcription as well as on the stability and degradation of mRNA. Therefore, we hypothesised that HDACi-induced regulation of p53 mRNA could be due to a reduced mRNA stability. To prove this hypothesis, we blocked mRNA synthesis using Actinomycin D, an antibiotic isolated from bacterial genus *Streptomyces*. It binds transcriptional initiation complex on the DNA and blocks *de novo* mRNA synthesis. Therefore, mRNA levels decrease after the treatment, due to the limited half-life. If HDACi-induced p53 mRNA depletion was due to the decreased mRNA stability, combined treatment with MS275 and Actinomycin D should lead to more pronounced decrease of mRNA level, compared to Actinomycin D treatment alone.

Contrary to our expectations, upon Actinomycin D treatment, p53 mRNA level was only decreased up to 30% (Figure 4.17A and B), even after treatment longer than 6h (data not shown). This indicates that p53 mRNA is remarkably stable. Furthermore, there was no significant additional down-regulation of p53 mRNA upon combined Actinomycin D + MS275 treatment, compared with treatment with Actinomycin D alone (Figure 4.17A and B). Therefore, we concluded that p53 mRNA down-regulation upon HDACi treatment is not due to decreased mRNA stability.

In Figure 4.17C, semi-quantitative PCR is depicted as a control experiment, showing that *c-MYC* mRNA levels were decreased in all four experiments. This experiment shows that Actinomycin D treatment was efficient for short living mRNAs.

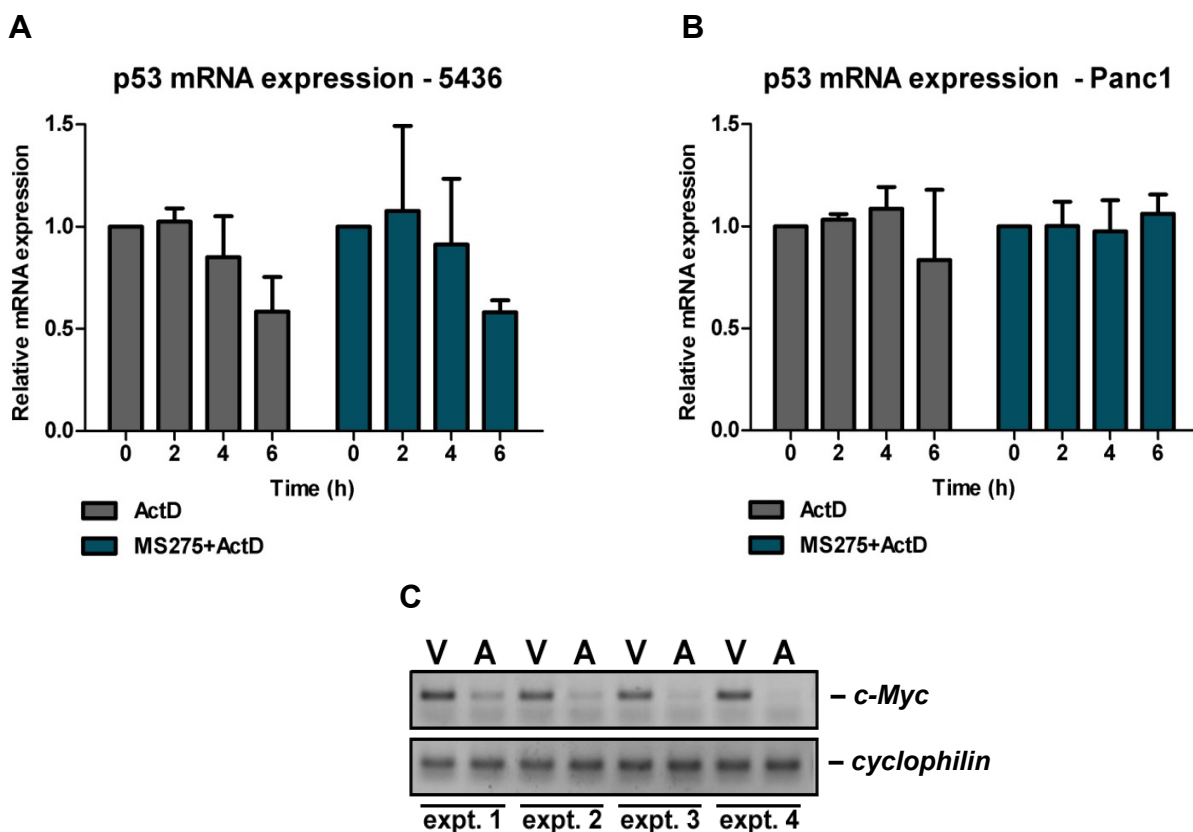


Figure 4.17. HDAC inhibitors SAHA and MS275 do not influence mRNA stability. **A** and **B** – PPT5436 and Panc1 cell lines were pre-treated with vehicle as a control group or with MS275 for 24h. Afterwards, both groups were treated with Actinomycin D for 0, 2, 4 and 6h. Every group is normalised to appropriate 0 time point. Relative mRNA levels were calculated with $\Delta\Delta Ct$ method using cyclophilin for normalisation. Mean values with SD are plotted. Statistical significance is tested with a two way ANOVA test for not repeated measurements and corrected for multiple testing ($p > 0,5$). Experiment is done three times. **C** – Semi-quantitative PCR for *c-MYC* in all four experiments. Cyclophilin A was used as a control. Experiment is done four times.

4.2.5 The role of HDAC1, 2 and 3 in p53 stabilisation

MS275 is a HDAC inhibitor that specifically blocks HDAC1, 2 and 3 activities (Bradner et al., 2010). To investigate which HDAC is responsible for p53 stabilisation, we combined chemical and genetic approaches. The role of H dac2 in p53 stabilisation is examined in *Hdac2* deficient (PPT F1042) and *Hdac2* proficient (PPT 5436) murine pancreatic cancer cell lines. Both cell lines harbour mutated *p53*^{R172H} which is stabilised on protein level in non-treated cells (Figure 4.18A). Upon treatment with SAHA or MS275 p53 is efficiently depleted

(Figure 4.18A). This result suggests that lack of Hdac2 is not sufficient to counteract the effect of HDAC inhibitors on p53 stability.

It is known that HDAC1 and 2 have a lot of overlapping functions, and one can partially complement the deficiency of another (Wilting et al., 2010). Therefore, we hypothesised that both HDAC1 and 2 need to be neutralised in order to destabilise p53. To test this hypothesis, we used the same cell lines like in figure 4.18A and, in addition, cell line F1047, which was isolated from the tumour of the mouse deficient for *Hdac2*. To deplete Hdac1, we performed siRNA mediated transitional knock down, and investigated p53 protein level. As it can be seen in Figure 4.18B, Hdac2 is present only in PPT5436 cell line, while F1042 and F1047 lack Hdac2. p53 was depleted only in *Hdac2* deficient cell lines in which Hdac1 was knocked down. This result argues that Hdac1 and 2 cooperate to maintain expression of p53 mutants.

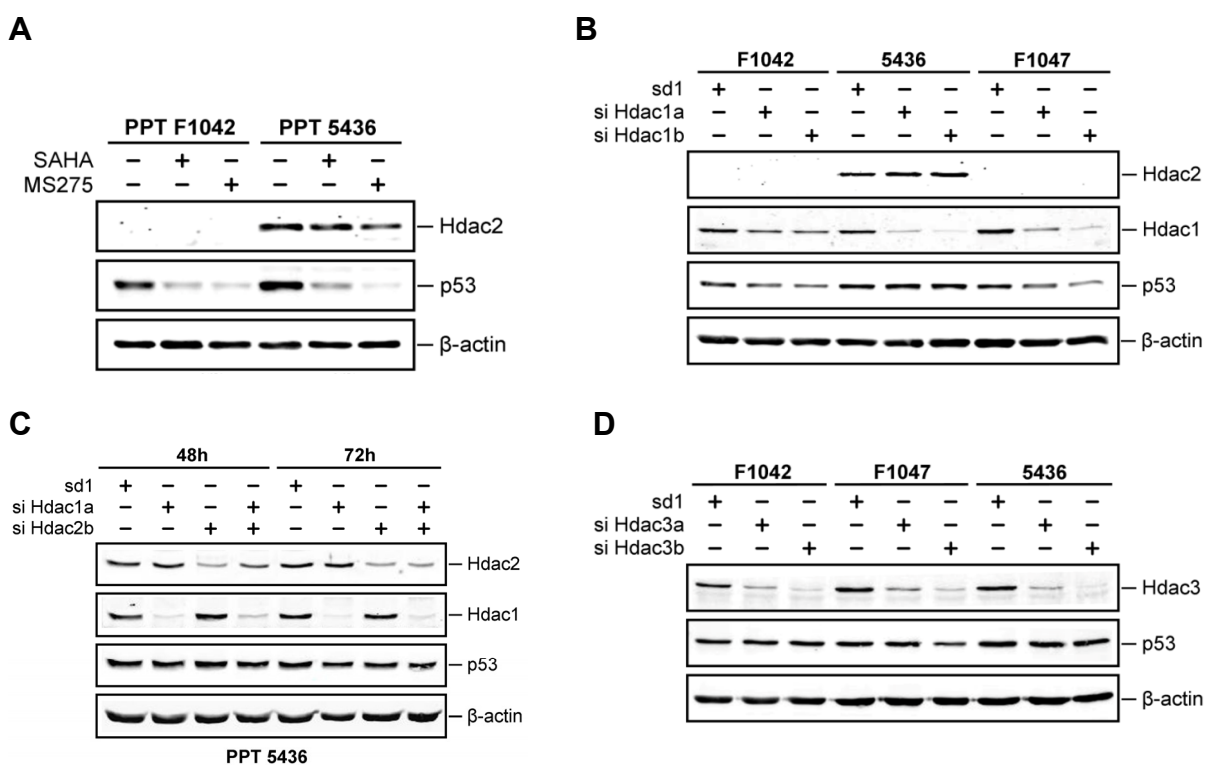


Figure 4.18. p53 regulation by Hdac1 and Hdac2. **A** – Western blot showing murine PDAC cell lines deficient (F1042) and proficient (PPT5436) for Hdac2. Cell lines were treated with SAHA (4 μ M) or MS275 (4 μ M) for 48h. Immunoblot for p53 and Hdac2. **B** – Western blot showing p53 protein decrease upon siRNA mediated *Hdac1* knock-down in F1042, F1047 and PPT5436 cell lines. Cells were transfected with two different siRNAs (100 nM each) against *Hdac1* or with control siRNA for 72h. **C** – Western blot showing HDAC1, HDAC2 and p53 protein levels after siRNA mediated *Hdac1* and/or *Hdac2* knock-down in PPT5436 cell line. Experiment was done twice. **D** – F1042, F1047 and PPT5436 cell lines were transfected with two different 100 nM siRNAs against HDAC3 or with control siRNA for 48h (immunoblot for HDAC3). P53 immunoblot shows stable protein levels upon Hdac3 knock-down independently of *Hdac2* status. β -actin is used as a loading control. All the experiments were done two times.

To confirm the regulation of p53 mutants by HDAC 1 and 2, we used *Hdac2* proficient cell line (PPT5436) and simultaneously knocked down *Hdac1* and *Hdac2*. As it can be seen in Figure 4.18C p53 was not regulated in HDAC1 and HDAC2 siRNA transfected PPT5436 cells over time. We further investigated the role of HDAC3 in p53 regulation since HDAC3 is also inhibited by MS275. For this purpose, we transiently knocked down *Hdac3* using siRNA. Independently of HDAC2 status, lack of HDAC3 could not destabilise p53 (Figure 4.18D). Therefore, we concluded that *Hdac3* plays no role in p53 regulation, while *Hdac1* and 2 act together to stabilise p53.

As it is shown in Figure 4.16A and 4.16B, HDAC inhibitors SAHA and MS275 deplete p53 mRNA. We wanted to investigate if this effect can be achieved by genetic inhibition of HDACs. Therefore, in the same setting like in the experiment shown in Figure 4.18B, we measured *p53* mRNA level after *Hdac1* knock-down. As it can be seen in Figure 4.19A, C and D, knock-down efficiency in all three cell lines was between 40% and 90%. However *p53* mRNA level did not decrease in this experiment. Instead *p53* mRNA was even slightly increased (Figure 4.19 B, D and F).

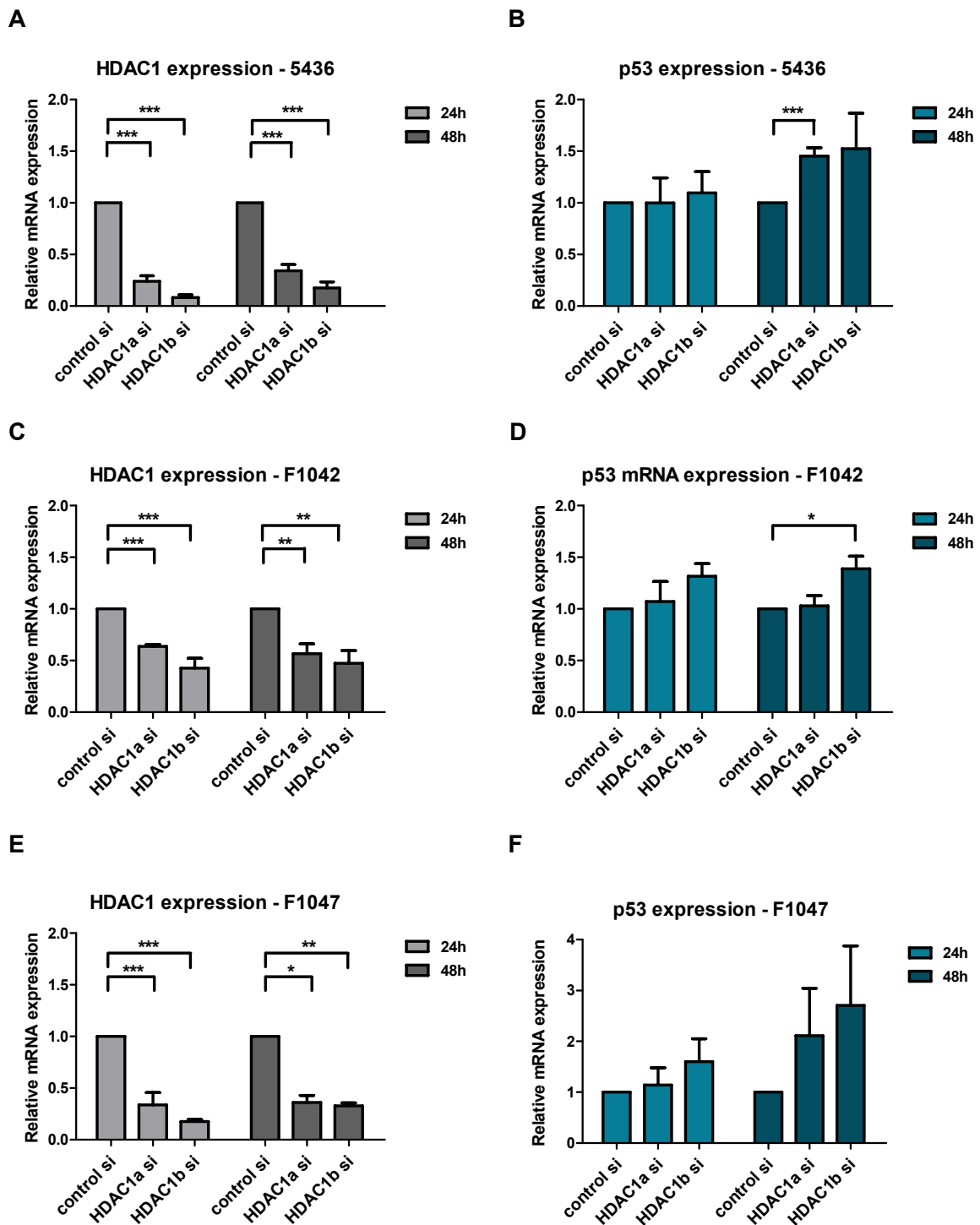


Figure 4.19. *p53* mRNA is not decreased upon *Hdac1* knock down in *Hdac2*-deficient cell lines. HDAC2 deficient (F1042 and F1047) and proficient (PPT5436) cell lines were transfected with two different *Hdac1* siRNA or a control siRNA (100 nm each). 48 hours after the transfection RNA is harvested and real time quantitative PCR is performed. **A**, **C** and **E** - *Hdac1* knock down; **B**, **D** and **F** - *p53* mRNA levels. Relative mRNA levels were calculated with $\Delta\Delta C_t$ approach normalised to cyclophilin. Mean values with SD are plotted. Statistical analyses were done with unpaired two tailed Student t-test and significance is depicted with asterisks above the columns.

4.2.6 The Role of HDAC8 in p53 stabilisation

HDAC8 is a member of the first class HDACs and it plays an important role in a diseases like acute myeloid leukaemia and T cell lymphomas (Gallinari et al., 2007). Recently, Yan and colleagues discovered that HDAC inhibitors, SAHA and sodium butyrate (NaB), suppress p53 transcription by HDAC8 via attenuation of transcription factor HoxA5 (Yan et al., 2013). As a model system, they used human cell lines from lung cancer, colorectal and pancreatic cancer as well as human keratinocytes. Therefore, we investigated contribution of HDAC8.

In both investigated cell lines F1042 and PPT5436, HDAC8 protein level was not changed upon treatment with MS275 or with SAHA (Figure 4.20A). Additionally, in all three cell lines no effect on Hdac8 protein level upon transfection with siRNA against *Hdac1* (4.20B) was observed. Therefore, we excluded the possibility that p53 depletion is a consequence of HDAC8 block by HDAC inhibitors or that HDAC8 is off target of siRNAs against *Hdac1*.

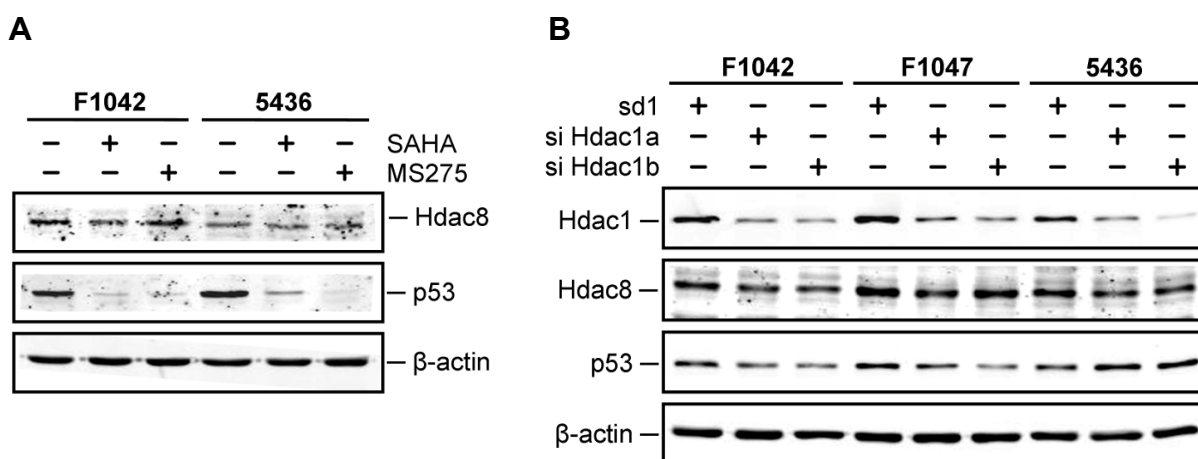


Figure 4.20. HDAC 8 is not off target of *Hdac1* siRNA and its protein level is not affected by SAHA nor MS275 treatment. **A** – Western blot showing HDAC8 and p53 protein levels after 48 hours of SAHA (4 μ M) or MS275 (4 μ M) treatment in F1042 and PPT5436. Experiment is done twice. **B** – Primary tumour cell lines F1042, F1047 and PPT5436 were transfected with control and two different siRNAs against *Hdac1* (100nM each) for 48h. HDAC1, HDAC8 and p53 protein levels are depicted. β -actin is used as a loading control.

4.2.7 Role of WRAP53 in p53 mRNA regulation

In the section 4.2.5, we have shown that HDAC inhibitors regulate p53 mRNA levels. Therefore, we wanted to investigate what is the molecular mechanism of p53 mRNA regulation.

WRAP53 was identified as an antisense RNA that binds to the 5' terminus of *p53* mRNA and stabilise it (Mahmoudi et al., 2009). To investigate if *WRAP53* is involved in HDACi mediated *p53* mRNA regulation, we determined its expression upon treatment with SAHA or MS275 in human pancreatic cancer cell line Panc1. As shown in Figure 4.21, *WRAP53- α* (A) as well as total *WRAP53* (B) levels were actually up-regulated upon SAHA and MS275 treatment. This result argues that *WRAP53* is not directly involved in destabilisation of *p53*.

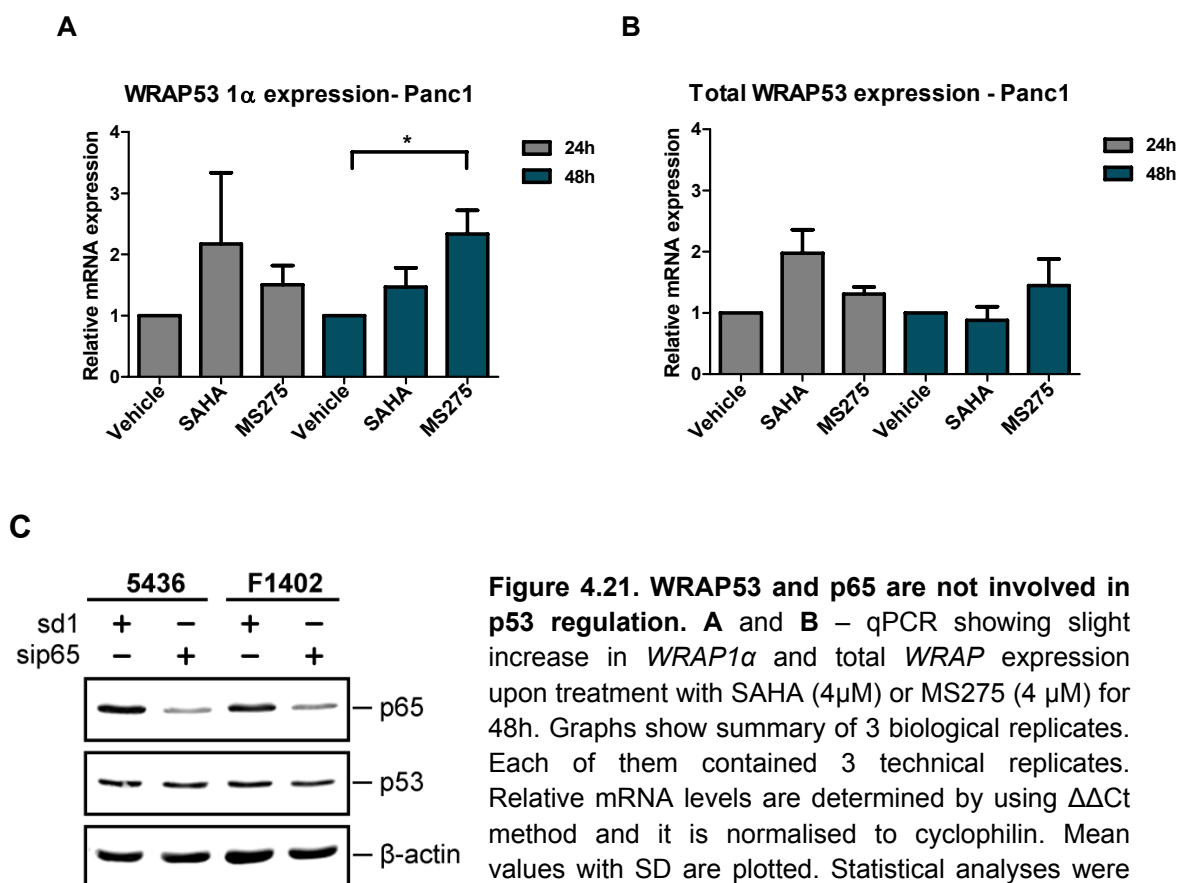


Figure 4.21. WRAP53 and p65 are not involved in p53 regulation. **A** and **B** – qPCR showing slight increase in *WRAP1 α* and total *WRAP* expression upon treatment with SAHA (4 μ M) or MS275 (4 μ M) for 48h. Graphs show summary of 3 biological replicates. Each of them contained 3 technical replicates. Relative mRNA levels are determined by using $\Delta\Delta$ Ct method and it is normalised to cyclophilin. Mean values with SD are plotted. Statistical analyses were done with unpaired two tailed Student t-test and significance is depicted with asterisks above the columns. **C** – Western blot. Panc 1 cell line was transfected with 100 nM siRNA against *p65* or with a control siRNA. After 48h proteins are isolated from harvested cells, and p53 and p65 are immunoblotted. This experiment was done twice.

Early reports from 1999 suggested that NFκB is one of the factors responsible for the basal activity of p53 promoter (Kirch et al., 1999). Since HDAC control NfκB/RelA activity in PDAC cell lines contribution of RelA in the regulation of p53 was investigated (Lehmann et al., 2009). As shown in Figure 4.20C, p53 protein abundance was unchanged by the knockdown of RelA/p65.

4.2.8 Hdac1/2 mediated p53 regulation *in vivo*

To investigate p53 regulation by HDAC1 and HDAC2 *in vivo*, we bred *Pdx1Cre; LSL-Kras^{G12D}; p53^{R172H/R172H}* mice with *Hdac1^{lox/lox}*; *Hdac2^{lox/lox}* mice. Mice with a resulting genotype should therefore have permanently activated oncogenic KRas, mutated p53 and lack of Hdac1 and Hdac2.

The objective was to compare p53 expression levels in the tumours of the mice with a final genotype (*Pdx1Cre; LSL-Kras^{G12D}; p53^{R172H/R172H}; Hdac1^{lox/lox}; Hdac2^{lox/lox}*) versus control mice (*Pdx1Cre; LSL-Kras^{G12D}; p53^{R172H/R172H}*). Up to now, we analysed one mouse with the genotype *Pdx1Cre; LSL-Kras^{G12D}; p53^{R172H/wt}; Hdac1^{lox/wt}; Hdac2^{lox/lox}*. This animal developed large tumour and lived only for 3.5 months. The tumour consisted of three parts that developed from head, body and tail of the pancreas. Histology of the tumour shows typical ductal structures in head and body of the tumour as well as acinar tumour in the tail of the pancreas (Figure 4.22). When we analysed immunohistochemical staining for p53, head-, body- and tail-derived tumours did not show huge difference in p53 stabilisation. Since immunohistochemistry cannot be considered as a quantitative approach, we have isolated cell lines from all three parts of the pancreatic cancer and compared their morphology, p53 protein and mRNA level as it can be seen in Figure 4.23.

Cells from the head of the pancreas showed highly mesenchymal morphology which is similar to the morphology of the cells isolated from ascites. Contrary, cells isolated from the tail of the pancreas show typical epithelial morphology. Cells from body of the pancreas are on the transition between two states. Surprisingly, when we analysed Hdac1 protein levels in isolated cells, we recognised that it decreases, starting from the cells isolated from the head and further on from the body. Finally, in the cells isolated from the pancreatic tail, Hdac1 protein level was the lowest. Furthermore, *p53* mRNA (Figure 4.23C) as well as protein (Figure 4.23E) showed the identical pattern of expression like the Hdac1.

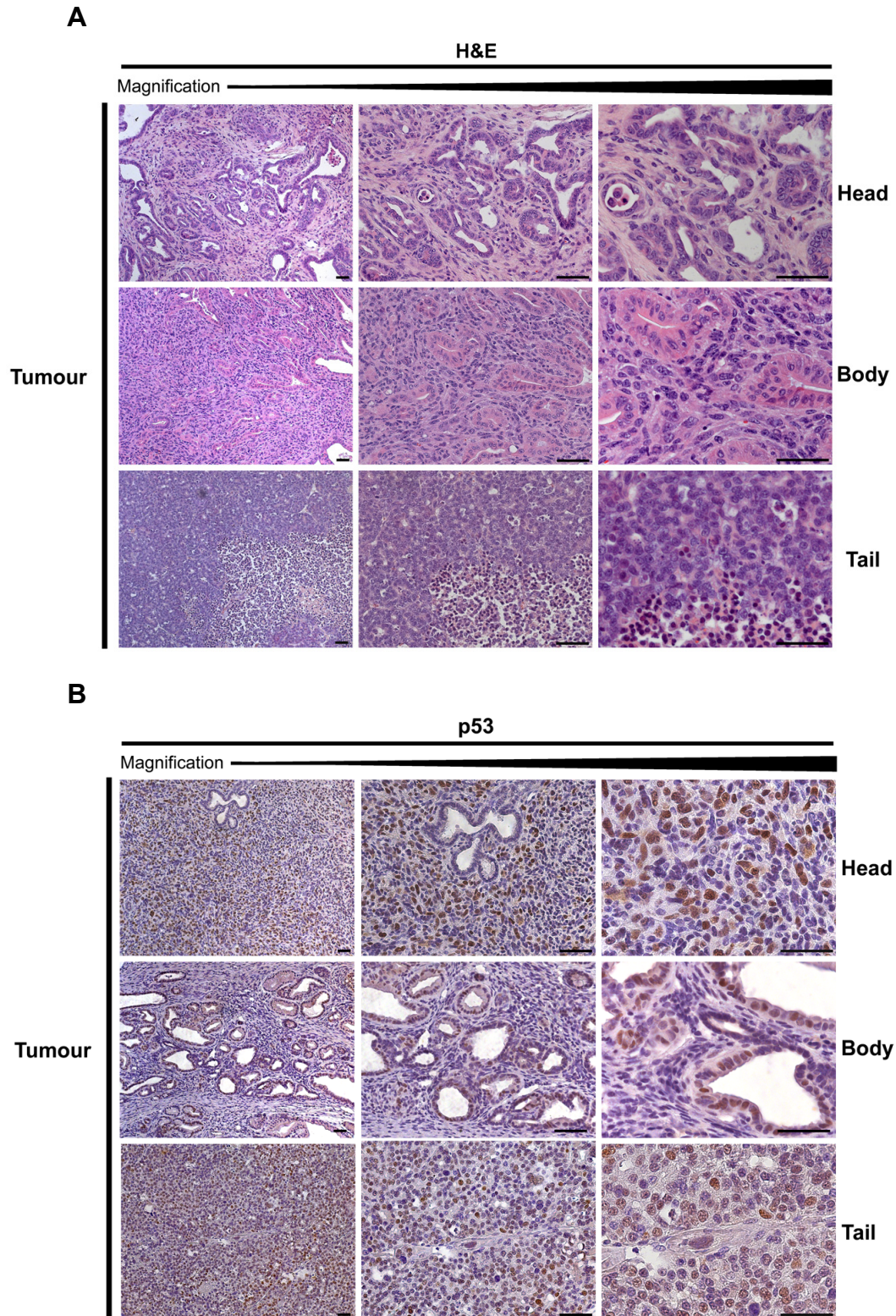


Figure 4.22. *Pdx1Cre; LSL-Kras^{G12D}; Hdac1^{lox/wt}; Hdac2^{lox/lox}; p53^{R172H/wt}* mice histology. **A** – HE staining performed on the paraffin sections from the head, body and tail of the pancreatic cancer developed in the mouse with a genotype *Pdx1Cre^{+/-}; LSL-Kras^{+/-}; Hdac1^{lox/wt}; hdac2^{lox/lox}; p53^{R172H/wt}*, at the age of 3,5 months (NSH55). **B** – Immunohistochemistry staining for p53 in paraffin sections of head, body and tail of the pancreatic cancer derived from the same mouse like in part **A**. Scale bar – 50µm.

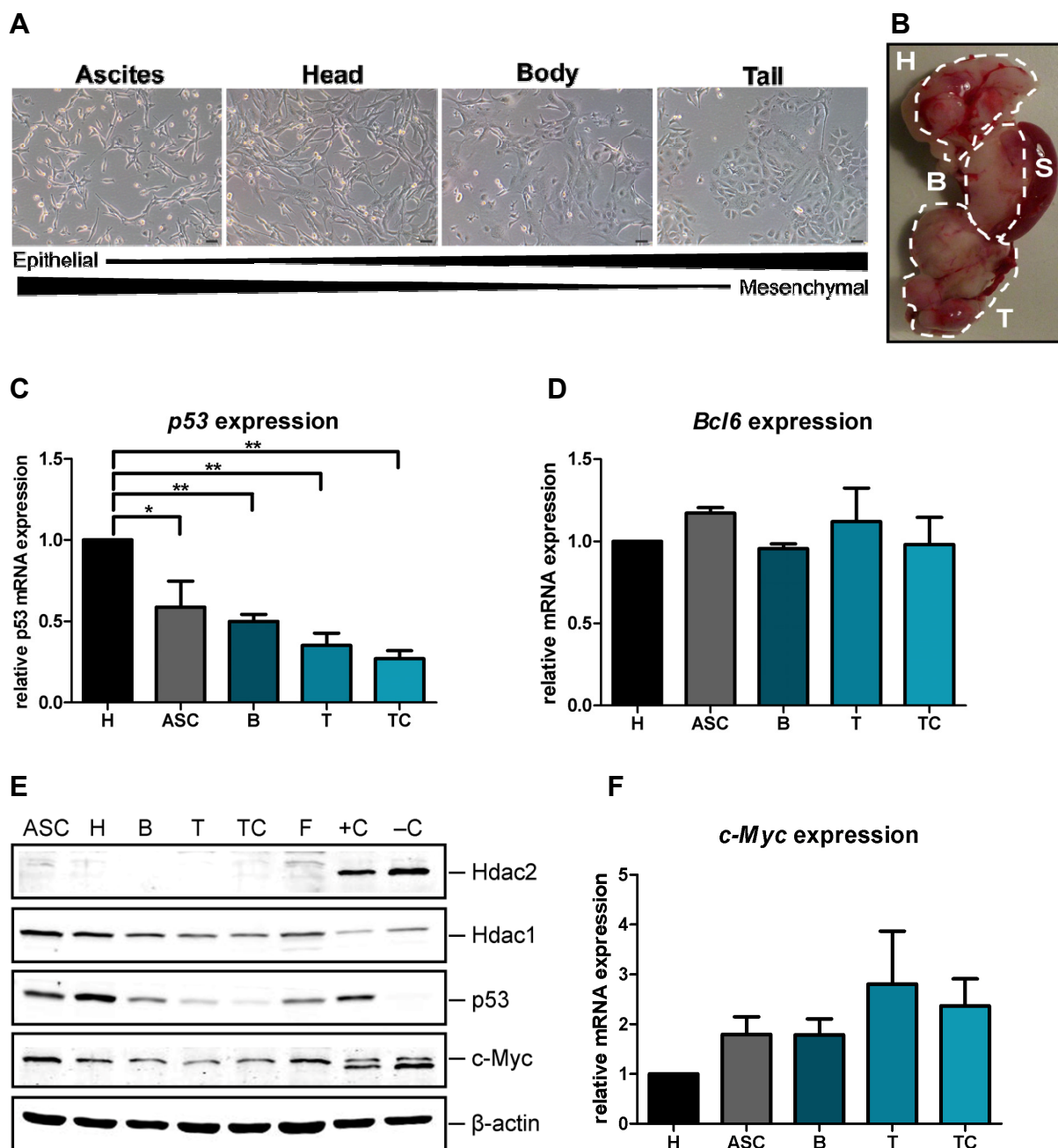


Figure 4.23. Protein levels of Hdac1, p53 and c-Myc correlate to each other in Hdac2 deficient background. **A** – Cell lines isolated from ascites (ASC), head (H), body (B) and tail (T) of the pancreatic cancer from the same mouse as in Figure 4.21. Scale bar – 100 μ M. **B** – macroscopic view of pancreatic cancer. **C**, **D** and **F** – qPCR showing relative mRNA expression of *p53*, *Bcl6* and *c-Myc* respectively in H, Asc, B, T and TC (derived from the tail cyst) cell lines from the same mouse like in figure 4.21. Relative mRNA levels are calculated with $\Delta\Delta$ Ct method and normalised to cyclophilin A using the values from 3 independent experiments. Each of experiments contained 3 technical replicates. Bars show mean values with standard deviation. Statistical significance is tested with two-tailed, unpaired t-test. **E** – Western blot showing correlation between Hdac1, Trp53 and c-Myc protein levels in *Hdac2* deficient murine cell lines ASC, H, B, T and TC cell lines. **F** is cell line derived from the mouse with a genotype *Pdx1Cre*^{+/-}; *LSL-KRas*^{+/-}; *Hdac1*^{lox/lox}; *Hdac2*^{lox/lox}; *p53*^{R172H/wt}, which retained high Hdac1 levels. Positive control (+C) for p53 is murine cell line (AA373) derived from the mouse with genotype *Pdx1Cre*^{+/-}; *LSL-KRas*^{+/-}; *p53*^{R172H/wt} and negative control (-C) is the cell line (5671) derived from the cancer of the mouse with a genotype *Pdx1Cre*^{+/-}; *LSL-KRas* *p53*^{wt/wt}. The experiment was done three times. β actin is used as a loading control.

In addition, c-Myc protein levels were high in the cell lines having high levels of Hdac1 and it gradually decreased with decreased level of Hdac1. Therefore, c-Myc protein showed the same expression pattern like the p53 protein in this system. Still, when *c-Myc* mRNA levels were investigated, we observed that *c-Myc* expression is lowest in the cells with highest level of Hdac1 and it further increases with Hdac1 decrease. From these experiments we concluded that there is a positive correlation between Hdac1, p53 and c-Myc protein levels in Hdac2 deficient cell lines. Still, the same does not apply to *c-Myc* mRNA.

It is known that human *p53* promoter has two binding sites for the BCL6 proto-oncogene which, when bound, functions as a transcriptional repressor of *p53* gene (Phan and Dalla-Favera, 2004). Therefore, we investigated *Bcl6* mRNA levels in murine cell lines with gradual expression of Hdac1, expecting that *Bcl6* might be expressed inversely to the *p53* mRNA. As it can be seen in Figure 4.23D, *Bcl6* mRNA expression remained the same independently of Hdac1 level. This result discouraged us to further investigate role of BCL6 as a potential negative regulator of *p53*.

4.2.9 The role of c-MYC in p53 regulation

Since p53 is a Myc target gene and MYC expression correlates with p53 expression in the cell lines isolated from *Pdx1Cre^{+/-};LSL-Kras^{+/-}; Hdac1^{lox/wt}; hdac2^{lox/lox}; p53^{R172H/wt}* mice, we investigated c-MYC mRNA and protein expression level upon SAHA and MS275 treatment. As it can be seen in Figure 4.24A and B, upon the treatment c-MYC was decreased on the protein but not on mRNA level.

Furthermore, we treated the Panc1 cell line with JQ1 inhibitor which inhibits c-MYC expression due to the blocked BET-bromodomain-containing proteins. Lack of BRD4 leads to the lack in recruitment of pTEF-t, transcription elongation factor whose presence and activity is necessary for successful transcription (Mertz et al., 2011). It is known that JQ1 depleats c-MYC and we could show the same in Panc1 cell line. As it can be seen in Figure 4.24C, both, c-MYC and p53 protein levels decrease when the BRD4 inhibitor is applied.

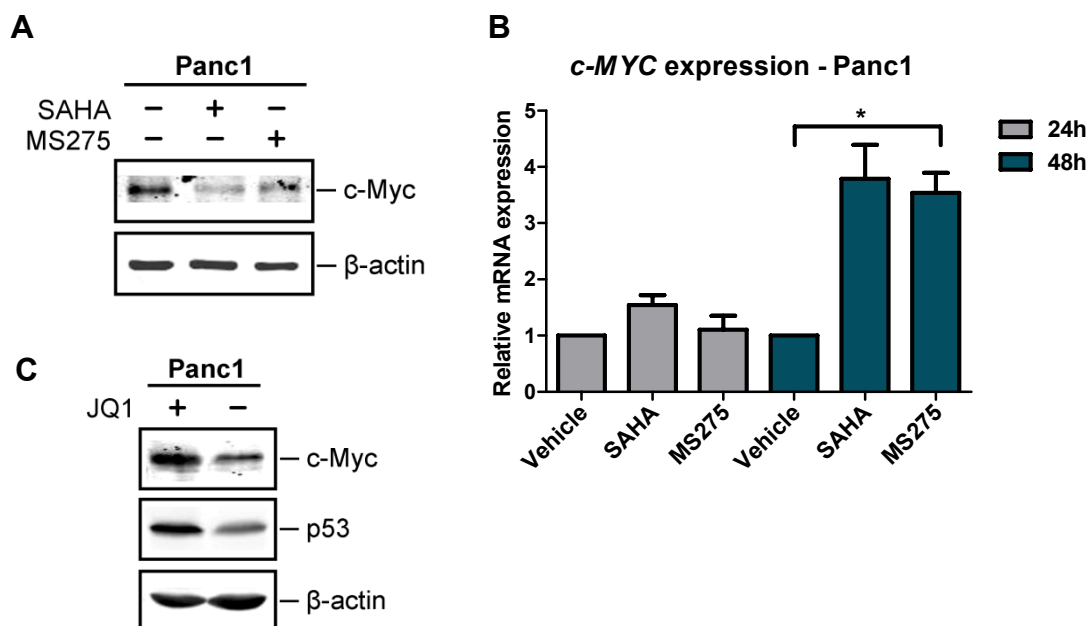


Figure 4.24. p53 and c-Myc display similar protein expression pattern. **A** – Panc1 cells were treated with SAHA (4 μ M) or MS275 (4 μ M) for 48h. Western blot showing c-MYC protein level upon the treatment. β -actin is used as a loading control. **B** – qPCR showing increased *c-Myc* mRNA expression levels upon SAHA (4 μ M) or MS275 (4 μ M) treatment. Relative mRNA levels are calculated with $\Delta\Delta$ Ct method normalised to cyclophilin, using the values from 3 independent experiments. Each of experiments contained 3 technical replicates. Bars showing mean values with standard deviation. Statistical significance is tested with two-tailed, paired t-test. P values are corrected for multiple testing. 48h: Vehicle vs SAHA, $p=0,0866$; Vehicle vs MS275, $p=0,0386$. **C** – Panc1 cells were treated with JQ1 inhibitor (0,5 μ M) for 12h. Western blot showing c-MYC and p53 protein levels upon the treatment. β actin is used as a loading control.

4.2.10 MYC bind to the p53 gene promoter and binding is regulated by HDACi

To investigate binding of MYC to the p53 gene promoter, p53 promoter scanning by chromatin immunoprecipitation (ChIP) was performed. We investigated conserved MYC binding sites predicted by software Contra in the p53 promoter, first exon, proximal part of the intron 1 and exon 2 and the 3' UTR as a control.

As it is shown in Figure 4.25A, MYC was highly present at the transcription start site, as well as in the first exon and at the beginning of the first intron. Upon MS275 treatment c-MYC binding decreased which may be the cause of the p53 mRNA down-regulation. Additionally, RNA Polymerase II (Pol II) was recruited at the transcription start site (TSS) but also in the exon 1 and proximal region of the intron 1. When cells were treated with MS275, Pol II binding was increased over the whole investigated region which is in agreement with general higher accessibility of the chromatin upon HDAC inhibitor treatment.

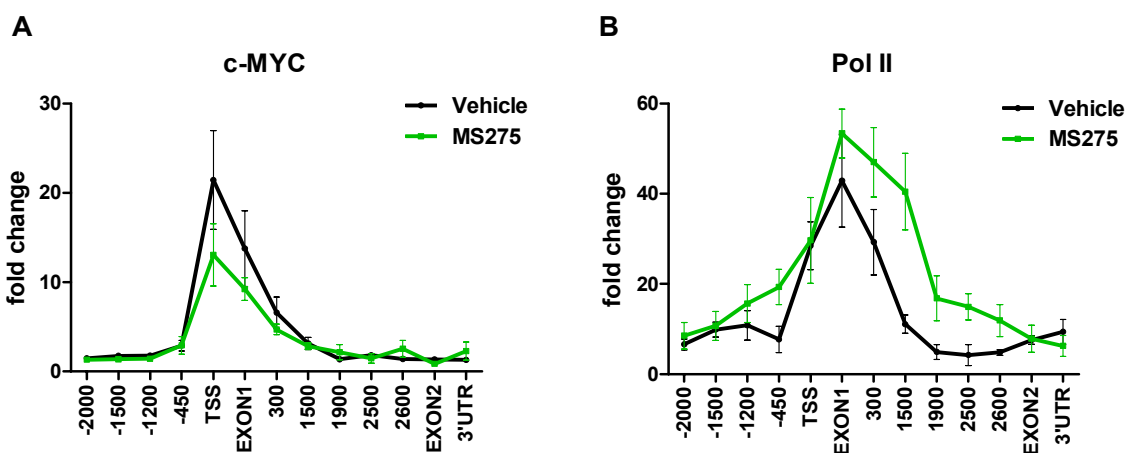


Figure 4.25, c-MYC and Pol II binding towards p53 gene upon MS275 treatment. Panc 1 cells were treated with MS275 for 24h and the whole cell lysate is used for chromatin immunoprecipitation with general anti-c-MYC (**A**) and anti-Pol II (**B**) antibodies. DNA quantification was performed with real time quantitative PCR using IgG as a negative control, and it was normalised to input (whole cell lysate without antibodies). Experiment was done four times.

We further investigated histone marks in the *p53* gene and found out that activation and repression marks were excluding each other. The marks which are in association with active chromatin, Ach3, H3K4Me3 and H3K27Ac, showed higher abundance at the TSS, exon 1 and proximal region of the intron 1, following Pol II and MYC pattern. Additionally, upon the treatment with MS275, all three marks had high peaks at the position +2500 within the first intron but they were not present at the position +1900 (Figure 4.26A, C and E). Contrary, histone marks typical for repressed regions, H3K27Me3, H3K9Me1 and H3K9Me3 had high peaks at the position +1900 but they were not present at the position +2500 (Figure 4.26B, D and F).

Since it is known that CTCF binds to the *p53* promoter and that it can serve as a barrier between transcriptionally active and non-active regions of the gene, we investigated its position on the *p53* gene (Soto-Reyes and Recillas-Targa, 2010). In both treated and non-treated cell lines CTCF showed highest recruitment in the promoter and at the TSS but lack of binding at the position 1900, where the rest of silencing marks was present (Fig 2.27A).

Additionally, increased H3K27Ac is also in agreement with blocked activity of HDACs and it is usually seen in the promoter or enhancer of the actively transcribed genes, but it also serves as a docking point for the Polycomb repression complex. In addition, we observed increase of H3K27Me3 at the region 1900. Therefore we investigated binding of the EZH2, component of the Polycomb complex, but the distribution was similar through the whole investigated region (Figure 27B).

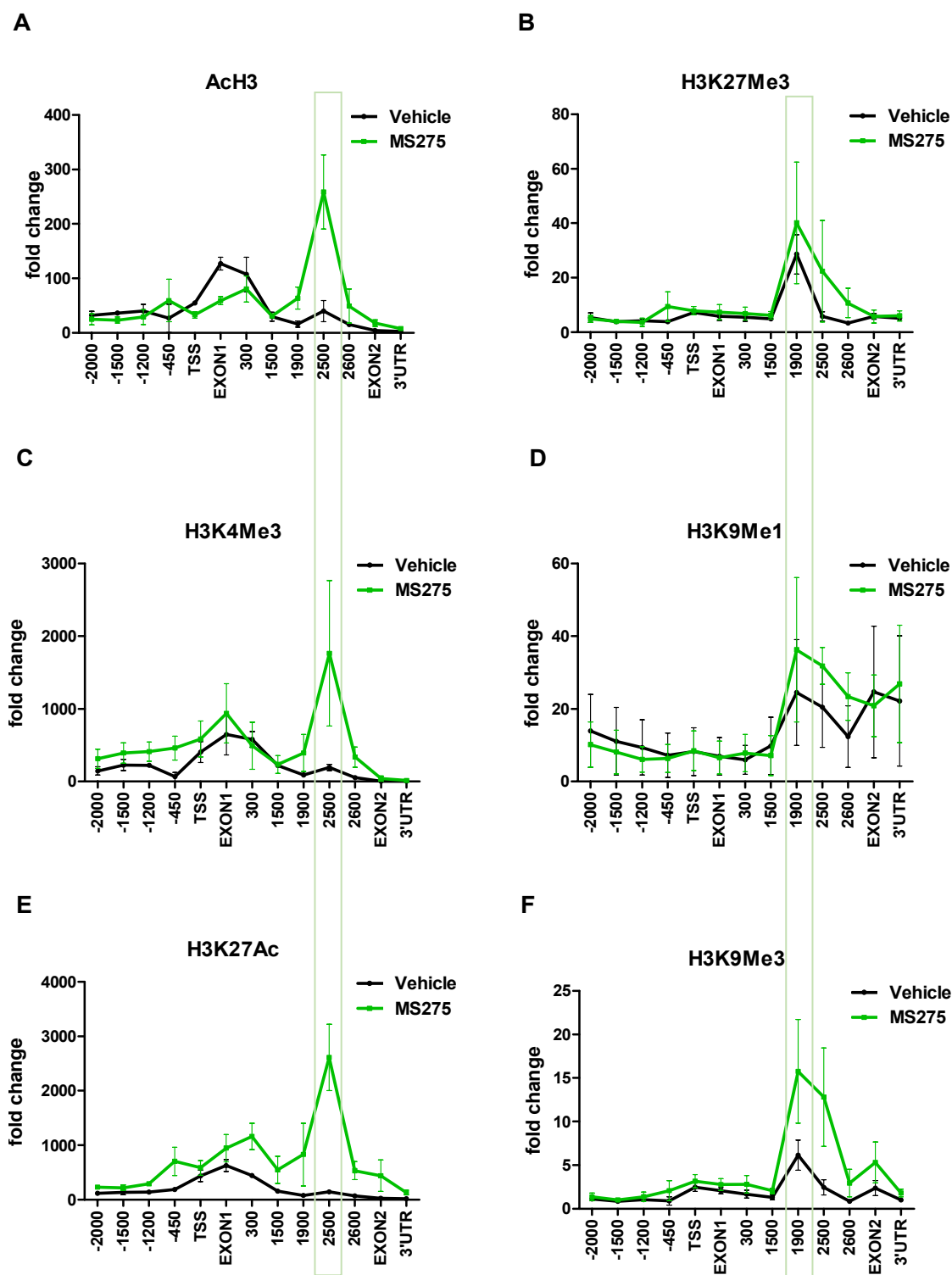


Figure 4.26. Activating and repressing histone marks upon MS275 treatment in the p53 gene. Panc 1 cells were treated with MS275 for 24h and the whole cell lysate is used for Chromatine Immunoprecipitation with antibodies against activating marks ACh3 (A), H3K4Me3 (C), H3K27Ac (E) and repressive marks H3K27Me3 (B), H3K9Me1 (D) and H3K9Me3 (F). DNA quantification was performed with real time-quantitative PCR using IgG as a negative control, and it was normalised to the abundance of histone H3.

As a part of the Polycomb repressive complex, and as an interaction partner of MYC, HDAC1 was an interesting target to investigate. In Figure 2.27C, the recruitment of HDAC1 is shown. There were no striking changes of the HDAC1 binding with a possible exception in the TSS region. Similar results were obtained for the HDAC2 (Figure 2.27D).

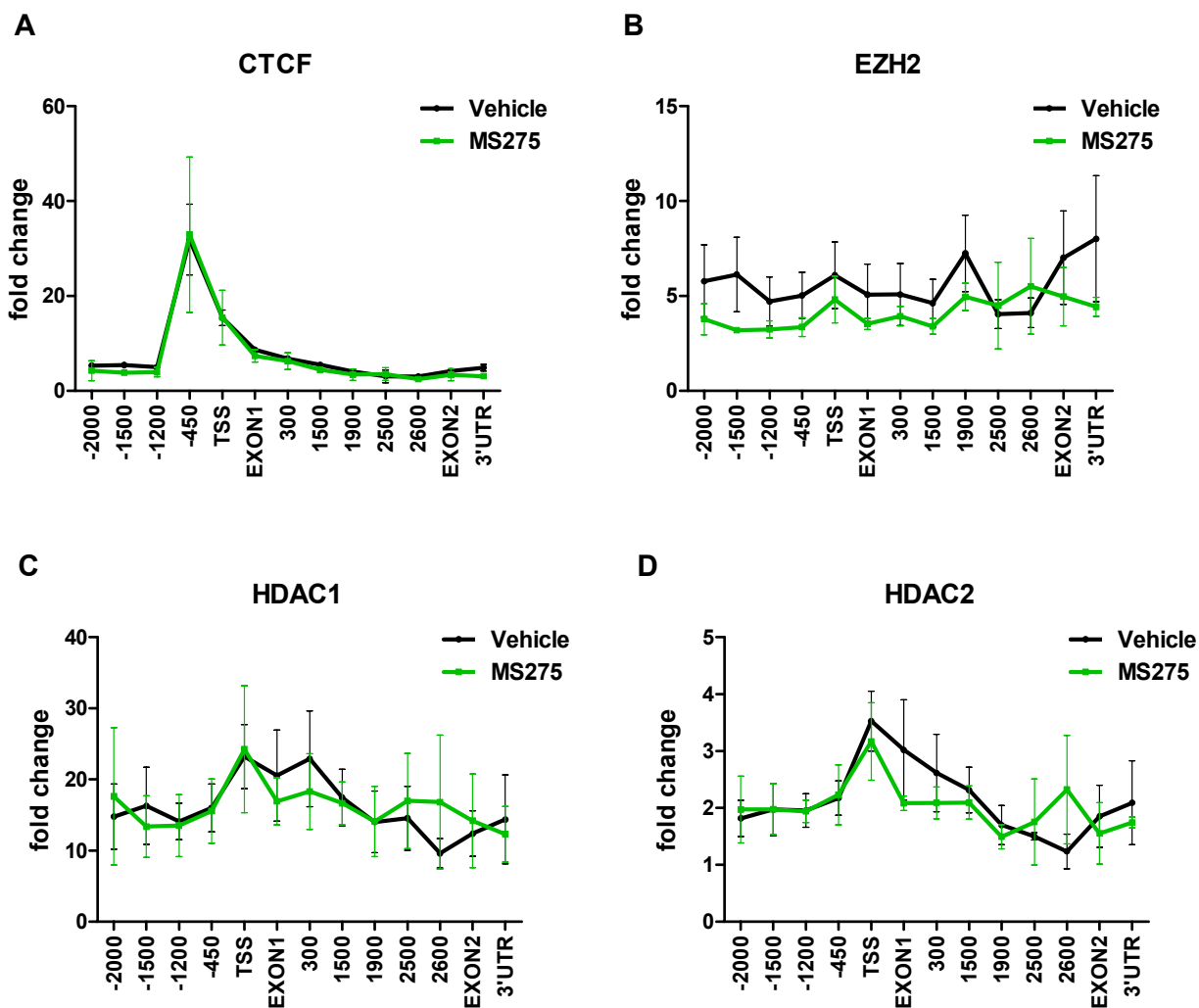


Figure 4.27. c-MYC and Pol II binding upon MS275 treatment towards p53 gene. Panc 1 cells were treated with MS275 for 24h and the whole cell lysate is used for chromatin immunoprecipitation with general anti-CTCF (**A**), anti-EZH2 (**B**) anti-HDAC1 (**C**) and anti-HDAC2 (**D**) antibodies. DNA quantification was performed with real time quantitative PCR using IgG as a negative control, and it was normalised to input (whole cell lysate without antibodies).

5 Discussion

5.1 Murine models for investigating p53^{R172H} gain of function in PDAC

Mouse models are powerful for investigating molecular mechanisms engaged in carcinogenesis, for testing therapeutics, and for analyzing tumour response and relapse. To generate site-specific modifications in the genome, *Cre-loxP* and *Flp-*frt** systems are introduced (Hoess et al., 1982; McLeod et al., 1986). Tissue specific activation of above mentioned systems is enabled by the control of their expression using tissue-specific promoters. Furthermore, introducing an additional inducible recombinase (*Flp/Cre*^{ERT2} dual recombinase system) provides tissue specific recombination at the specific time point (Section 1.3) (Metzger et al., 1995).

In this work we investigated p53^{R172H} gain of function properties, mostly in *in vitro* systems, derived from dual recombination mouse model. Morton et al., reported p53^{R172H} 'gain of function' in pancreatic cancer mouse model, in terms of higher metastatic rate of *KC*; p53^{R172H/wt} compared with *KC*; p53^{lox/wt} mice (Morton et al., 2010). The mechanisms how p53 mutants drive observed metastasis pattern are still lacking. The concept of p53 'gain of function' is very well established. Still, criteria that constitute 'gain of function' are not precisely defined.

p53^{R172H} 'gain of function' in the system we investigated, is based on the increased cell growth, as well as migratory potential, upon p53^{R172H} expression in the cell lines derived from the mouse with dual recombination system (*Flp/Cre*^{ERT2}). The mice in which p53^{R172H} was induced *in vivo*, tended to live shorter in comparison to control mice (not induced). Still, the difference was not statistically significant, which might be due to the low number of mice investigated (3 per group). It should be considered that this mouse model can have certain shortcomings which refer to early loss of wt p53. Therefore, shorter survival might also be due to the lack of wt p53 tumour suppressor function.

Mice expressing p53^{R172H} which were exposed to tamoxifen enriched food for four weeks and then sacrificed at the age of 7 weeks, stabilised p53 only within preneoplastic lesions. Using reporter system, we confirmed that recombination took place in the rest of the pancreas. This argues that p53 mutant stabilisation depends on the activated pathways that provide stabilisation and not only on the mutation itself (Terzian et al., 2008). This result is in the line with former observations coming from p53 mutant knock-in models, in which

stabilisation of p53 mutant was not detected in the normal tissue (Lang et al., 2004; Olive et al., 2004). It would be interesting to further investigate conditions which provide stabilisation of p53^{R172H}. If the pathways involved would be druggable, they might be considered as indirect way to target p53 mutant.

Relying on the 'gain of function' data, as well as on the strong p65 gene set enrichment in the cell lines harbouring p53 mutant, we analysed *p65*^{lox/lox} mice in a *KC* background with a different p53 status (*KC; p53*^{lox/lox}, *KC; p53*^{R172H/lox}, *KC; p53*^{R172H/R172}).

In contrast to dual recombinase system, p53^{R172H} did not show 'gain of function' in the sense of shorter survival in conventional model (*KC; p53*^{R172H/R172} compared with *KC; p53*^{lox/lox}). Also, *KC; p53*^{R172H/lox} mice lived significantly shorter than *KC; p53*^{R172H/R172H}, but the explanation still remains unknown. What is definitively necessary is to increase number of analysed *KC; p53*^{lox/lox} and *KC; p53*^{R172H/lox} animals. In difference to the data published by Morton et al., none of the mentioned mice developed macro-metastasis, while presence of micro-metastasis remains to be analysed. The effect can be due to the very short survival of the mice, which does not provide enough time for overgrowth of distant metastases.

Mice harbouring *p65*^{lox/lox} allele lived longer independently of the p53 status. Moreover, only the mice with *KC; p53*^{R172H/lox}; *p65*^{lox/lox} developed macro-metastasis which might be p53^{R172H} effect manifesting in those animals since they lived longer than *KC; p53*^{R172H/lox} due to the p65 truncation. To prove such a concept, analysis of more animals would be needed. In addition, the role of p65 remains to be investigated. There is a raising number of reports about p53/p65 cross-signalling and p53 'gain of function' through activation of p65 (Cooks et al., 2013; Schneider et al., 2010). Unfortunately, we could not confirm it in terms of survival in conventional *KCP* mouse model. Still, the outcome might be different in dual recombinase (*Flp/Cre*^{ERT2}) model. Together, these results indicate that 'gain of function' concept should be taken with caution with regards to criteria and systems in which it is investigated.

5.2 p53^{R172H} prepare the cell for the synthesis and increase metabolic processes

The results concerning gene expression which arose from KEGG database analysis of the cell lines in which p53^{R172H} was induced by 4'OH-tamoxifen indicate that p53^{R172H} activates genes and pathways that prepare cells for the synthesis. Those pathways involve: basal transcription factors, DNA replication, RNA polymerase, spliceosome, ribosome, aminoacyl-tRNA biosynthesis, RNA degradation, protein export, proteasome pathways and metabolic processes. All these processes might contribute to p53^{R172H} oncogenic function by promoting proliferation. Still, individual targets remain to be validated.

The most significantly enriched pathway was the ribosomal pathway. Ribosome biogenesis was formerly thought to be involved only in a production of ribosomes. Lately, increasing number of deregulated ribosomal proteins are related to malignant diseases (Holzel et al., 2010). Some of them have anticancer effect and can be considered as targets for the anti-cancer therapy. Also, surprising number of ribosomal proteins play a role in regulation of p53. By binding MDM2 they do not permit p53–MDM2 interaction and therefore lead to the stabilisation of p53 upon ribosomal stress. Ribosomal proteins S25 and S27a which were part of the enrichment core in our analysis are recently published to engage mentioned mechanism (Zhang et al., 2013; Sun et al., 2011). Additionally, RPL31 as well as RPL22 showed significant effect on the inhibition of cell growth (Su et al., 2012) and RPL37a was shown to be deregulated in numerous tumours (MacDonald et al., 2007).

Wild-type p53 suppresses protein biosynthesis machinery and therefore exerts part of its tumour-suppressive function. This is achieved by inhibiting Pol I and Pol III activity. Pol I driven transcription is blocked by association of p53 with initiation complex on the rRNA promoter (Budde and Grummt, 1999; Zhai and Comai, 2000). Transcription of tRNA can be repressed by direct interaction of p53 with Pol III transcription machinery (Crighton et al., 2003; Stein et al., 2002). tRNA transcription can be indirectly repressed by p53 dependent degradation of TFIIIB (Eichhorn and Jackson, 2001). The influence which p53 mutant has on the already mentioned regulation remains to be further investigated.

5.3 Targeting p53

WT p53 regulates cell cycle, senescence and cell death as a response to the different stimuli like DNA damage, hypoxia and oncogene activation (Vousden and Prives, 2009). Recent research confirmed the role of the p53 in aging and metabolism (Jones et al., 2005; Maddocks and Vousden, 2011; Matheu et al., 2007). All this mechanisms can be recruited by the tumour cell in order to provide selective advantage. Therefore, it is quite common that p53 wt pathway in tumours is disrupted by inactivating wt or by selecting for the mutant p53 (Soussi and Wiman, 2007).

Reactivation of p53 wt is an attractive strategy and it was confirmed as a successful approach in *in vivo* systems. Tumours in which the p53 was reactivated showed reduction of tumour size by massive apoptosis and senescence (Martins et al., 2006; Ventura et al., 2007). Moreover, small molecules, Nutlins, inhibitors of MDM2-p53 binding are very efficient in stabilisation of p53 and they are already in clinical trials (Vassilev et al., 2004). Important limitation of this strategy is that numerous tumours have lost wt p53, and therefore its reactivation is not possible. The rest of the tumours harbour mutant p53, which also needs to

be neutralised. p53 mutant can have dominant negative effect over wt p53, in which case p53 wt reactivation would not bring much. On the other hand, p53 mutant can engage pathways which are not typical for p53 wt, what constitutes 'gain of function', but they are still favoured by the tumour cell and remain unaffected by wt p53 reactivation.

Reactivation of mutant p53 transcriptional activity is rather difficult because it would require structural changes in order to renew contacts with DNA and other transcription partners. PRIMA-1 restores wt conformation and DNA binding of mutant p53 (Bykov et al., 2002). P53R3 enhances binding of the wt and mutant to the p53 promoters and induces expression of p53 targets p21 and Puma (Weinmann et al., 2008). SCH529074 binds to the core domain and restore p53 wt conformation (Demma et al., 2010). RETRA disrupt complex between p53 and p73 and release p73 which can induce apoptosis (Kravchenko et al., 2008). Still, detailed molecular mechanisms behind all those processes need to be revealed.

In addition to the attempts to reactivate wt function of p53, destabilisation of the p53 mutant offers possibility to dampen the gain of function of mutant p53. Even without reactivation of wt, this would be beneficial considering all the function of the mutant p53 that are favoured by cancer cell (Wiman, 2010). For the last twenty years few agents able to destabilise p53 mutant were reported, but the detailed mechanism of their action is mostly unknown.

5.4 HDAC inhibitors as destabilisers of p53 mutants

In addition to the reports about small molecules targeting p53 mutant, there are also reports, which claim that high stability of mutant p53 is not caused by the mutation, but rather by activated pathways which provide its stabilisation (Terzian et al., 2008). Since the therapy with small molecules is still not available, it seems reasonable to target mentioned pathways.

HDAC inhibitors are rising as a promising anticancer therapeutics and they are shown to induce cell cycle arrest, apoptosis and cellular senescence (Ogryzko et al., 1996; Roy et al., 2005). SAHA and romidepsin are shown to be efficient treatments against T cell lymphomas (Prince et al., 2009). Lot of other HDACi are developed towards higher specificity for single HDACs in order to limit side effects. Almost ten years ago it was reported for the first time that p53 is destabilised upon treatment with HDACi, FR901228, as well as trichostatin A (Blagosklonny et al., 2005). Since then, few groups tried to elucidate the mechanism of HDACi mediated p53 regulation and how the HDACs stabilise p53 mutant.

In 2011 Moll group reported that HDACi SAHA destabilises p53 mutant protein, while the p53 wt is not affected (Li et al., 2011). Additionally, SAHA is losing cytotoxic effect when

p53 mutant level in the cell is low. The destabilisation occurs due to the block of HDAC6, which subsequently leads to the acetylation and destabilisation of Hsp90. Hsp90 is necessary for stabilisation of the p53 mutant, because in the normal cell the mutant would be degraded due to the aberrant conformation (Li et al., 2011). Exact molecular mechanism engaged by existing inhibitors is mostly not known in details, but those compounds can be used as valuable research tools to study p53 biology. Knowledge derived in this way may facilitate the development of novel drugs or combinations of existing drugs to achieve more pronounced effect and to avoid resistance.

In this work, we investigated the effect of HDAC inhibitors SAHA and MS275 on the p53 mutant stability in pancreatic cancer cell lines. The human cell lines harboured spontaneously developed p53 mutations, while the murine cell lines contained p53^{R172H} and derived from genetically engineered mice. Depletion of p53 by both HDACi occurred in all investigated cell lines, which confirms it as a general effect independent of the mutation. By using nutlin3 (MDM2 inhibitor) and MG132 (proteasomal inhibitor) we showed that MDM2-mediated destabilisation of p53 protein is not the main mechanism engaged by the HDAC inhibitors, and that degradation of p53 mutant did not occur in the proteasomes.

5.5 HDACi regulate p53 mRNA levels

MS275 specifically inhibits HDAC1,-2 and -3 (Bradner et al., 2010). Therefore, the effect on p53 should not be the consequence of blocked HDAC6, and it does not have to occur on protein level, like reported by Li et al. (Li et al., 2011). In contrast, we observed 50% reduction in p53 mRNA level upon HDACi treatment (both SAHA and MS275). This result indicates that protein depletion that we observed was not totally dependent on the p53 protein stability, but rather was determined by the mRNA levels available for further translation. p53 mRNA regulation by the HDACi was additionally confirmed by Yan et al. They reported that HDAC8 inhibition by SAHA and sodium-butyrate (NaB) causes p53 mRNA decrease by the transcription factor HOXA5, which then fails to induce transcription of the p53 gene (Yan et al., 2013).

5.6 HDAC1 and HDAC2 cooperate to stabilise p53

Murine cell line deficient for HDAC2 did not show any lower level of the p53 compared with HDAC2 proficient cell line. When treated with SAHA or MS275, we observed the same ratio of p53 reduction like in HDAC2 proficient cell line, arguing that p53 destabilisation cannot be explained just by inactivation of the HDAC2.

Worth noticing is that HDAC1 and HDAC2 share 83% amino acid homology and are found together in almost all repressive transcriptional complexes (Grozinger and Schreiber, 2002). High homology indicates their functional redundancy (Wilting et al., 2010). We confirmed this hypothesis by siRNA mediated genetic approach and found out that HDAC1 and HDAC2 both need to be depleted in order to destabilise p53, while the single knock downs of *HDAC1* or *HDAC2* do not show this effect. Yan et al., showed that only siRNA against *HDAC8* led to the depletion of the p53, but they didn't test simultaneous depletion of the *HDAC1* and 2. Although HDAC8 was not our subject of interest, because it is not affected by MS275, we further eliminated any possible effect of HDAC8 on p53 stability in our system. p53 depletion could not be due to the off target effect of the siRNAs used against HDAC1 or -2 and upon SAHA or MS275 treatment, since HDAC8 level remained the same. Additionally, we did not notice any effect of HDAC3 on p53 mutant stabilisation.

5.7 Regulation of p53 transcription and mRNA stability

Investigating how the p53 gene expression is regulated was interesting for small number of scientists, compared to those who were investigating transcriptional regulation of p53 target genes. p53 expression can be regulated through different transcription factors, noncoding RNAs, its antisense RNA *Wrap53*, but still a lot of genetic and epigenetic mechanisms remain unknown.

DNA methylation, as one of the epigenetic modifications, is a general marker of silenced chromatin. Concerning methylation of the *p53* promoter, literature stays controversial. There are reports about methylated, mostly wt, *p53* promoter in breast cancer (Paroah et al., 1999), hepatocellular carcinoma (Pogribny et al., 2000) and in acute lymphoblastic leukaemia (Agirre et al., 2003) but there are also other studies claiming the lack of methylation of the *p53* promoter.

Mahmoudi and colleagues had discovered novel way of *p53* regulation (Mahmoudi et al., 2009). They have identified antisense RNA *WRAP53*, transcribed partly from the *p53* gene, but in opposite direction. The isoform *WRAP53-1 α* overlaps with *p53* exon 1 up to 1479 bp and it binds directly to 5' terminus of the *p53* mRNA, stabilizes it and provides successful translation (Mahmoudi et al., 2011).

Furthermore, *p53* mRNA can be stabilised by the proteins which are binding AU rich elements (ARE). Mostly those proteins are negative regulators, but there are two of them which can also act as positive regulators. Wig1 is a p53 target and together they build positive feedback loop. Wig1 binds to the ARE in the 3'UTR region of the *p53* mRNA and protects it from deadenylation (Vilborg et al., 2009). Also, human antigen R (HuR) is known to

increase p53 mRNA stability as well as its translation (Mazan-Mamczarz et al., 2003; Zou et al., 2006). All of these mechanisms might be the potential regulators of p53 mRNA upon HDACi treatments.

To address the question if depletion of p53 mRNA upon HDACi treatment depends on its stability or on the transcription factors involved in p53 regulation we blocked *de novo* synthesis of mRNA by applying Actinomycin D. We did not observe additional decrease in mRNA abundance in combined treatment (MS275+ActD). Therefore, we concluded that mRNA stability is not changed upon MS275 treatment. WRAP53 mRNA expression was increased upon HDACi treatment, arguing against a contribution of a WRAP53 dependent mechanism. Therefore, we focused on transcriptional regulation of p53.

For two decades it is known that c-MYC regulates p53 on a transcriptional level. Reisman et al. reported in 1993, that c-MYC/MAX binding motif (CACGTG) is present in the p53 gene. Soon after, it was confirmed that c-MYC enhances expression of p53 (Tavtigian et al., 1994). Additionally, AP1 as well as NFκB can activate p53 promoter (Kirch et al., 1999) while PAX2, 5 and 8 are known as a p53 repressors (Stuart et al., 1995). More detailed overview of p53 regulators as well as binding regions of transcription factors on p53 human and murine promoter is shown in the figure 5.1.

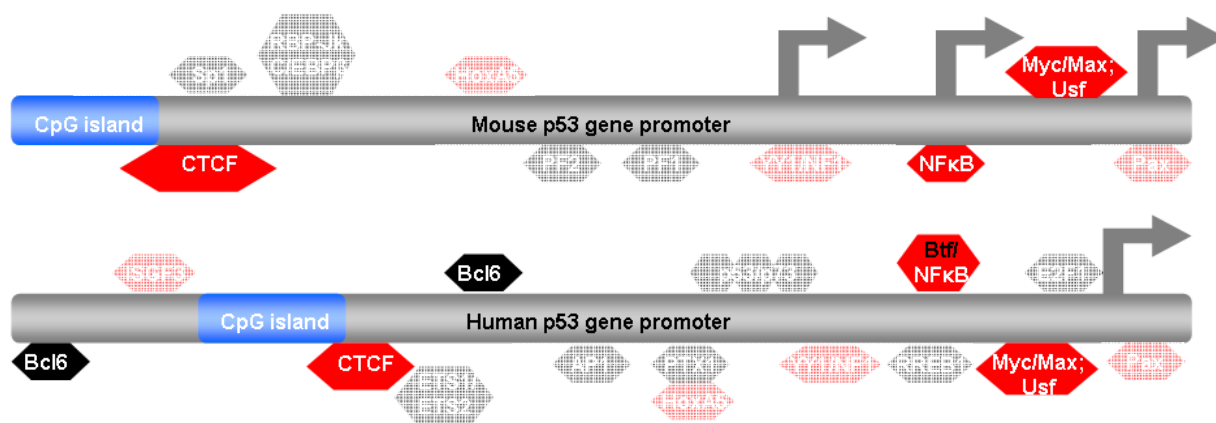


Figure 5.1 Murine and human p53 promoter occupancy. Transcription factors shown have binding motifs in the p53 promoter. Red – evolutionary conserved binding motifs for depicted transcription factors in the mouse and human. Black – binding motifs unique for the species. CpG islands as well as a transcription start sites are depicted in blue and with arrows, respectively. Modified according to (Saldana-Meyer and Recillas-Targa, 2011). The highlighted transcription factor have also been object of our research.

5.8 c-MYC binding on the p53 promoter is regulated by MS275

The observation that c-MYC undergoes same pattern of changes like the p53 on the protein level, prompted us to further focus on the c-MYC as a transcription factor possibly enrolled in regulation of p53 mRNA. c-MYC is for a long time known as an important regulator of the p53. Together with its interaction partner MAX, MYC binds to the consensus motif in the p53 gene and enhances its expression (Reisman et al., 1993; Tavitigian et al., 1994). Additionally, c-MYC is known as one of the HDAC2 targets (Marshall et al., 2010).

We and others reported previously that c-MYC protein level decreases upon HDACi treatment (Labisso et al., 2012; Xu et al., 2005). Additionally, JQ1 inhibitor treatment led to depletion of c-MYC as well as p53 protein levels. Moreover, c-MYC and p53 proteins showed similar expression patterns in the cell lines isolated from HDAC1 semi-deficient and HDAC2 deficient mice. Considering this correlation in expression, we tested for c-MYC occupancy on the p53 gene. In the ChIP analysis of the Panc1 cell line, c-MYC showed high affinity for the TSS, exon1, and the proximal region of the intron1 in vehicle treated cells. The binding was decreased upon MS275 treatment which was in line with fewer amounts of c-MYC protein available upon HDACi treatment. This result argues that lack of c-MYC protein and decreased binding at the p53 TSS after MS275 treatment contribute to the decline in the p53 mRNA and protein level. Additionally, repressive histone marks argue for an ongoing transcriptional repression.

We additionally investigated RNA Polymerase II (PolII) recruitment as well as histone marks typical for active and repressed chromatin. In non-treated cells, Pol II showed high occupancy at the TSS and exon1, but also in the proximal region of the first intron. Upon the MS275 treatment, Pol II binding was even higher towards the TSS and intron 1, which is in line with higher availability of the chromatin due to the inactive HDACs. Additionally, p53 gene transcription is regulated by three promoters. P1 is located 100-250bp upstream from the non-translated exon1. P2 is roughly 50 fold stronger than P1 and it spreads within 5' 1.2 kbp of intron 1 (Reisman et al., 1988). P3 is located within intron 4 and it harbours RE for p53 itself, being therefore part of the self-regulatory loop (Bourdon et al., 2005). Presence of the P2 might be the reason for such a spread binding of the Pol II within intron1. Problematic aspect of the p53 gene regulation is also the overlap with WRAP53 which is transcribed partly from the same sequence like p53, but in opposite direction, as it is shown in the Figure 5.2 (Hollstein and Hainaut, 2010; Mahmoudi et al., 2009).

Since it is almost impossible to elucidate in which direction Pol II is progressing, it is hard to distinguish if the recruitment is due to the necessity for p53 or WRAP53 transcription.

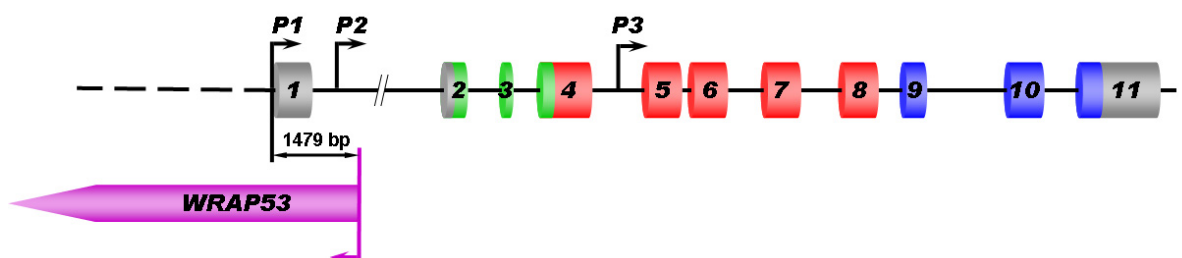


Figure 5.2. p53 gene organization and overlap with WRAP53. Structure of chromosome 17p13.1 region, showing the position and orientation of the *TP53* locus and the overlapping *WRAP53* locus. Intron/exon structure of *TP53* showing the position of P1, P2 and P3 promoters. Intron sizes are not to scale. Grey boxes, non-coding regions; green boxes, regions encoding the N-terminal, transcriptional activation domain; red boxes, regions encoding the central, DNA-binding domain; blue boxes, regions encoding the C-terminal, oligomerization domain. Modified according to (Hollstein and Hainaut, 2010).

Additionally, in many genes Pol II is recruited at the 5' end of the gene, but held paused (Core et al., 2008). Therefore it is necessary to investigate Pol II status. Phosphorylation of the Pol II at the Ser5 by the kinase subunit of the GTF TFIIF is a characteristic of the paused status. During paused status negative elongation factor (NELF) is bound, not allowing Pol II to proceed along DNA strand. To activate Pol II, it is necessary to phosphorylate Ser 2, which is done by the positive-transcription elongation factor b (P-TEF-b)(Fuda et al., 2009). Then, NELF dissociates and transcription can proceed further. To investigate if the Pol II is active or not, it is necessary to examine binding of Pol II phosphorylated at the Ser2 and 5 as well as the presence of NELF, TFIIF and pTEF-b on the p53 promoter and on the distant exons. This is going to be subject of our further research.

Another aspect of p53 transcription are PAX proteins which are known as a potent repressors. They bind within 3' end of the exon 1, but there are also reports arguing that within intron 1, PAX responsive elements exist. Up to now, we do not know if the PAX proteins are regulated by acetylation and if they are targeted by HDACs, but it would be worth investigating it.

5.9 MS275 treatment reveals repressed region within first intron of the p53 gene

P53 gene harbours 10 kb long intron 1. It is common case that within those long introns lot of regulative sequences exists or some of regulatory RNAs are coded. We found within p53 intron 1 high chromatin activating marks (AcH3, H3K4Me3 and H3K27Ac) at the position +2500, where only low amounts of Pol II were present. The repressive marks (H3K9Me3, H3K27Me3 and H3K9Me1) were highly increased at the position +1900. From this perspective, the final explanation cannot be made. However, the scenario might be that p53

is constitutively expressed in non-treated cells and upon MS275 treatment high repressive marks appear and the transcription is blocked. In other words, MS275 is switching an active promoter to an poised promoter with a paused RNA Pol II. Such a scenario definitely needs further supporting data, specifically about the phosphorylation state of RNA Pol II and the co-recruitment of NELF.

According to the induction of the repressive marks, one possible mechanism could be that an insulator is present in the position +1900. Insulators are complex regulatory elements on the DNA that provide gene isolation from the influence of the regulatory elements that belong to the other genes (Burgess-Beusse et al., 2002). The factor which is usually associated with chromatin boundaries is zinc finger protein, CTCF (Phillips and Corces, 2009). CTCF commonly occupies intergenic regions, but it is also known that there are exceptions like the *PUMA* gene where CTCF binds at the intragenic boundaries (Gomes and Espinosa, 2010; Kim et al., 2007). Therefore, we investigated binding of the CTCF towards p53 gene, but CTCF was not bound to the +1900 region. It was rather present in the region which is already known as a CTCF binding region in the p53 gene between -781 and -381 and its abundance was not influenced by the treatment. Still, different types of insulators exist and not all of them depend on the CTCF binding, but they are going to be subject of further investigation.

5.10 Potential role of the repressive complexes in the regulation of the p53 transcription

H3K27Ac mark is characteristic for the active promoters and enhancers, and it can serve as a signal for recruitment of the Polycomb complex members. Proteins of the Polycomb group (PcG) are responsible for epigenetic repression of transcription (Schwartz and Pirrotta, 2013). The members can be part of the Polycomb repressive complexes PRC1 or PRC2 which are recruited to PcG target genes (Schwartz and Pirrotta, 2013). In mammalian PRC2 complex, enzymatic function is performed by EZH2 (enhancer of zeste homologue 2) which acts as a methyltransferase and they can transfer monomethyl, dimethyl or trimethyl groups to the lysine 27 at the histone 3 (H3K27) (Cao et al., 2002). It is also well known that H3K27Me3 is competitive to the acetylation of H3K27, which is the mark usually seen in promoter or enhancer of the actively transcribed genes.

Since we observed accumulation of the H3K27Me3 at the position +1900 and H3K27Ac at the position +2500, an exclusive pattern of the appearance of those two histone marks, we investigated binding of the EZH2 within the *p53* gene. As it is shown in the Figure 2.27B, EZH2 was present through the whole investigated region of the p53 gene without any

significant peaks. Therefore, we could not argue about recruitment of the Polycomb complex. Still, additional methyltransferases like G9a, GLP or SUV39H are known to be responsible for H3K27Me3 and they will be tested in further experiments.

Moreover, other Polycomb-dependent scenarios can be involved in this type of regulation. For instance, elongation of transcription by RNA Pol II highly depends on the ubiquitination of H2A by RING1 or RING2 which also belong to the Polycomb complex (Zhou et al., 2008). It could be that by the recruitment of one of those two Polycomb members, elongation is stalled at the position +1900, but this still remains speculation.

HDAC1 can be part of the RING2–L3MBTL2 – alternative Polycomb complex, in appropriate context (Schwartz and Pirrotta, 2013). Thus, we examined binding of the HDAC1 and also HDAC2 on the p53 gene. There was no significant change in binding, except marginal recruitment at the TSS (Fig. 4.27C and D). Still, this result does not exclude HDACs as relevant targets because, through modified acetylation, HDACs are able to modify activity of the TF which are part of the huge transcriptional machineries. Their binding properties do not have to be changed to provide alterations in the function of the whole complex. Therefore, it might be impossible to determine HDAC1 and 2 role with a CHIP but rather with enzymatic assays.

6 Summary

Pancreatic ductal adenocarcinoma is a severe disease with a 5-year survival rates under 5% due to the lack of the efficient therapy, as well as due to the inefficient diagnostic tools. Tumour suppressor p53 is mutated in 50-70% of PDACs and current reports indicate its pronounced oncogenic function (gain of function, GOF) which might mediate therapeutic resistance. Molecular mechanisms behind p53 mutant GOF are still not understood and need to be addressed.

In this work *in vivo* and cell based *ex-vivo* models for investigating p53^{R172H} GOF in pancreatic cancer were developed and characterised. For this purpose, mice harbouring p53^{R172H} was crossed in the mouse model with double recombinase (Flp/Cre) system and mutated KRas. This model provided pancreas specific sequential activation of the oncogenic Kras^{G12D} and p53^{R172H}. Generated *ex-vivo* models provided a tool for investing molecular mechanisms of p53 biology in malignant (tumour cell lines) and non-malignant (pancreatic ductal epithelial cells) environment. Furthermore, in this work p53^{R172H} was shown to improve cell growth and facilitate cell migration (gain of function) in cell lines derived from the dual recombinase system. Still, for proving its equivalent function in *in vivo* models additional animals need to be analysed.

Contrary, we were not able to prove p53^{R172H} GOF in terms of prolonged survival in the conventional model (KC model), mainly due to the short survival of control, as well p53^{R172H} expressing mice. Taking in consideration p53/p65 cross signalling as well as recent reports of the role of p65 in p53 mediated GOF, we investigated the influence of p65 inactivation on the mouse survival in conventional model (KC) with different p53 status. We observed prolonged survival of the mice carrying p65^{lox/lox} allele, independently of their p53 status. The mechanism behind this phenomenon is not known and it remains to be further investigated.

Additionally, p53 responded on the potential therapeutics, histone deacetylase inhibitors (HDACi), by drastic destabilization on mRNA and protein level, upon SAHA and MS275 treatment. We found that partly this was due to the lack of c-Myc mediated transcriptional activation. The epigenetic landscape indicates that additional players, like transcriptional repressive complexes might be involved. In this work, novel mechanism of p53 stabilization is discovered, and it is mediated by HDAC1 and HDAC2. Still, detailed regulation will be further investigated.

Potential mechanisms for destabilisation of p53^{R172H} should be considered as a promising way to overcome p53 mutant GOF and decrease p53^{R172H} dependent therapeutic resistance. The results achieved in this work provide important new insights into transcriptional regulation of the p53 gene and role of HDACs in it. Further investigation of molecular mechanisms of p53 GOF and p53 regulation might open potential novel therapeutic strategies.

7 References

- Agirre, X., Novo, F. J., Calasanz, M. J., Larrayoz, M. J., Lahortiga, I., Valganon, M., Garcia-Delgado, M., and Vizmanos, J. L. (2003). TP53 is frequently altered by methylation, mutation, and/or deletion in acute lymphoblastic leukaemia. *Mol Carcinog* 38, 201-208.
- Alberts B, J. A., Lewis J, Raff M, Roberts K, Walter P (2012). *Molecular Biology of the Cell*, Fifth edition (New York: Garland Science, Taylor & Francis Group).
- Algul, H., Treiber, M., Lesina, M., Nakhai, H., Saur, D., Geisler, F., Pfeifer, A., Paxian, S., and Schmid, R. M. (2007). Pancreas-specific RelA/p65 truncation increases susceptibility of acini to inflammation-associated cell death following cerulein pancreatitis. *J Clin Invest* 117, 1490-1501.
- Arrowsmith, C. H., Bountra, C., Fish, P. V., Lee, K., and Schapira, M. (2012). Epigenetic protein families: a new frontier for drug discovery. *Nat Rev Drug Discov* 11, 384-400.
- Baker, S. J., Preisinger, A. C., Jessup, J. M., Paraskeva, C., Markowitz, S., Willson, J. K., Hamilton, S., and Vogelstein, B. (1990). p53 gene mutations occur in combination with 17p allelic deletions as late events in colorectal tumorigenesis. *Cancer Res* 50, 7717-7722.
- Bantscheff, M., and Drewes, G. (2012). Chemoproteomic approaches to drug target identification and drug profiling. *Bioorg Med Chem* 20, 1973-1978.
- Bartlett, J., Blagojevic, J., Carter, D., Eskiw, C., Fromaget, M., Job, C., Shamsher, M., Trindade, I. F., Xu, M., and Cook, P. R. (2006). Specialized transcription factories. *Biochem Soc Symp*, 67-75.
- Barton, C. M., Staddon, S. L., Hughes, C. M., Hall, P. A., O'Sullivan, C., Kloppel, G., Theis, B., Russell, R. C., Neoptolemos, J., Williamson, R. C., and et al. (1991). Abnormalities of the p53 tumour suppressor gene in human pancreatic cancer. *Br J Cancer* 64, 1076-1082.
- Blagosklonny, M. V., Trostel, S., Kayastha, G., Demidenko, Z. N., Vassilev, L. T., Romanova, L. Y., Bates, S., and Fojo, T. (2005). Depletion of mutant p53 and cytotoxicity of histone deacetylase inhibitors. *Cancer Res* 65, 7386-7392.
- Bourdon, J. C., Fernandes, K., Murray-Zmijewski, F., Liu, G., Diot, A., Xirodimas, D. P., Saville, M. K., and Lane, D. P. (2005). p53 isoforms can regulate p53 transcriptional activity. *Genes Dev* 19, 2122-2137.
- Bradford, M. M. (1976). A rapid and sensitive method for the quantitation of microgram quantities of protein utilizing the principle of protein-dye binding. *Anal Biochem* 72, 248-254.
- Bradner, J. E., West, N., Grachan, M. L., Greenberg, E. F., Haggarty, S. J., Warnow, T., and Mazitschek, R. (2010). Chemical phylogenetics of histone deacetylases. *Nat Chem Biol* 6, 238-243.

- Bradner, J. E., Mak, R., Tanguturi, S. K., Mazitschek, R., Haggarty, S. J., Ross, K., Chang, C. Y., Bosco, J., West, N., Morse, E., et al. (2010). Chemical genetic strategy identifies histone deacetylase 1 (HDAC1) and HDAC2 as therapeutic targets in sickle cell disease. *Proc Natl Acad Sci U S A* 107, 12617-12622.
- Budde, A., and Grummt, I. (1999). p53 represses ribosomal gene transcription. *Oncogene* 18, 1119-1124.
- Burgess-Beusse, B., Farrell, C., Gaszner, M., Litt, M., Mutskov, V., Recillas-Targa, F., Simpson, M., West, A., and Felsenfeld, G. (2002). The insulation of genes from external enhancers and silencing chromatin. *Proc Natl Acad Sci U S A* 99 Suppl 4, 16433-16437.
- Burnette, W. N. (1981). "Western blotting": electrophoretic transfer of proteins from sodium dodecyl sulfate--polyacrylamide gels to unmodified nitrocellulose and radiographic detection with antibody and radioiodinated protein A. *Anal Biochem* 112, 195-203.
- Bykov, V. J., Issaeva, N., Shilov, A., Hultcrantz, M., Pugacheva, E., Chumakov, P., Bergman, J., Wiman, K. G., and Selivanova, G. (2002). Restoration of the tumor suppressor function to mutant p53 by a low-molecular-weight compound. *Nat Med* 8, 282-288.
- Cadwell, C., and Zambetti, G. P. (2001). The effects of wild-type p53 tumor suppressor activity and mutant p53 gain-of-function on cell growth. *Gene* 277, 15-30.
- Cao, R., Wang, L., Wang, H., Xia, L., Erdjument-Bromage, H., Tempst, P., Jones, R. S., and Zhang, Y. (2002). Role of histone H3 lysine 27 methylation in Polycomb-group silencing. *Science* 298, 1039-1043.
- Chang, C., Simmons, D. T., Martin, M. A., and Mora, P. T. (1979). Identification and partial characterization of new antigens from simian virus 40-transformed mouse cells. *J Virol* 31, 463-471.
- Conroy, T., Desseigne, F., Ychou, M., Bouche, O., Guimbaud, R., Becouarn, Y., Adenis, A., Raoul, J. L., Gourgou-Bourgade, S., de la Fouchardiere, C., et al. (2011). FOLFIRINOX versus gemcitabine for metastatic pancreatic cancer. *N Engl J Med* 364, 1817-1825.
- Cooks, T., Pateras, I. S., Tarcic, O., Solomon, H., Schetter, A. J., Wilder, S., Lozano, G., Pikarsky, E., Forshe, T., Rosenfeld, N., et al. (2013). Mutant p53 prolongs NF-kappaB activation and promotes chronic inflammation and inflammation-associated colorectal cancer. *Cancer Cell* 23, 634-646.
- Core, L. J., Waterfall, J. J., and Lis, J. T. (2008). Nascent RNA sequencing reveals widespread pausing and divergent initiation at human promoters. *Science* 322, 1845-1848.
- Crawford, L. V., Pim, D. C., and Bulbrook, R. D. (1982). Detection of antibodies against the cellular protein p53 in sera from patients with breast cancer. *Int J Cancer* 30, 403-408.

- Crichton, D., Woiwode, A., Zhang, C., Mandavia, N., Morton, J. P., Warnock, L. J., Milner, J., White, R. J., and Johnson, D. L. (2003). p53 represses RNA polymerase III transcription by targeting TBP and inhibiting promoter occupancy by TFIIIB. *EMBO J* 22, 2810-2820.
- Darnell, J. E., Jr. (2002). Transcription factors as targets for cancer therapy. *Nat Rev Cancer* 2, 740-749.
- Das, C., Lucia, M. S., Hansen, K. C., and Tyler, J. K. (2009). CBP/p300-mediated acetylation of histone H3 on lysine 56. *Nature* 459, 113-117.
- de Ruijter, A. J., van Gennip, A. H., Caron, H. N., Kemp, S., and van Kuilenburg, A. B. (2003). Histone deacetylases (HDACs): characterization of the classical HDAC family. *Biochem J* 370, 737-749.
- de Vries, A., Flores, E. R., Miranda, B., Hsieh, H. M., van Oostrom, C. T., Sage, J., and Jacks, T. (2002). Targeted point mutations of p53 lead to dominant-negative inhibition of wild-type p53 function. *Proc Natl Acad Sci U S A* 99, 2948-2953.
- Demma, M., Maxwell, E., Ramos, R., Liang, L., Li, C., Hesk, D., Rossman, R., Mallams, A., Doll, R., Liu, M., et al. (2010). SCH529074, a small molecule activator of mutant p53, which binds p53 DNA binding domain (DBD), restores growth-suppressive function to mutant p53 and interrupts HDM2-mediated ubiquitination of wild type p53. *J Biol Chem* 285, 10198-10212.
- Deppert, W., Gohler, T., Koga, H., and Kim, E. (2000). Mutant p53: "gain of function" through perturbation of nuclear structure and function? *J Cell Biochem Suppl* 35, 115-122.
- Dimri, G. P., Lee, X., Basile, G., Acosta, M., Scott, G., Roskelley, C., Medrano, E. E., Linskens, M., Rubelj, I., Pereira-Smith, O., and et al. (1995). A biomarker that identifies senescent human cells in culture and in aging skin in vivo. *Proc Natl Acad Sci U S A* 92, 9363-9367.
- Dovey, O. M., Foster, C. T., Conte, N., Edwards, S. A., Edwards, J. M., Singh, R., Vassiliou, G., Bradley, A., and Cowley, S. M. (2013). Histone deacetylase 1 and 2 are essential for normal T-cell development and genomic stability in mice. *Blood* 121, 1335-1344.
- Eichhorn, K., and Jackson, S. P. (2001). A role for TAF3B2 in the repression of human RNA polymerase III transcription in nonproliferating cells. *J Biol Chem* 276, 21158-21165.
- Eliyahu, D., Michalovitz, D., Eliyahu, S., Pinhasi-Kimhi, O., and Oren, M. (1989). Wild-type p53 can inhibit oncogene-mediated focus formation. *Proc Natl Acad Sci U S A* 86, 8763-8767.
- Eliyahu, D., Raz, A., Gruss, P., Givol, D., and Oren, M. (1984). Participation of p53 cellular tumour antigen in transformation of normal embryonic cells. *Nature* 312, 646-649.
- Esposito, I., Konukiewitz, B., Schlitter, A. M., and Kloppel, G. (2012). [New insights into the origin of pancreatic cancer. Role of atypical flat lesions in pancreatic carcinogenesis]. *Pathologe* 33 Suppl 2, 189-193.
- Faure, A. J., Schmidt, D., Watt, S., Schwalie, P. C., Wilson, M. D., Xu, H., Ramsay, R. G., Odom, D. T., and Flicek, P. (2012). Cohesin regulates tissue-specific expression by stabilizing highly occupied cis-regulatory modules. *Genome Res* 22, 2163-2175.

- Feil, R., Wagner, J., Metzger, D., and Chambon, P. (1997). Regulation of Cre recombinase activity by mutated estrogen receptor ligand-binding domains. *Biochem Biophys Res Commun* 237, 752-757.
- Finlay, C. A., Hinds, P. W., Tan, T. H., Eliyahu, D., Oren, M., and Levine, A. J. (1988). Activating mutations for transformation by p53 produce a gene product that forms an hsc70-p53 complex with an altered half-life. *Mol Cell Biol* 8, 531-539.
- Finlay, C. A., Hinds, P. W., and Levine, A. J. (1989). The p53 proto-oncogene can act as a suppressor of transformation. *Cell* 57, 1083-1093.
- Finnin, M. S., Donigian, J. R., Cohen, A., Richon, V. M., Rifkind, R. A., Marks, P. A., Breslow, R., and Pavletich, N. P. (1999). Structures of a histone deacetylase homologue bound to the TSA and SAHA inhibitors. *Nature* 401, 188-193.
- Freed-Pastor, W. A., and Prives, C. (2012). Mutant p53: one name, many proteins. *Genes Dev* 26, 1268-1286.
- Friedman, P. N., Chen, X., Bargonetti, J., and Prives, C. (1993). The p53 protein is an unusually shaped tetramer that binds directly to DNA. *Proc Natl Acad Sci U S A* 90, 3319-3323.
- Fuda, N. J., Ardehali, M. B., and Lis, J. T. (2009). Defining mechanisms that regulate RNA polymerase II transcription in vivo. *Nature* 461, 186-192.
- Gallinari, P., Di Marco, S., Jones, P., Pallaoro, M., and Steinkuhler, C. (2007). HDACs, histone deacetylation and gene transcription: from molecular biology to cancer therapeutics. *Cell Res* 17, 195-211.
- Glozak, M. A., Sengupta, N., Zhang, X., and Seto, E. (2005). Acetylation and deacetylation of non-histone proteins. *Gene* 363, 15-23.
- Gomes, N. P., and Espinosa, J. M. (2010). Gene-specific repression of the p53 target gene PUMA via intragenic CTCF-Cohesin binding. *Genes Dev* 24, 1022-1034.
- Grant, S., Easley, C., and Kirkpatrick, P. (2007). Vorinostat. *Nat Rev Drug Discov* 6, 21-22.
- Grozinger, C. M., and Schreiber, S. L. (2002). Deacetylase enzymes: biological functions and the use of small-molecule inhibitors. *Chem Biol* 9, 3-16.
- Guenther, M. G., Levine, S. S., Boyer, L. A., Jaenisch, R., and Young, R. A. (2007). A chromatin landmark and transcription initiation at most promoters in human cells. *Cell* 130, 77-88.
- Hainaut, P., and Hollstein, M. (2000). p53 and human cancer: the first ten thousand mutations. *Adv Cancer Res* 77, 81-137.
- Hamacher, R., Schmid, R. M., Saur, D., and Schneider, G. (2008). Apoptotic pathways in pancreatic ductal adenocarcinoma. *Mol Cancer* 7, 64.
- Hanel, W., Marchenko, N., Xu, S., Yu, S. X., Weng, W., and Moll, U. (2013). Two hot spot mutant p53 mouse models display differential gain of function in tumorigenesis. *Cell Death Differ* 20, 898-909.

- Harms, K. L., and Chen, X. (2007). Histone deacetylase 2 modulates p53 transcriptional activities through regulation of p53-DNA binding activity. *Cancer Res* 67, 3145-3152.
- Harris, C. C., and Hollstein, M. (1993). Clinical implications of the p53 tumor-suppressor gene. *N Engl J Med* 329, 1318-1327.
- Haupt, Y., Maya, R., Kazaz, A., and Oren, M. (1997). Mdm2 promotes the rapid degradation of p53. *Nature* 387, 296-299.
- M.S. Hayden, S. Ghosh, Shared principles in NF-kappaB signaling, *Cell* 132 (2008) 344–362.
- Hayden, M. S., and Ghosh, S. (2011). NF-kappaB in immunobiology. *Cell Res* 21, 223-244.
- Hezel, A. F., Kimmelman, A. C., Stanger, B. Z., Bardeesy, N., and Depinho, R. A. (2006). Genetics and biology of pancreatic ductal adenocarcinoma. *Genes Dev* 20, 1218-1249.
- Hingorani, S. R., Wang, L., Multani, A. S., Combs, C., Deramaudt, T. B., Hruban, R. H., Rustgi, A. K., Chang, S., and Tuveson, D. A. (2005). Trp53R172H and KrasG12D cooperate to promote chromosomal instability and widely metastatic pancreatic ductal adenocarcinoma in mice. *Cancer Cell* 7, 469-483.
- Hingorani, S. R., Petricoin, E. F., Maitra, A., Rajapakse, V., King, C., Jacobetz, M. A., Ross, S., Conrads, T. P., Veenstra, T. D., Hitt, B. A., et al. (2003). Preinvasive and invasive ductal pancreatic cancer and its early detection in the mouse. *Cancer Cell* 4, 437-450.
- Hoess, R. H., Ziese, M., and Sternberg, N. (1982). P1 site-specific recombination: nucleotide sequence of the recombining sites. *Proc Natl Acad Sci U S A* 79, 3398-3402.
- Hollstein, M., and Hainaut, P. (2010). Massively regulated genes: the example of TP53. *J Pathol* 220, 164-173.
- Holzel, M., Burger, K., Muhl, B., Orban, M., Kellner, M., and Eick, D. (2010). The tumor suppressor p53 connects ribosome biogenesis to cell cycle control: a double-edged sword. *Oncotarget* 1, 43-47.
- Hruban, R. H., Adsay, N. V., Albores-Saavedra, J., Compton, C., Garrett, E. S., Goodman, S. N., Kern, S. E., Klimstra, D. S., Kloppel, G., Longnecker, D. S., et al. (2001). Pancreatic intraepithelial neoplasia: a new nomenclature and classification system for pancreatic duct lesions. *Am J Surg Pathol* 25, 579-586.
- Hruban, R. H., Goggins, M., Parsons, J., and Kern, S. E. (2000a). Progression model for pancreatic cancer. *Clin Cancer Res* 6, 2969-2972.
- Hruban, R. H., Wilentz, R. E., and Kern, S. E. (2000b). Genetic progression in the pancreatic ducts. *Am J Pathol* 156, 1821-1825.
- Insinga, A., Monestiroli, S., Ronzoni, S., Gelmetti, V., Marchesi, F., Viale, A., Altucci, L., Nervi, C., Minucci, S., and Pelicci, P. G. (2005). Inhibitors of histone deacetylases induce tumor-selective apoptosis through activation of the death receptor pathway. *Nat Med* 11, 71-76.

- Jackson, E. L., Willis, N., Mercer, K., Bronson, R. T., Crowley, D., Montoya, R., Jacks, T., and Tuveson, D. A. (2001). Analysis of lung tumor initiation and progression using conditional expression of oncogenic K-ras. *Genes Dev* 15, 3243-3248.
- Jeffrey, P. D., Gorina, S., and Pavletich, N. P. (1995). Crystal structure of the tetramerization domain of the p53 tumor suppressor at 1.7 angstroms. *Science* 267, 1498-1502.
- Jones, P. A., and Baylin, S. B. (2007). The epigenomics of cancer. *Cell* 128, 683-692.
- Jones, R. G., Plas, D. R., Kubek, S., Buzzai, M., Mu, J., Xu, Y., Birnbaum, M. J., and Thompson, C. B. (2005). AMP-activated protein kinase induces a p53-dependent metabolic checkpoint. *Mol Cell* 18, 283-293.
- Jones, S. N., Roe, A. E., Donehower, L. A., and Bradley, A. (1995). Rescue of embryonic lethality in Mdm2-deficient mice by absence of p53. *Nature* 378, 206-208.
- Jonkers, J., Meuwissen, R., van der Gulden, H., Peterse, H., van der Valk, M., and Berns, A. (2001). Synergistic tumor suppressor activity of BRCA2 and p53 in a conditional mouse model for breast cancer. *Nat Genet* 29, 418-425.
- Kagey, M. H., Newman, J. J., Bilodeau, S., Zhan, Y., Orlando, D. A., van Berkum, N. L., Ebmeier, C. C., Goossens, J., Rahl, P. B., Levine, S. S., et al. (2010). Mediator and cohesin connect gene expression and chromatin architecture. *Nature* 467, 430-435.
- Karagiannis, T. C., and Ververis, K. (2012). Potential of chromatin modifying compounds for the treatment of Alzheimer's disease. *Pathobiol Aging Age Relat Dis* 2.
- Karin, M. (2006). Nuclear factor-kappaB in cancer development and progression. *Nature* 441, 431-436.
- Kim, T. H., Abdullaev, Z. K., Smith, A. D., Ching, K. A., Loukinov, D. I., Green, R. D., Zhang, M. Q., Lobanenko, V. V., and Ren, B. (2007). Analysis of the vertebrate insulator protein CTCF-binding sites in the human genome. *Cell* 128, 1231-1245.
- Kirch, H. C., Flaswinkel, S., Rumpf, H., Brockmann, D., and Esche, H. (1999). Expression of human p53 requires synergistic activation of transcription from the p53 promoter by AP-1, NF-kappaB and Myc/Max. *Oncogene* 18, 2728-2738.
- Klein, S., Seidler, B., Kettenberger, A., Sibae, A., Rohn, M., Feil, R., Allescher, H. D., Vanderwinden, J. M., Hofmann, F., Schemann, M., et al. (2013). Interstitial cells of Cajal integrate excitatory and inhibitory neurotransmission with intestinal slow-wave activity. *Nat Commun* 4, 1630.
- Knudson, A. G., Jr. (1971). Mutation and cancer: statistical study of retinoblastoma. *Proc Natl Acad Sci U S A* 68, 820-823.
- Kornberg, R. D., and Lorch, Y. (1999). Twenty-five years of the nucleosome, fundamental particle of the eukaryote chromosome. *Cell* 98, 285-294.
- Kouzarides, T. (2007). Chromatin modifications and their function. *Cell* 128, 693-705.

- Krapp, A., Knofler, M., Ledermann, B., Burki, K., Berney, C., Zoerkler, N., Hagenbuchle, O., and Wellauer, P. K. (1998). The bHLH protein PTF1-p48 is essential for the formation of the exocrine and the correct spatial organization of the endocrine pancreas. *Genes Dev* 12, 3752-3763.
- Kravchenko, J. E., Ilyinskaya, G. V., Komarov, P. G., Agapova, L. S., Kochetkov, D. V., Strom, E., Frolova, E. I., Kovriga, I., Gudkov, A. V., Feinstein, E., and Chumakov, P. M. (2008). Small-molecule RETRA suppresses mutant p53-bearing cancer cells through a p73-dependent salvage pathway. *Proc Natl Acad Sci U S A* 105, 6302-6307.
- Kress, M., May, E., Cassingena, R., and May, P. (1979). Simian virus 40-transformed cells express new species of proteins precipitable by anti-simian virus 40 tumor serum. *J Virol* 31, 472-483.
- Kruse, J. P., and Gu, W. (2009). Modes of p53 regulation. *Cell* 137, 609-622.
- Kubbutat, M. H., Jones, S. N., and Vousden, K. H. (1997). Regulation of p53 stability by Mdm2. *Nature* 387, 299-303.
- Kumar, A., Takada, Y., Boriek, A. M., and Aggarwal, B. B. (2004). Nuclear factor-kappaB: its role in health and disease. *J Mol Med (Berl)* 82, 434-448.
- Labisso, W. L., Wirth, M., Stojanovic, N., Stauber, R. H., Schnieke, A., Schmid, R. M., Kramer, O. H., Saur, D., and Schneider, G. (2012). MYC directs transcription of MCL1 and eIF4E genes to control sensitivity of gastric cancer cells toward HDAC inhibitors. *Cell Cycle* 11, 1593-1602.
- Lane, D. P. (1992). Cancer. p53, guardian of the genome. *Nature* 358, 15-16.
- Lane, D. P., and Crawford, L. V. (1979). T antigen is bound to a host protein in SV40-transformed cells. *Nature* 278, 261-263.
- Lang, G. A., Iwakuma, T., Suh, Y. A., Liu, G., Rao, V. A., Parant, J. M., Valentin-Vega, Y. A., Terzian, T., Caldwell, L. C., Strong, L. C., et al. (2004). Gain of function of a p53 hot spot mutation in a mouse model of Li-Fraumeni syndrome. *Cell* 119, 861-872.
- Lavon, I., Pikarsky, E., Gutkovich, E., Goldberg, I., Bar, J., Oren, M., and Ben-Neriah, Y. (2003). Nuclear factor-kappaB protects the liver against genotoxic stress and functions independently of p53. *Cancer Res* 63, 25-30.
- Lehmann, A., Denkert, C., Budczies, J., Buckendahl, A. C., Darb-Esfahani, S., Noske, A., Muller, B. M., Bahra, M., Neuhaus, P., Dietel, M., et al. (2009). High class I HDAC activity and expression are associated with RelA/p65 activation in pancreatic cancer in vitro and in vivo. *BMC Cancer* 9, 395.
- Levine, A. J., and Oren, M. (2009). The first 30 years of p53: growing ever more complex. *Nat Rev Cancer* 9, 749-758.
- Li, D., Marchenko, N. D., and Moll, U. M. (2011). SAHA shows preferential cytotoxicity in mutant p53 cancer cells by destabilizing mutant p53 through inhibition of the HDAC6-Hsp90 chaperone axis. *Cell Death Differ* 18, 1904-1913.

- Linzer, D. I., and Levine, A. J. (1979). Characterization of a 54K dalton cellular SV40 tumor antigen present in SV40-transformed cells and uninfected embryonal carcinoma cells. *Cell* 17, 43-52.
- Liu, G., McDonnell, T. J., Montes de Oca Luna, R., Kapoor, M., Mims, B., El-Naggar, A. K., and Lozano, G. (2000). High metastatic potential in mice inheriting a targeted p53 missense mutation. *Proc Natl Acad Sci U S A* 97, 4174-4179.
- Livak, K. J., and Schmittgen, T. D. (2001). Analysis of relative gene expression data using real-time quantitative PCR and the 2(-Delta Delta C(T)) Method. *Methods* 25, 402-408.
- Luger, K., Mader, A. W., Richmond, R. K., Sargent, D. F., and Richmond, T. J. (1997). Crystal structure of the nucleosome core particle at 2.8 Å resolution. *Nature* 389, 251-260.
- MacDonald, T. J., Pollack, I. F., Okada, H., Bhattacharya, S., and Lyons-Weiler, J. (2007). Progression-associated genes in astrocytoma identified by novel microarray gene expression data reanalysis. *Methods Mol Biol* 377, 203-222.
- Maddocks, O. D., and Vousden, K. H. (2011). Metabolic regulation by p53. *J Mol Med (Berl)* 89, 237-245.
- Mahmoudi, S., Henriksson, S., Corcoran, M., Mendez-Vidal, C., Wiman, K. G., and Farnebo, M. (2009). Wrap53, a natural p53 antisense transcript required for p53 induction upon DNA damage. *Mol Cell* 33, 462-471.
- Mahmoudi, S., Henriksson, S., Farnebo, L., Roberg, K., and Farnebo, M. (2011). WRAP53 promotes cancer cell survival and is a potential target for cancer therapy. *Cell Death Dis* 2, e114.
- Margolis, D. (2005). Depletion of Latent HIV Infection & the Goal of Eradication. Physicians' research network.
- Marshall, G. M., Gherardi, S., Xu, N., Neiron, Z., Trahair, T., Scarlett, C. J., Chang, D. K., Liu, P. Y., Jankowski, K., Iraci, N., et al. (2010). Transcriptional upregulation of histone deacetylase 2 promotes Myc-induced oncogenic effects. *Oncogene* 29, 5957-5968.
- Martins, C. P., Brown-Swigart, L., and Evan, G. I. (2006). Modeling the therapeutic efficacy of p53 restoration in tumors. *Cell* 127, 1323-1334.
- Matheu, A., Maraver, A., Klatt, P., Flores, I., Garcia-Cao, I., Borrás, C., Flores, J. M., Vina, J., Blasco, M. A., and Serrano, M. (2007). Delayed ageing through damage protection by the Arf/p53 pathway. *Nature* 448, 375-379.
- Mattioni, T., Louvion, J. F., and Picard, D. (1994). Regulation of protein activities by fusion to steroid binding domains. *Methods Cell Biol* 43 Pt A, 335-352.
- Mazan-Mamczarz, K., Galban, S., Lopez de Silanes, I., Martindale, J. L., Atasoy, U., Keene, J. D., and Gorospe, M. (2003). RNA-binding protein HuR enhances p53 translation in response to ultraviolet light irradiation. *Proc Natl Acad Sci U S A* 100, 8354-8359.

- McLeod, M., Craft, S., and Broach, J. R. (1986). Identification of the crossover site during FLP-mediated recombination in the *Saccharomyces cerevisiae* plasmid 2 microns circle. *Mol Cell Biol* 6, 3357-3367.
- Meek, D. W. (1994). Post-translational modification of p53. *Semin Cancer Biol* 5, 203-210.
- Melero, J. A., Stitt, D. T., Mangel, W. F., and Carroll, R. B. (1979). Identification of new polypeptide species (48-55K) immunoprecipitable by antiserum to purified large T antigen and present in SV40-infected and -transformed cells. *Virology* 93, 466-480.
- Mertz, J. A., Conery, A. R., Bryant, B.M., Sandy, P., Balasubramanian, S., Mele, D. A., Bergeron, L., and Sims, R. J., (2011). Targeting MYC dependence in cancer by inhibiting BET bromodomains. *Proc Natl Acad Sci U S A* 108, 16669–16674.
- Metzger, D., Clifford, J., Chiba, H., and Chambon, P. (1995). Conditional site-specific recombination in mammalian cells using a ligand-dependent chimeric Cre recombinase. *Proc Natl Acad Sci U S A* 92, 6991-6995.
- Momand, J., Zambetti, G. P., Olson, D. C., George, D., and Levine, A. J. (1992). The mdm-2 oncogene product forms a complex with the p53 protein and inhibits p53-mediated transactivation. *Cell* 69, 1237-1245.
- Montgomery, R. L., Davis, C. A., Potthoff, M. J., Haberland, M., Fielitz, J., Qi, X., Hill, J. A., Richardson, J. A., and Olson, E. N. (2007). Histone deacetylases 1 and 2 redundantly regulate cardiac morphogenesis, growth, and contractility. *Genes Dev* 21, 1790-1802.
- Morris, J. P. t., Wang, S. C., and Hebrok, M. (2010). KRAS, Hedgehog, Wnt and the twisted developmental biology of pancreatic ductal adenocarcinoma. *Nat Rev Cancer* 10, 683-695.
- Morton, J. P., Timpson, P., Karim, S. A., Ridgway, R. A., Athineos, D., Doyle, B., Jamieson, N. B., Oien, K. A., Lowy, A. M., Brunton, V. G., et al. (2010). Mutant p53 drives metastasis and overcomes growth arrest/senescence in pancreatic cancer. *Proc Natl Acad Sci U S A* 107, 246-251.
- Mosmann, T. (1983). Rapid colorimetric assay for cellular growth and survival: application to proliferation and cytotoxicity assays. *J Immunol Methods* 65, 55-63.
- Muller, P. A. J. and Vousden, K. H. (2013). p53 mutations and cancer. *Nat. Cell Biol.* 15, 2–8
- Mullis, K., Faloona, F., Scharf, S., Saiki, R., Horn, G., and Erlich, H. (1986). Specific enzymatic amplification of DNA in vitro: the polymerase chain reaction. *Cold Spring Harb Symp Quant Biol* 51 Pt 1, 263-273.
- Muzumdar, M. D., Tasic, B., Miyamichi, K., Li, L., and Luo, L. (2007). A global double-fluorescent Cre reporter mouse. *Genesis* 45, 593-605.
- Neoptolemos, J. P., Stocken, D. D., Friess, H., Bassi, C., Dunn, J. A., Hickey, H., Beger, H., Fernandez-Cruz, L., Dervenis, C., Lacaine, F., et al. (2004). A randomized trial of

- chemoradiotherapy and chemotherapy after resection of pancreatic cancer. *N Engl J Med* 350, 1200-1210.
- Offield, M. F., Jetton, T. L., Labosky, P. A., Ray, M., Stein, R. W., Magnuson, M. A., Hogan, B. L., and Wright, C. V. (1996). PDX-1 is required for pancreatic outgrowth and differentiation of the rostral duodenum. *Development* 122, 983-995.
- Ogryzko, V. V., Hirai, T. H., Russanova, V. R., Barbie, D. A., and Howard, B. H. (1996). Human fibroblast commitment to a senescence-like state in response to histone deacetylase inhibitors is cell cycle dependent. *Mol Cell Biol* 16, 5210-5218.
- Olive, K. P., Tuveson, D. A., Ruhe, Z. C., Yin, B., Willis, N. A., Bronson, R. T., Crowley, D., and Jacks, T. (2004). Mutant p53 gain of function in two mouse models of Li-Fraumeni syndrome. *Cell* 119, 847-860.
- Olivier, M., Langerod, A., Carrieri, P., Bergh, J., Klaar, S., Eyfjord, J., Theillet, C., Rodriguez, C., Lidereau, R., Bieche, I., et al. (2006). The clinical value of somatic TP53 gene mutations in 1,794 patients with breast cancer. *Clin Cancer Res* 12, 1157-1167.
- Orban, P. C., Chui, D., and Marth, J. D. (1992). Tissue- and site-specific DNA recombination in transgenic mice. *Proc Natl Acad Sci U S A* 89, 6861-6865.
- Oren, M., Bienz, B., Givol, D., Rechavi, G., and Zakut, R. (1983). Analysis of recombinant DNA clones specific for the murine p53 cellular tumor antigen. *EMBO J* 2, 1633-1639.
- Osborne, C. S., Chakalova, L., Brown, K. E., Carter, D., Horton, A., Debrand, E., Goyenechea, B., Mitchell, J. A., Lopes, S., Reik, W., and Fraser, P. (2004). Active genes dynamically colocalize to shared sites of ongoing transcription. *Nat Genet* 36, 1065-1071.
- Pahl, H. L. (1999). Activators and target genes of Rel/NF-kappaB transcription factors. *Oncogene* 18, 6853-6866.
- Palani, C. D., Beck, J. F., and Sonnemann, J. (2012). Histone deacetylase inhibitors enhance the anticancer activity of nutlin-3 and induce p53 hyperacetylation and downregulation of MDM2 and MDM4 gene expression. *Invest New Drugs* 30, 25-36.
- Parada, L. F., Land, H., Weinberg, R. A., Wolf, D., and Rotter, V. (1984). Cooperation between gene encoding p53 tumour antigen and ras in cellular transformation. *Nature* 312, 649-651.
- Phan, R. T., and Dalla-Favera, R. (2004). The BCL6 proto-oncogene suppresses p53 expression in germinal-centre B cells. *Nature* 432, 635-639.
- Pharoah, P. D., Day, N. E., and Caldas, C. (1999). Somatic mutations in the p53 gene and prognosis in breast cancer: a meta-analysis. *Br J Cancer* 80, 1968-1973.
- Phillips, J. E., and Corces, V. G. (2009). CTCF: master weaver of the genome. *Cell* 137, 1194-1211.
- Place, R. F., Noonan, E. J., and Giardina, C. (2005). HDAC inhibition prevents NF-kappa B activation by suppressing proteasome activity: down-regulation of proteasome subunit expression stabilizes I kappa B alpha. *Biochem Pharmacol* 70, 394-406.

- Pogribny, I. P., Pogribna, M., Christman, J. K., and James, S. J. (2000). Single-site methylation within the p53 promoter region reduces gene expression in a reporter gene construct: possible in vivo relevance during tumorigenesis. *Cancer Res* 60, 588-594.
- Pollack, V. A., Savage, D. M., Baker, D. A., Tsaparikos, K. E., Sloan, D. E., Moyer, J. D., Barbacci, E. G., Pustilnik, L. R., Smolarek, T. A., Davis, J. A., et al. (1999). Inhibition of epidermal growth factor receptor-associated tyrosine phosphorylation in human carcinomas with CP-358,774: dynamics of receptor inhibition in situ and antitumor effects in athymic mice. *J Pharmacol Exp Ther* 291, 739-748.
- Prince, H. M., Bishton, M. J., and Harrison, S. J. (2009). Clinical studies of histone deacetylase inhibitors. *Clin Cancer Res* 15, 3958-3969.
- Redston, M. S., Caldas, C., Seymour, A. B., Hruban, R. H., da Costa, L., Yeo, C. J., and Kern, S. E. (1994). p53 mutations in pancreatic carcinoma and evidence of common involvement of homocopolymer tracts in DNA microdeletions. *Cancer Res* 54, 3025-3033.
- Reisman, D., Elkind, N. B., Roy, B., Beamon, J., and Rotter, V. (1993). c-Myc trans-activates the p53 promoter through a required downstream CACGTG motif. *Cell Growth Differ* 4, 57-65.
- Reisman, D., Greenberg, M., and Rotter, V. (1988). Human p53 oncogene contains one promoter upstream of exon 1 and a second, stronger promoter within intron 1. *Proc Natl Acad Sci U S A* 85, 5146-5150.
- Richter, E. D., Friedman, L. S., Tamir, Y., Berman, T., Levy, O., Westin, J. B., and Peretz, T. (2003). Cancer risks in naval divers with multiple exposures to carcinogens. *Environ Health Perspect* 111, 609-617.
- Riley, T., Sontag, E., Chen, P., and Levine, A. (2008). Transcriptional control of human p53-regulated genes. *Nat Rev Mol Cell Biol* 9, 402-412.
- Roemer, K. (1999). Mutant p53: gain-of-function oncoproteins and wild-type p53 inactivators. *Biol Chem* 380, 879-887.
- Roy, S., Packman, K., Jeffrey, R., and Tenniswood, M. (2005). Histone deacetylase inhibitors differentially stabilize acetylated p53 and induce cell cycle arrest or apoptosis in prostate cancer cells. *Cell Death Differ* 12, 482-491.
- Rozen, S., and Skaletsky, H. (2000). Primer3 on the WWW for general users and for biologist programmers. *Methods Mol Biol* 132, 365-386.
- Ruggeri, B., Zhang, S. Y., Caamano, J., DiRado, M., Flynn, S. D., and Klein-Szanto, A. J. (1992). Human pancreatic carcinomas and cell lines reveal frequent and multiple alterations in the p53 and Rb-1 tumor-suppressor genes. *Oncogene* 7, 1503-1511.
- Sakaguchi, K., Herrera, J. E., Saito, S., Miki, T., Bustin, M., Vassilev, A., Anderson, C. W., and Appella, E. (1998). DNA damage activates p53 through a phosphorylation-acetylation cascade. *Genes Dev* 12, 2831-2841.

- Saldana-Meyer, R., and Recillas-Targa, F. (2011). Transcriptional and epigenetic regulation of the p53 tumor suppressor gene. *Epigenetics* 6, 1068-1077.
- Sauve, A. A., Wolberger, C., Schramm, V. L., and Boeke, J. D. (2006). The biochemistry of sirtuins. *Annu Rev Biochem* 75, 435-465.
- Schmitt, C. A., Fridman, J. S., Yang, M., Baranov, E., Hoffman, R. M., and Lowe, S. W. (2002). Dissecting p53 tumor suppressor functions in vivo. *Cancer Cell* 1, 289-298.
- Schneider, G., Kramer, O. H., Fritsche, P., Schuler, S., Schmid, R. M., and Saur, D. (2010). Targeting histone deacetylases in pancreatic ductal adenocarcinoma. *J Cell Mol Med* 14, 1255-1263.
- Schneider, G., Henrich, A., Greiner, G., Wolf, V., Lovas, A., Wieczorek, M., Wagner, T., Reichardt, S., von Werder, A., Schmid, R. M., et al. (2010). Cross talk between stimulated NF-kappaB and the tumor suppressor p53. *Oncogene* 29, 2795-2806.
- Schneider, G., and Kramer, O. H. (2011). NFkappaB/p53 crosstalk-a promising new therapeutic target. *Biochim Biophys Acta* 1815, 90-103.
- Schönhuber N, Seidler B, Schuck K, Veltkamp C, Schachtler C, Zukowska M, Eser S, Feyerabend TB, Paul MC, Saur D et al., (2014) A next-generation dual-recombinase system for time- and host-specific targeting of pancreatic cancer. *Nat Med.*,2014. 1340-1347.
- Schwartz, Y. B., and Pirrotta, V. (2013). A new world of Polycombs: unexpected partnerships and emerging functions. *Nat Rev Genet* 14, 853-864.
- Shvarts, A., Steegenga, W. T., Riteco, N., van Laar, T., Dekker, P., Bazuine, M., van Ham, R. C., van der Houven van Oordt, W., Hateboer, G., van der Eb, A. J., and Jochemsen, A. G. (1996). MDMX: a novel p53-binding protein with some functional properties of MDM2. *EMBO J* 15, 5349-5357.
- Siegel, R., Ma, J., Zou, Z., and Jemal, A. (2014). Cancer statistics, 2014. *CA Cancer J Clin* 64, 9-29.
- Soriano, P. (1999). Generalized lacZ expression with the ROSA26 Cre reporter strain. *Nat Genet* 21, 70-71.
- Soto-Reyes, E., and Recillas-Targa, F. (2010). Epigenetic regulation of the human p53 gene promoter by the CTCF transcription factor in transformed cell lines. *Oncogene* 29, 2217-2227.
- Soussi, T., Caron de Fromentel, C., Mechali, M., May, P., and Kress, M. (1987). Cloning and characterization of a cDNA from *Xenopus laevis* coding for a protein homologous to human and murine p53. *Oncogene* 1, 71-78.
- Soussi, T., and Wiman, K. G. (2007). Shaping genetic alterations in human cancer: the p53 mutation paradigm. *Cancer Cell* 12, 303-312.
- Stein, T., Crighton, D., Warnock, L. J., Milner, J., and White, R. J. (2002). Several regions of p53 are involved in repression of RNA polymerase III transcription. *Oncogene* 21, 5540-5547.

- Stenger, J. E., Mayr, G. A., Mann, K., and Tegtmeyer, P. (1992). Formation of stable p53 homotetramers and multiples of tetramers. *Mol Carcinog* 5, 102-106.
- Strano, S., Dell'Orso, S., Di Agostino, S., Fontemaggi, G., Sacchi, A., and Blandino, G. (2007). Mutant p53: an oncogenic transcription factor. *Oncogene* 26, 2212-2219.
- Stuart, E. T., Haffner, R., Oren, M., and Gruss, P. (1995). Loss of p53 function through PAX-mediated transcriptional repression. *EMBO J* 14, 5638-5645.
- Su, X. L., Hou, Y. L., Yan, X. H., Ding, X., Hou, W. R., Sun, B., and Zhang, S. N. (2012). Expression, purification, and evaluation for anticancer activity of ribosomal protein L31 gene (RPL31) from the giant panda (*Ailuropoda melanoleuca*). *Mol Biol Rep* 39, 8945-8954.
- Subramanian, A., Tamayo, P., Mootha, V. K., Mukherjee, S., Ebert, B. L., Gillette, M. A., Paulovich, A., Pomeroy, S. L., Golub, T. R., Lander, E. S., and Mesirov, J. P. (2005). Gene set enrichment analysis: a knowledge-based approach for interpreting genome-wide expression profiles. *Proc Natl Acad Sci U S A* 102, 15545-15550.
- Sun, X. X., DeVine, T., Challagundla, K. B., and Dai, M. S. (2011). Interplay between ribosomal protein S27a and MDM2 protein in p53 activation in response to ribosomal stress. *J Biol Chem* 286, 22730-22741.
- Takahashi, T., D'Amico, D., Chiba, I., Buchhagen, D. L., and Minna, J. D. (1990). Identification of intronic point mutations as an alternative mechanism for p53 inactivation in lung cancer. *J Clin Invest* 86, 363-369.
- Tavtigian, S. V., Zabludoff, S. D., and Wold, B. J. (1994). Cloning of mid-G1 serum response genes and identification of a subset regulated by conditional myc expression. *Mol Biol Cell* 5, 375-388.
- Tergaonkar, V., Pando, M., Vafa, O., Wahl, G., and Verma, I. (2002). p53 stabilization is decreased upon NFkappaB activation: a role for NFkappaB in acquisition of resistance to chemotherapy. *Cancer Cell* 1, 493-503.
- Terzian, T., Suh, Y. A., Iwakuma, T., Post, S. M., Neumann, M., Lang, G. A., Van Pelt, C. S., and Lozano, G. (2008). The inherent instability of mutant p53 is alleviated by Mdm2 or p16INK4a loss. *Genes Dev* 22, 1337-1344.
- Towbin, H., Staehelin, T., and Gordon, J. (1979). Electrophoretic transfer of proteins from polyacrylamide gels to nitrocellulose sheets: procedure and some applications. *Proc Natl Acad Sci U S A* 76, 4350-4354.
- Tsuda, H., and Hirohashi, S. (1994). Association among p53 gene mutation, nuclear accumulation of the p53 protein and aggressive phenotypes in breast cancer. *Int J Cancer* 57, 498-503.
- Turner, B. M. (2002). Cellular memory and the histone code. *Cell* 111, 285-291.
- Vassilev, L. T., Vu, B. T., Graves, B., Carvajal, D., Podlaski, F., Filipovic, Z., Kong, N., Kammlott, U., Lukacs, C., Klein, C., et al. (2004). In vivo activation of the p53 pathway by small-molecule antagonists of MDM2. *Science* 303, 844-848.

- Ventura, A., Kirsch, D. G., McLaughlin, M. E., Tuveson, D. A., Grimm, J., Lintault, L., Newman, J., Reczek, E. E., Weissleder, R., and Jacks, T. (2007). Restoration of p53 function leads to tumour regression in vivo. *Nature* 445, 661-665.
- Vilborg, A., Glahder, J. A., Wilhelm, M. T., Bersani, C., Corcoran, M., Mahmoudi, S., Rosenstierne, M., Grander, D., Farnebo, M., Norrild, B., and Wiman, K. G. (2009). The p53 target Wig-1 regulates p53 mRNA stability through an AU-rich element. *Proc Natl Acad Sci U S A* 106, 15756-15761.
- Von Hoff, D. D., Ervin, T., Arena, F. P., Chiorean, E. G., Infante, J., Moore, M., Seay, T., Tjulandin, S. A., Ma, W. W., Saleh, M. N., et al. (2013). Increased survival in pancreatic cancer with nab-paclitaxel plus gemcitabine. *N Engl J Med* 369, 1691-1703.
- Vousden, K. H., and Prives, C. (2009). Blinded by the Light: The Growing Complexity of p53. *Cell* 137, 413-431.
- Vousden, K. H., and Lu, X. (2002). Live or let die: the cell's response to p53. *Nat Rev Cancer* 2, 594-604.
- Weinberg, R. A. (1991). Tumor suppressor genes. *Science* 254, 1138-1146.
- Weinmann, L., Wischhusen, J., Demma, M. J., Naumann, U., Roth, P., Dasmahapatra, B., and Weller, M. (2008). A novel p53 rescue compound induces p53-dependent growth arrest and sensitises glioma cells to Apo2L/TRAIL-induced apoptosis. *Cell Death Differ* 15, 718-729.
- Wilting, R. H., Yanover, E., Heideman, M. R., Jacobs, H., Horner, J., van der Torre, J., DePinho, R. A., and Dannenberg, J. H. (2010). Overlapping functions of Hdac1 and Hdac2 in cell cycle regulation and haematopoiesis. *EMBO J* 29, 2586-2597.
- Wiman, K. G. (2010). Pharmacological reactivation of mutant p53: from protein structure to the cancer patient. *Oncogene* 29, 4245-4252.
- Wirth, M., Fritsche, P., Stojanovic, N., Brandl, M., Jaeckel, S., Schmid, R. M., Saur, D., and Schneider, G. (2011). A simple and cost-effective method to transfect small interfering RNAs into pancreatic cancer cell lines using polyethylenimine. *Pancreas* 40, 144-150.
- Wu, Y., and Zhou, B. P. (2010). TNF-alpha/NF-kappaB/Snail pathway in cancer cell migration and invasion. *Br J Cancer* 102, 639-644.
- Xiong, S., Pant, V., Suh, Y. A., Van Pelt, C. S., Wang, Y., Valentin-Vega, Y. A., Post, S. M., and Lozano, G. (2010). Spontaneous tumorigenesis in mice overexpressing the p53-negative regulator Mdm4. *Cancer Res* 70, 7148-7154.
- Xu, Y., Voelter-Mahlknecht, S., and Mahlkecht, U. (2005). The histone deacetylase inhibitor suberoylanilide hydroxamic acid down-regulates expression levels of Bcr-abl, c-Myc and HDAC3 in chronic myeloid leukemia cell lines. *Int J Mol Med* 15, 169-172.
- Yan, J., Enge, M., Whittington, T., Dave, K., Liu, J., Sur, I., Schmierer, B., Jolma, A., Kivioja, T., Taipale, M., and Taipale, J. (2013). Transcription factor binding in human cells occurs in dense clusters formed around cohesin anchor sites. *Cell* 154, 801-813.

- Yan, W., Liu, S., Xu, E., Zhang, J., Zhang, Y., and Chen, X. (2013). Histone deacetylase inhibitors suppress mutant p53 transcription via histone deacetylase 8. *Oncogene* 32, 599-609.
- Zambrowicz, B. P., Imamoto, A., Fiering, S., Herzenberg, L. A., Kerr, W. G., and Soriano, P. (1997). Disruption of overlapping transcripts in the ROSA beta geo 26 gene trap strain leads to widespread expression of beta-galactosidase in mouse embryos and hematopoietic cells. *Proc Natl Acad Sci U S A* 94, 3789-3794.
- Zhai, W., and Comai, L. (2000). Repression of RNA polymerase I transcription by the tumor suppressor p53. *Mol Cell Biol* 20, 5930-5938.
- Zhang, X., Wang, W., Wang, H., Wang, M. H., Xu, W., and Zhang, R. (2013). Identification of ribosomal protein S25 (RPS25)-MDM2-p53 regulatory feedback loop. *Oncogene* 32, 2782-2791.
- Zhao, L., Chen, C. N., Hajji, N., Oliver, E., Cotroneo, E., Wharton, J., Wang, D., Li, M., McKinsey, T. A., Stenmark, K. R., and Wilkins, M. R. (2012). Histone deacetylation inhibition in pulmonary hypertension: therapeutic potential of valproic acid and suberoylanilide hydroxamic acid. *Circulation* 126, 455-467.
- Zhou, V. W., Goren, A., and Bernstein, B. E. (2011). Charting histone modifications and the functional organization of mammalian genomes. *Nat Rev Genet* 12, 7-18.
- Zhou, W., Zhu, P., Wang, J., Pascual, G., Ohgi, K. A., Lozach, J., Glass, C. K., and Rosenfeld, M. G. (2008). Histone H2A monoubiquitination represses transcription by inhibiting RNA polymerase II transcriptional elongation. *Mol Cell* 29, 69-80.
- Zhu, X. D., and Sadowski, P. D. (1995). Cleavage-dependent ligation by the FLP recombinase. Characterization of a mutant FLP protein with an alteration in a catalytic amino acid. *J Biol Chem* 270, 23044-23054.
- Zou, T., Mazan-Mamczarz, K., Rao, J. N., Liu, L., Marasa, B. S., Zhang, A. H., Xiao, L., Pullmann, R., Gorospe, M., and Wang, J. Y. (2006). Polyamine depletion increases cytoplasmic levels of RNA-binding protein HuR leading to stabilization of nucleophosmin and p53 mRNAs. *J Biol Chem* 281, 19387-19394.

Acknowledgements

The experimental part of this Doctoral thesis was performed at the Medical clinic and polyclinic II, Klinikum Rechts der Isar, TU Munich, Germany, within the TUM PhD Programme 'Medical Life Science and Technology'

I would like to thank to

PD Dr. med. Günter Schneider, for accepting me as a part of his research group, and giving me the opportunity to work on a number of exciting projects. I am thankful for his support, trust, tolerance, and enthusiasm. His help in the final steps of the writing of this thesis was essential.

Dr. rer. nat. Matthias Wirth, who helped me while I made first steps in this research field, for continuous support, knowledge he selflessly shared, endless patience, answering my numerous questions, and proofreading of the thesis.

Prof. Dr. med. Dieter Saur for insightful discussions, providing mouse models, and constant help and support.

PD Dr. rer. nat. Klaus Peter Jansen, for being the member of the thesis committee, great support, patience, and scientific advice.

Prof. Dr. rer. nat. Oliver Krämer, for years-long cooperation, and for giving me the opportunity to do part of my project in his research group. His great advice, support, and friendliness mean a lot to me.

Dr. rer. nat. Mariel Paul and Dr. Melanie Dobler, for moral support, careful reading and correcting of my thesis, and giving suggestions which contributed significantly to the completion of this work.

Sandra Diersch and Sabine Klein, for selfless help, and sharing their methodical experiences.

All the colleagues from the working group Schneider and Saur for an extraordinary supportive team work and creative and warm atmosphere in which I had a privilege to work.

Dr. Katrin Offe, for excellent organization of the PhD programme and administrative support and ***Desislava Zlatanova***, for great help and support, advice, and patience.

Special thanks to my Miodrag for selfless scientific and overall support and advice, for help and patience during all these years, and for his endless love.